

# CITATION REPORT

List of articles citing

**Development of an improved four-site water model for biomolecular simulations: TIP4P-Ew**

**DOI: 10.1063/1.1683075**

**Journal of Chemical Physics, 2004, 120, 9665-78.**

**Source:** <https://exaly.com/paper-pdf/37443286/citation-report.pdf>

**Version:** 2024-04-28

This report has been generated based on the citations recorded by exaly.com for the above article. For the latest version of this publication list, visit the link given above.

The third column is the impact factor (IF) of the journal, and the fourth column is the number of citations of the article.

#	Paper	IF	Citations
1619	Role of Water Molecules in ProteinLigand Dissociation and Selectivity Discrimination: Analysis of the Mechanisms and Kinetics of Biomolecular Solvation Using Molecular Dynamics.		
1618	Restructuring a Deep Eutectic Solvent by Water: The Nanostructure of Hydrated Choline Chloride/Urea.		
1617	Demonstrating an Order-of-Magnitude Sampling Enhancement in Molecular Dynamics Simulations of Complex Protein Systems.		
1616	Further along the Road Less Traveled: AMBER ff15ipq an Original Protein Force Field Built on a Self-Consistent Physical Model.		
1615	Reparameterization of SoluteSolute Interactions for Amino AcidSugar Systems Using Isopiestic Osmotic Pressure Molecular Dynamics Simulations.		
1614	Correction to Reparameterization of SoluteSolute Interactions for Amino AcidSugar Systems Using Isopiestic Osmotic Pressure Molecular Dynamics Simulations.		
1613	Force Field for Mg <sup>2+</sup> , Mn <sup>2+</sup> Zn <sup>2+</sup> , and Cd <sup>2+</sup> Ions That Have Balanced Interactions with Nucleic Acids.		
1612	Refining Disordered Peptide Ensembles with Computational Amide I Spectroscopy: Application to Elastin-Like Peptides.		
1611	Homology Modeling and Molecular Dynamics Simulation Combined with Xray Solution Scattering Defining Protein Structures of Thromboxane and Prostacyclin Synthases.		
1610	Seven-Site Effective Pair Potential for Simulating Liquid Water.		
1609	Systematic Optimization of Water Models Using Liquid/Vapor Surface Tension Data.		
1608	Water Structure and Transport in Zeolites with Pores in One or Three Dimensions from Molecular Dynamics Simulations.		
1607	Accurate Structure Prediction and Conformational Analysis of Cyclic Peptides with Residue-Specific Force Fields.		
1606	Substrate Channeling of Prostaglandin H <sub>2</sub> on the Stereochemical Control of a Cascade Cyclization Route.		
1605	Observing Solvation Dynamics with Simultaneous Femtosecond Xray Emission Spectroscopy and Xray Scattering.		
1604	Crowding Stabilizes DMSOWater Hydrogen-Bonding Interactions.		
1603	Dynamical Model for the Counteracting Effects of Trimethylamine NOxide on Urea in Aqueous Solutions under Pressure.		

1602 LiquidLiquid Phase Separation Produces Fast HBond Dynamics in DMSOWater Mixtures.

1601 Two-Dimensional Infrared Spectroscopy Reveals Cosolvent-Composition-Dependent Crossover in Intermolecular Hydrogen-Bond Dynamics.

1600 Extending the Nonbonded Cationic Dummy Model to Account for Ion-Induced Dipole Interactions.

1599 Cleaning Up Mechanistic Debris Generated by Twister Ribozymes Using Computational RNA Enzymology.

1598 Molecular Simulations Reveal Terminal Group Mediated Stabilization of Helical Conformers in Both Amyloid-42 and Synuclein.

1597 Binding Hydrated Anions with Hydrophobic Pockets.

1596 Molecular Recognition of Hydrophilic Molecules in Water by Combining the Hydrophobic Effect with Hydrogen Bonding.

1595 Heterochiral Knottin Protein: Folding and Solution Structure.

1594 Solubility of Water in Hydrogen at High Pressures: A Molecular Simulation Study.

1593 Osmolyte Induced Changes in Peptide Conformational Ensemble Correlate with Slower Amyloid Aggregation: A Coarse-Grained Simulation Study.

1592 Further along the Road Less Traveled: AMBER ff15ipq an Original Protein Force Field Built on a Self-Consistent Physical Model.

1591 A Multidimensional BSpline Correction for Accurate Modeling Sugar Puckering in QM/MM Simulations.

1590 Revisiting Hydrogen Bond Thermodynamics in Molecular Simulations.

1589 Force Field Parametrization from the Hirshfeld Molecular Electronic Density.

1588 Computing Bulk Phase Resonance Raman Spectra from ab Initio Molecular Dynamics and Real-Time TDDFT.

1587 A new approach for the prediction of partition functions using machine learning techniques. **1989**, 55, 963-965

24

1586 Molecular modeling of nucleic acid structure: electrostatics and solvation. **2001**, Chapter 7, Unit 7.9

2

1585 An Assessment of Potential of Mean Force Calculations with Implicit Solvent Models. **2004**, 108, 16525-16532

21

1584	WIGGLE: A new constrained molecular dynamics algorithm in Cartesian coordinates. <b>2005</b> , 210, 171-182		9
1583	Solvation free energies of amino acid side chain analogs for common molecular mechanics water models. <i>Journal of Chemical Physics</i> , <b>2005</b> , 122, 134508	3.9	329
1582	Fluctuating charge normal modes: An algorithm for implementing molecular dynamics simulations with polarizable potentials. <b>2005</b> , 26, 699-707		35
1581	The Amber biomolecular simulation programs. <b>2005</b> , 26, 1668-88		6155
1580	Wasser: Anomalien und Reisel. <b>2005</b> , 39, 164-175		16
1579	How well can simulation predict protein folding kinetics and thermodynamics?. <b>2005</b> , 34, 43-69		209
1578	Characterization of the TIP4P-Ew water model: vapor pressure and boiling point. <i>Journal of Chemical Physics</i> , <b>2005</b> , 123, 194504	3.9	86
1577	Polypeptide foldings obtained with effective pair potentials. <i>Journal of Chemical Physics</i> , <b>2005</b> , 122, 244908	3.9	6
1576	Relation between the melting temperature and the temperature of maximum density for the most common models of water. <i>Journal of Chemical Physics</i> , <b>2005</b> , 123, 144504	3.9	107
1575	Melting temperature of ice Ih calculated from coexisting solid-liquid phases. <i>Journal of Chemical Physics</i> , <b>2005</b> , 123, 36101	3.9	57
1574	Chapter 5 A Review of the TIP4P, TIP4P-Ew, TIP5P, and TIP5P-E Water Models. <b>2005</b> , 1, 59-74		12
1573	Can simple models describe the phase diagram of water?. <b>2005</b> , 17, S3283-S3288		62
1572	Computational Free Energy Studies of a New Ice Polymorph Which Exhibits Greater Stability than Ice Ih. <b>2005</b> , 1, 662-7		31
1571	Cutoff size need not strongly influence molecular dynamics results for solvated polypeptides. <b>2005</b> , 44, 609-16		138
1570	Potential energy functions for atomic-level simulations of water and organic and biomolecular systems. <b>2005</b> , 102, 6665-70		770
1569	Molecular origin of anticooperativity in hydrophobic association. <b>2005</b> , 109, 8108-19		26
1568	Exploring the helix-coil transition via all-atom equilibrium ensemble simulations. <b>2005</b> , 88, 2472-93		557
1567	A potential model for the study of ices and amorphous water: TIP4P/Ice. <i>Journal of Chemical Physics</i> , <b>2005</b> , 122, 234511	3.9	765

1566	The melting temperature of the most common models of water. <i>Journal of Chemical Physics</i> , <b>2005</b> , 122, 114507	3.9	302
1565	A general purpose model for the condensed phases of water: TIP4P/2005. <i>Journal of Chemical Physics</i> , <b>2005</b> , 123, 234505	3.9	2342
1564	Liquid-liquid phase transitions in supercooled water studied by computer simulations of various water models. <i>Journal of Chemical Physics</i> , <b>2005</b> , 123, 044515	3.9	141
1563	Molecular dynamics simulations of liquid water using various long-range electrostatics techniques. <b>2005</b> , 103, 1945-1960		46
1562	Vapor-liquid equilibria from the triple point up to the critical point for the new generation of TIP4P-like models: TIP4P/Ew, TIP4P/2005, and TIP4P/ice. <i>Journal of Chemical Physics</i> , <b>2006</b> , 125, 34503	3.9	175
1561	Osmotic coefficients of atomistic NaCl (aq) force fields. <i>Journal of Chemical Physics</i> , <b>2006</b> , 124, 164509	3.9	122
1560	Four phases of amorphous water: Simulations versus experiment. <i>Journal of Chemical Physics</i> , <b>2006</b> , 124, 164505	3.9	20
1559	The melting point of ice Ih for common water models calculated from direct coexistence of the solid-liquid interface. <i>Journal of Chemical Physics</i> , <b>2006</b> , 124, 144506	3.9	320
1558	Computational study of structural and dynamical properties of formamide-water mixtures. <i>Journal of Chemical Physics</i> , <b>2006</b> , 125, 184506	3.9	90
1557	The Origin of Layer Structure Artifacts in Simulations of Liquid Water. <b>2006</b> , 2, 1-11		164
1556	Liquid water simulation: a critical examination of cutoff length. <i>Journal of Chemical Physics</i> , <b>2006</b> , 124, 204501	3.9	51
1555	Flexible simple point-charge water model with improved liquid-state properties. <i>Journal of Chemical Physics</i> , <b>2006</b> , 124, 024503	3.9	742
1554	Revisiting the hexane-water interface via molecular dynamics simulations using nonadditive alkane-water potentials. <i>Journal of Chemical Physics</i> , <b>2006</b> , 124, 204706	3.9	54
1553	Structural correlations and motifs in liquid water at selected temperatures: ab initio and empirical model predictions. <b>2006</b> , 110, 3540-54		76
1552	Developing optimal Wertheim-like models of water for use in Statistical Associating Fluid Theory (SAFT) and related approaches. <b>2006</b> , 104, 3561-3581		146
1551	Absence of superheating for ice Ih with a free surface: a new method of determining the melting point of different water models. <b>2006</b> , 104, 3583-3592		56
1550	Molecular dynamics simulations of microwave effects on water using different long-range electrostatics methodologies. <b>2006</b> , 104, 243-253		57
1549	Solvation in modified water models: towards understanding hydrophobic effects. <b>2006</b> , 104, 3593-3605		44

1548	Molecular dynamics study of diffusion of formaldehyde in ice. <b>2006</b> , 432, 78-83		19
1547	On the re-engineered TIP4P water models for the prediction of vapor-liquid equilibrium. <b>2006</b> , 129, 120-124		19
1546	Hydration thermodynamic properties of amino acid analogues: a systematic comparison of biomolecular force fields and water models. <b>2006</b> , 110, 17616-26		271
1545	Limitations of the rigid planar nonpolarizable models of water. <i>Journal of Chemical Physics</i> , <b>2006</b> , 124, 74507	3.9	23
1544	Quantum effects in liquid water and ice: model dependence. <i>Journal of Chemical Physics</i> , <b>2006</b> , 125, 054512	3.9	51
1543	Dynamical properties of the soft sticky dipole-quadrupole-octupole water model: a molecular dynamics study. <i>Journal of Chemical Physics</i> , <b>2006</b> , 125, 144513	3.9	39
1542	Computer simulation of two new solid phases of water: Ice XIII and ice XIV. <i>Journal of Chemical Physics</i> , <b>2006</b> , 125, 116101	3.9	15
1541	Capillary waves at the liquid-vapor interface and the surface tension of water. <i>Journal of Chemical Physics</i> , <b>2006</b> , 125, 014702	3.9	142
1540	A potential model for methane in water describing correctly the solubility of the gas and the properties of the methane hydrate. <i>Journal of Chemical Physics</i> , <b>2006</b> , 125, 074510	3.9	121
1539	Solubility of simple, nonpolar compounds in TIP4P-Ew. <i>Journal of Chemical Physics</i> , <b>2006</b> , 124, 16102	3.9	20
1538	An accurate and simple quantum model for liquid water. <i>Journal of Chemical Physics</i> , <b>2006</b> , 125, 184507	3.9	165
1537	1. Features of the state of bound water in Bio-Objects as an example of the nature of sorbed in swelling sorbents. <b>2007</b> , 13, 5-40		
1536	Nonlinear scaling schemes for Lennard-Jones interactions in free energy calculations. <i>Journal of Chemical Physics</i> , <b>2007</b> , 127, 214108	3.9	240
1535	Free energy of liquid water from a computer simulation via cell theory. <i>Journal of Chemical Physics</i> , <b>2007</b> , 126, 064504	3.9	62
1534	Single particle and collective hydration dynamics for hydrophobic and hydrophilic peptides. <i>Journal of Chemical Physics</i> , <b>2007</b> , 126, 215101	3.9	17
1533	Surface tension of the most popular models of water by using the test-area simulation method. <i>Journal of Chemical Physics</i> , <b>2007</b> , 126, 154707	3.9	530
1532	Proposed high-pressure calorimetric experiment to probe theoretical predictions on the liquid-liquid critical point hypothesis. <b>2007</b> , 76, 021503		5
1531	Dipole-quadrupole force ratios determine the ability of potential models to describe the phase diagram of water. <b>2007</b> , 98, 237801		62

1530	TIP5P-Consistent Treatment of Electrostatics for Biomolecular Simulations. <b>2007</b> , 3, 1721-1733		24
1529	Disorder in ice polymorphs: A Monte Carlo simulation study. <b>2007</b> , 353, 2698-2707		2
1528	Replica exchange simulation of reversible folding/unfolding of the Trp-cage miniprotein in explicit solvent: on the structure and possible role of internal water. <b>2007</b> , 157, 524-33		105
1527	Classical interaction model for the water molecule. <i>Journal of Chemical Physics</i> , <b>2007</b> , 126, 184508	3.9	14
1526	Protein-folding dynamics: overview of molecular simulation techniques. <b>2007</b> , 58, 57-83		278
1525	Comparison of charge models for fixed-charge force fields: small-molecule hydration free energies in explicit solvent. <b>2007</b> , 111, 2242-54		232
1524	Representability problems for coarse-grained water potentials. <i>Journal of Chemical Physics</i> , <b>2007</b> , 126, 144509	3.9	172
1523	The Water Forcefield: Importance of Dipolar and Quadrupolar Interactions□ <b>2007</b> , 111, 15811-15822		45
1522	The melting point of hexagonal ice (Ih) is strongly dependent on the quadrupole of the water models. <b>2007</b> , 9, 2775-8		29
1521	Consequences of chain networks on thermodynamic, dielectric and structural properties for liquid water. <b>2007</b> , 9, 83-91		34
1520	Equation of State, Thermal Expansion Coefficient, and Isothermal Compressibility for Ices Ih, II, III, V, and VI, as Obtained from Computer Simulation□ <b>2007</b> , 111, 15877-15888		35
1519	Development of a polarizable intermolecular potential function (PIPF) for liquid amides and alkanes. <b>2007</b> , 3, 1878-1889		102
1518	Rapid estimation of relative protein-ligand binding affinities using a high-throughput version of MM-PBSA. <b>2007</b> , 47, 1493-503		53
1517	Accurate and efficient corrections for missing dispersion interactions in molecular simulations. <b>2007</b> , 111, 13052-63		141
1516	Solid-Liquid Interfacial Free Energy of Water: A Molecular Dynamics Simulation Study. <b>2007</b> , 3, 1494-8		20
1515	Molecular Dynamics Simulations of Proteins: Can the Explicit Water Model Be Varied?. <b>2007</b> , 3, 1550-60		46
1514	Thermal conductivity of methane hydrate from experiment and molecular simulation. <b>2007</b> , 111, 13194-205		90
1513	Long-range Lennard-Jones and electrostatic interactions in interfaces: application of the isotropic periodic sum method. <b>2007</b> , 111, 4393-400		71

1512	Methods in Membrane Lipids. <b>2007</b> ,	16
1511	Pressure and salt effects in simulated water: two sides of the same coin?. <b>2007</b> , 46, 8907-11	76
1510	Druck- und Salzeffekte in simuliertem Wasser: zwei Seiten einer Medaille?. <b>2007</b> , 119, 9065-9069	10
1509	Interfacing Q-Chem and CHARMM to perform QM/MM reaction path calculations. <b>2007</b> , 28, 1485-1502	170
1508	Molecular dynamic simulations of ionic liquids: a reliable description of structure, thermodynamics and dynamics. <b>2007</b> , 8, 2464-70	316
1507	Molecular dynamics simulations of pea ( <i>Pisum sativum</i> ) lectin structure with octyl glucoside detergents: the ligand interactions and dynamics. <b>2007</b> , 128, 215-30	10
1506	Molecular dynamics simulations of freezing of water and salt solutions. <b>2007</b> , 134, 64-70	52
1505	Testing the adequacy of simple water models at the opposite ends of the phase diagram. <b>2007</b> , 134, 94-98	7
1504	Ice: A fruitful source of information about liquid water. <b>2007</b> , 136, 214-220	14
1503	Hydrophobic potential of mean force as a solvation function for protein structure prediction. <b>2007</b> , 15, 727-40	41
1502	New model pair potential for water. Effect of inclusion of specific O-H interactions on the topology and dynamics of the hydrogen-bond network. <b>2007</b> , 77, 1700-1707	1
1501	On the validity of Stokes-Einstein and Stokes-Einstein-Debye relations in ionic liquids and ionic-liquid mixtures. <b>2008</b> , 9, 1851-8	127
1500	Thermodynamic and structural characterization of the transformation from a metastable low-density to a very high-density form of supercooled TIP4P-Ew model water. <b>2008</b> , 9, 2737-41	51
1499	The solvent-dependent shift of the amide I band of a fully solvated peptide as a local probe for the solvent composition in the peptide/solvent interface. <b>2008</b> , 9, 2742-50	11
1498	Temperature and concentration effects on the solvophobic solvation of methane in aqueous salt solutions. <b>2008</b> , 9, 2722-30	12
1497	Salt effects on the structure of water probed by attenuated total reflection infrared spectroscopy and molecular dynamics simulations. <b>2008</b> , 9, 2731-6	23
1496	Physicochemical properties of blue fluorescent protein determined via molecular dynamics simulation. <b>2008</b> , 89, 1136-43	7
1495	Chapter 1 Considerations for Lipid Force Field Development. <b>2008</b> , 1-48	51



1494	Water, Properties of. <b>2008</b> , 1			1
1493	Water inside a hydrophobic cavitand molecule. <b>2008</b> , 112, 10272-9			61
1492	Computational methods for biomolecular electrostatics. <b>2008</b> , 84, 843-70			55
1491	Determination of phase diagrams via computer simulation: methodology and applications to water, electrolytes and proteins. <b>2008</b> , 20, 153101			180
1490	Molecular simulation of protein-surface interactions: benefits, problems, solutions, and future directions. <b>2008</b> , 3, FC2-12			140
1489	Evaluating rotational diffusion from protein MD simulations. <b>2008</b> , 112, 6013-24			114
1488	Developing ab initio quality force fields from condensed phase quantum-mechanics/molecular-mechanics calculations through the adaptive force matching method. <i>Journal of Chemical Physics</i> , <b>2008</b> , 129, 064108	3.9		98
1487	Formation of ice-like water structure on the surface of an antifreeze protein. <b>2008</b> , 112, 6193-202			77
1486	Computing the free energy of molecular solids by the Einstein molecule approach: ices XIII and XIV, hard-dumbbells and a patchy model of proteins. <i>Journal of Chemical Physics</i> , <b>2008</b> , 129, 104704	3.9		53
1485	Protein folding revisited. <b>2008</b> , 84, 161-202			9
1484	Determination of alkali and halide monovalent ion parameters for use in explicitly solvated biomolecular simulations. <b>2008</b> , 112, 9020-41			1985
1483	The low-temperature dynamic crossover phenomenon in protein hydration water: simulations vs experiments. <b>2008</b> , 112, 1571-5			69
1482	Structure and dynamics of maltooligomer/water solutions and glasses. <b>2008</b> , 4, 1887			35
1481	Modeling of aqueous poly(oxyethylene) solutions: 1. Atomistic simulations. <b>2008</b> , 112, 2388-98			75
1480	Modeling of aqueous poly(oxyethylene) solutions: 2. Mesoscale simulations. <b>2008</b> , 112, 13561-71			51
1479	Classical and quantum gibbs free energies and phase behavior of water using simulation and cell theory. <b>2008</b> , 112, 9769-76			16
1478	Charge asymmetries in hydration of polar solutes. <b>2008</b> , 112, 2405-14			84
1477	Expressions for local contributions to the surface tension from the virial route. <b>2008</b> , 77, 031601			63

1476	Guanidinium chloride molecular diffusion in aqueous and mixed water-ethanol solutions. <b>2008</b> , 112, 8906-11		16
1475	Water simulation model with explicit three-molecule interactions. <b>2008</b> , 112, 8311-8		94
1474	Structure and dynamics of the Abeta(21-30) peptide from the interplay of NMR experiments and molecular simulations. <b>2008</b> , 130, 6145-58		142
1473	Comparing MD Simulations and NMR Relaxation Parameters. <b>2008</b> , 139-154		
1472	Shear thinning and shear dilatancy of liquid n-hexadecane via equilibrium and nonequilibrium molecular dynamics simulations: Temperature, pressure, and density effects. <i>Journal of Chemical Physics</i> , <b>2008</b> , 129, 014502	3.9	23
1471	Hydrophobic solvation of Gay-Berne particles in modified water models. <i>Journal of Chemical Physics</i> , <b>2008</b> , 128, 104506	3.9	8
1470	The importance of polarizability in the modeling of solubility: quantifying the effect of solute polarizability on the solubility of small nonpolar solutes in popular models of water. <i>Journal of Chemical Physics</i> , <b>2008</b> , 129, 024508	3.9	32
1469	An energy dispersive x-ray scattering and molecular dynamics study of liquid dimethyl carbonate. <i>Journal of Chemical Physics</i> , <b>2009</b> , 131, 244503	3.9	42
1468	Dynamic susceptibility of supercooled water and its relation to the dynamic crossover phenomenon. <b>2009</b> , 79, 040201		36
1467	Coarse-grained ions without charges: reproducing the solvation structure of NaCl in water using short-ranged potentials. <i>Journal of Chemical Physics</i> , <b>2009</b> , 131, 034107	3.9	61
1466	Properties of water along the liquid-vapor coexistence curve via molecular dynamics simulations using the polarizable TIP4P-QDP-LJ water model. <i>Journal of Chemical Physics</i> , <b>2009</b> , 131, 084709	3.9	35
1465	Single-molecule spectroscopy of the temperature-induced collapse of unfolded proteins. <b>2009</b> , 106, 20740-5		186
1464	Millisecond-scale molecular dynamics simulations on Anton. <b>2009</b> ,		166
1463	Assessing thermodynamic-dynamic relationships for waterlike liquids. <i>Journal of Chemical Physics</i> , <b>2009</b> , 130, 214510	3.9	31
1462	Theory for the three-dimensional Mercedes-Benz model of water. <i>Journal of Chemical Physics</i> , <b>2009</b> , 131, 194504	3.9	41
1461	Excited state properties of liquid water. <b>2009</b> , 21, 033101		21
1460	What far-infrared spectra can contribute to the development of force fields for ionic liquids used in molecular dynamics simulations. <b>2009</b> , 10, 1181-6		49
1459	In silico prediction of drug solubility: 4. Will simple potentials suffice?. <b>2009</b> , 30, 1859-71		20

1458	How hot? Systematic convergence of the replica exchange method using multiple reservoirs. <b>2010</b> , 31, 620-7	18
1457	How to obtain statistically converged MM/GBSA results. <b>2010</b> , 31, 837-46	129
1456	Conformational entropy changes upon lactose binding to the carbohydrate recognition domain of galectin-3. <b>2009</b> , 45, 157-69	67
1455	Investigations of structure and dynamics of water solvation of the type I antifreeze protein. <b>2009</b> , 109, 73-80	12
1454	A polarizable, four-point-charge model of water with size variation. <b>2009</b> , 148, 88-93	4
1453	Monte Carlo structure simulations for tertiary-butyl alcohol solutions in water/acetonitrile solvents. <b>2009</b> , 895, 116-126	12
1452	Molecular dynamics simulations of the dynamic and energetic properties of alkali and halide ions using water-model-specific ion parameters. <b>2009</b> , 113, 13279-90	354
1451	An elemental mercury diffusion coefficient for natural waters determined by molecular dynamics simulation. <b>2009</b> , 43, 3183-6	50
1450	Ice Nanocolumns: A Molecular Dynamics Study. <b>2009</b> , 113, 12699-12705	27
1449	Hydration water dynamics near biological interfaces. <b>2009</b> , 113, 4082-92	51
1448	Improving the point-charge description of hydrogen bonds by adaptive force matching. <b>2009</b> , 113, 1237-40	25
1447	Free energies and entropies of water molecules at the inhibitor-protein interface of DNA gyrase. <b>2009</b> , 131, 6608-13	36
1446	Thermodynamic properties of liquid water: an application of a nonparametric approach to computing the entropy of a neat fluid. <b>2009</b> , 5, 1462-1473	38
1445	A short guide for molecular dynamics simulations of RNA systems. <b>2009</b> , 47, 187-97	60
1444	Evaluating the performance of the ff99SB force field based on NMR scalar coupling data. <b>2009</b> , 97, 853-6	182
1443	Incorporating Phase-Dependent Polarizability in Non-Additive Electrostatic Models for Molecular Dynamics Simulations of the Aqueous Liquid-Vapor Interface. <b>2009</b> , 5, 359-373	33
1442	Optimized molecular dynamics force fields applied to the helix-coil transition of polypeptides. <b>2009</b> , 113, 9004-15	595
1441	Anomalies in water as obtained from computer simulations of the TIP4P/2005 model: density maxima, and density, isothermal compressibility and heat capacity minima. <b>2009</b> , 107, 365-374	131

1440	On the structure of water at the aqueous/air interface. <b>2009</b> , 113, 11672-9		113
1439	The properties of water: insights from quantum simulations. <b>2009</b> , 113, 5702-19		187
1438	Three-dimensional "Mercedes-Benz" model for water. <i>Journal of Chemical Physics</i> , <b>2009</b> , 131, 054505	3.9	52
1437	Ion pairing in molecular simulations of aqueous alkali halide solutions. <b>2009</b> , 113, 6782-91		242
1436	Evidence of dynamic crossover phenomena in water and other glass-forming liquids: experiments, MD simulations and theory. <b>2009</b> , 21, 504102		39
1435	Logarithmic decay in single-particle relaxation of hydrated lysozyme powder. <b>2009</b> , 103, 108102		36
1434	The influence of protein dynamics on the success of computational enzyme design. <b>2009</b> , 131, 14111-5		52
1433	Evaluation of various water models for simulation of adsorption in hydrophobic zeolites. <b>2009</b> , 35, 1067-1076		52
1432	Clusters of classical water models. <i>Journal of Chemical Physics</i> , <b>2009</b> , 131, 204310	3.9	43
1431	How Does Solute-Polarization Affect the Hydrophobic Hydration of Methane?. <b>2009</b> , 223, 1091-1104		8
1430	Correlation of Static and Dynamic Heterogeneities in Supercooled Water by Means of Molecular Dynamics Simulations. <b>2009</b> , 223, 1001-1010		5
1429	The Dynamic Response Function $\mathbb{I}(Q,t)$ of Confined Supercooled Water and its Relation to the Dynamic Crossover Phenomenon. <b>2010</b> , 224, 109-131		2
1428	A study of the structural and thermodynamic properties of water by the molecular dynamics method. <b>2010</b> , 4, 217-226		8
1427	UNDERSTANDING STRUCTURAL EFFECTS OF MULTIPOLE MOMENTS ON AQUEOUS SOLVATION OF IONS USING THE SOFT-STICKY DIPOLE-QUADRUPOLE-OCTUPOLE WATER MODEL. <b>2010</b> , 499, 219-225		13
1426	Discretization errors in molecular dynamics simulations with deterministic and stochastic thermostats. <b>2010</b> , 229, 9323-9346		22
1425	Structural changes induced in thionins by chloride anions as determined by molecular dynamics simulations. <b>2010</b> , 147, 42-52		3
1424	Predicting hydration free energies using all-atom molecular dynamics simulations and multiple starting conformations. <b>2010</b> , 24, 307-16		85
1423	Discovering Unique, Low-Energy Pure Water Isomers: Memetic Exploration, Optimization, and Landscape Analysis. <b>2010</b> , 14, 419-437		29

1422	Ion interactions with the carbon nanotube surface in aqueous solutions: understanding the molecular mechanisms. <b>2010</b> , 11, 2612-6		38
1421	Solvation of Glucose, Trehalose, and Sucrose by the Soft Sticky Dipole-Quadrupole-Octupole Water Model. <b>2010</b> , 491, 218-223		25
1420	Improved side-chain torsion potentials for the Amber ff99SB protein force field. <b>2010</b> , 78, 1950-8		3395
1419	15. Computer Simulations on Phase Transitions in Ice. <b>2010</b> , 315-336		
1418	Tip-sample interaction force mediated by water molecules for AFM in water: Three-dimensional reference interaction site model theory. <b>2010</b> , 82,		24
1417	Small-angle scattering and the structure of ambient liquid water. <b>2010</b> , 107, 14003-7		153
1416	Calculation of interfacial properties using molecular simulation with the reaction field method: Results for different water models. <i>Journal of Chemical Physics</i> , <b>2010</b> , 132, 184102	3.9	31
1415	Assessing the thermodynamic signatures of hydrophobic hydration for several common water models. <i>Journal of Chemical Physics</i> , <b>2010</b> , 132, 124504	3.9	64
1414	Temperature and pressure dependence of the optimized soft-sticky dipole-quadrupole-octupole water model. <i>Journal of Chemical Physics</i> , <b>2010</b> , 132, 114511	3.9	24
1413	A statistical mechanical theory for a two-dimensional model of water. <i>Journal of Chemical Physics</i> , <b>2010</b> , 132, 224507	3.9	23
1412	Evidence of functional protein dynamics from X-ray crystallographic ensembles. <b>2010</b> , 6, e1000911		31
1411	Therapeutic implications of the IL-21: IL-4 receptor system in children with common variable immunodeficiency syndrome. <b>2010</b> , 222, 362-7		5
1410	Two-phase thermodynamic model for efficient and accurate absolute entropy of water from molecular dynamics simulations. <b>2010</b> , 114, 8191-8		218
1409	The structure of ambient water. <b>2010</b> , 108, 1415-1433		183
1408	Water is the key to nonclassical nucleation of amorphous calcium carbonate. <b>2010</b> , 132, 17623-34		283
1407	Sodium perchlorate effects on the helical stability of a mainly alanine peptide. <b>2010</b> , 98, 186-96		22
1406	Construction, MD simulation, and hydrodynamic validation of an all-atom model of a monoclonal IgG antibody. <b>2010</b> , 99, 905-13		67
1405	Metadynamics as a tool for mapping the conformational and free-energy space of peptides--the alanine dipeptide case study. <b>2010</b> , 114, 5632-42		50

1404	Nonpolar Solvation Free Energies of Protein-Ligand Complexes. <b>2010</b> , 6, 3558-68	21
1403	Accounting for polarization cost when using fixed charge force fields. I. Method for computing energy. <b>2010</b> , 114, 8621-30	39
1402	Water's Contribution to the Energetic Roughness from Peptide Dynamics. <b>2010</b> , 6, 2591-7	23
1401	Nuclear quantum effects in water clusters: the role of the molecular flexibility. <b>2010</b> , 114, 2484-92	27
1400	Nonadditive empirical force fields for short-chain linear alcohols: methanol to butanol. Hydration free energetics and Kirkwood-Buff analysis using charge equilibration models. <b>2010</b> , 114, 11076-92	42
1399	Calculations of the free energy of interaction of the c-Fos-c-Jun coiled coil: effects of the solvation model and the inclusion of polarization effects. <b>2010</b> , 50, 2201-12	14
1398	Current status of the AMOEBA polarizable force field. <b>2010</b> , 114, 2549-64	914
1397	Starting-Condition Dependence of Order Parameters Derived from Molecular Dynamics Simulations. <b>2010</b> , 6, 2176-90	33
1396	Helix formation in a pentapeptide: experiment and force-field dependent dynamics. <b>2010</b> , 114, 12391-402	36
1395	A systematic molecular dynamics study of nearest-neighbor effects on base pair and base pair step conformations and fluctuations in B-DNA. <b>2010</b> , 38, 299-313	299
1394	Protein simulations with an optimized water model: cooperative helix formation and temperature-induced unfolded state collapse. <b>2010</b> , 114, 14916-23	195
1393	Understanding the interactions of cellulose with ionic liquids: a molecular dynamics study. <b>2010</b> , 114, 4293-301	269
1392	An MM/3D-RISM approach for ligand binding affinities. <b>2010</b> , 114, 8505-16	117
1391	Accounting for polarization cost when using fixed charge force fields. II. Method and application for computing effect of polarization cost on free energy of hydration. <b>2010</b> , 114, 8631-45	29
1390	Computer Simulations on Phase Transitions in Ice. <b>2010</b> , 71, 315-335	8
1389	Widom line and the liquid-liquid critical point for the TIP4P/2005 water model. <i>Journal of Chemical Physics</i> , <b>2010</b> , 133, 234502	3-9 239
1388	Exploring solvent effects upon the Menshutkin reaction using a polarizable force field. <b>2010</b> , 114, 8425-30	48
1387	Solvation theory to provide a molecular interpretation of the hydrophobic entropy loss of noble-gas hydration. <b>2010</b> , 22, 284108	20

1386	Heat capacity of water: A signature of nuclear quantum effects. <i>Journal of Chemical Physics</i> , <b>2010</b> , 132, 046101	3.9	81
1385	Derivation of an Accurate Force-Field for Simulating the Growth of Calcium Carbonate from Aqueous Solution: A New Model for the Calcite-Water Interface. <b>2010</b> , 114, 5997-6010		195
1384	The Use of Anisotropic Potentials in Modeling Water and Free Energies of Hydration. <b>2010</b> , 6, 1590-607		27
1383	A second generation distributed point polarizable water model. <i>Journal of Chemical Physics</i> , <b>2010</b> , 132, 014309	3.9	102
1382	Practical Aspects of Computational Chemistry. <b>2010</b> ,		11
1381	The thermodynamics of charge transfer in DNA photolyase: using thermodynamic integration calculations to analyse the kinetics of electron transfer reactions. <b>2010</b> , 12, 9516-25		28
1380	Transport in nanofluidic systems: a review of theory and applications. <b>2010</b> , 12, 015004		171
1379	Water adsorption in hydrophobic MOF channels. <b>2010</b> , 12, 8123-9		66
1378	A computational investigation of the properties of a reverse osmosis membrane. <b>2010</b> , 20, 7788		62
1377	Experimental test of the thermodynamic model of protein cooperativity using temperature-induced unfolding of a Ubq-UIM fusion protein. <b>2010</b> , 49, 8455-67		7
1376	Influence of water-protein hydrogen bonding on the stability of Trp-cage miniprotein. A comparison between the TIP3P and TIP4P-Ew water models. <b>2011</b> , 13, 19840-7		63
1375	Predicting hydration Gibbs energies of alkyl-aromatics using molecular simulation: a comparison of current force fields and the development of a new parameter set for accurate solvation data. <b>2011</b> , 13, 17384-94		19
1374	Limiting diffusion coefficients of ionic liquids in water and methanol: a combined experimental and molecular dynamics study. <b>2011</b> , 13, 3268-73		29
1373	The ice-vapor interface and the melting point of ice I(h) for the polarizable POL3 water model. <b>2011</b> , 115, 5973-82		18
1372	Homogeneous and heterogeneous tertiary structure ensembles of amyloid- $\beta$ peptides. <b>2011</b> , 50, 7612-28		114
1371	Molecular Mechanics Investigation of an Adenine-Adenine Non-Canonical Pair Conformational Change. <b>2011</b> , 7, 3779-3792		12
1370	Molecular Dynamics Simulations Predict a Favorable and Unique Mode of Interaction between Lithium (Li(+)) Ions and Hydrophobic Molecules in Aqueous Solution. <b>2011</b> , 7, 818-24		8
1369	The extent of conformational rigidity determines hydration in nonaromatic hexacyclic systems. <b>2011</b> , 115, 2608-16		9

1368	Comparison of Charge Models for Fixed-Charge Force Fields: Small Molecule Hydration Free Energies in Explicit Solvent. <b>2011</b> , 115, 1329-1332		17
1367	Driving force for hydrophobic interaction at different length scales. <b>2011</b> , 115, 2303-11		58
1366	Dielectric constant of ices and water: a lesson about water interactions. <b>2011</b> , 115, 5745-58		94
1365	Atomistic kinetic model for population shift and allostery in biomolecules. <b>2011</b> , 133, 18999-9005		43
1364	Correction to "Charge Asymmetries in Hydration of Polar Solutes" <b>2011</b> , 115, 15145-15145		3
1363	Polarizable Atomic Multipole-based Molecular Mechanics for Organic Molecules. <b>2011</b> , 7, 3143-3161		320
1362	Calculation of local water densities in biological systems: a comparison of molecular dynamics simulations and the 3D-RISM-KH molecular theory of solvation. <b>2011</b> , 115, 319-28		72
1361	Enhanced small-angle scattering connected to the Widom line in simulations of supercooled water. <i>Journal of Chemical Physics</i> , <b>2011</b> , 134, 214506	3.9	61
1360	Role of hydration in collagen recognition by bacterial adhesins. <b>2011</b> , 100, 2253-61		22
1359	Thermodynamics of liquids: standard molar entropies and heat capacities of common solvents from 2PT molecular dynamics. <b>2011</b> , 13, 169-81		113
1358	Tautomerism in 7-hydroxyquinoline: a combined experimental and theoretical study in water. <b>2011</b> , 115, 4195-201		28
1357	Prediction of self-diffusion coefficient and shear viscosity of water and its binary mixtures with methanol and ethanol by molecular simulation. <i>Journal of Chemical Physics</i> , <b>2011</b> , 134, 074508	3.9	161
1356	A molecular dynamics study of water nucleation using the TIP4P/2005 model. <i>Journal of Chemical Physics</i> , <b>2011</b> , 135, 244505	3.9	27
1355	Local and bulk hydration of zwitterionic glycine and its analogues through molecular simulations. <b>2011</b> , 115, 660-7		57
1354	A coarse-grained model of DNA with explicit solvation by water and ions. <b>2011</b> , 115, 132-42		69
1353	Structure and dynamics of 1,2-dimethoxyethane and 1,2-dimethoxypropane in aqueous and non-aqueous solutions: a molecular dynamics study. <i>Journal of Chemical Physics</i> , <b>2011</b> , 135, 164501	3.9	34
1352	A non-polarizable model of water that yields the dielectric constant and the density anomalies of the liquid: TIP4Q. <b>2011</b> , 13, 19728-40		38
1351	Temperature-dependent infrared spectroscopy of water from a first-principles approach. <b>2011</b> , 115, 6861-71		23



1350	Molecular Simulation Methods to Investigate Protein Adsorption Behavior at the Atomic Level. <b>2011</b> , 171-192	4
1349	References. 557-640	
1348	Development of the CHARMM Force Field for Lipids. <b>2011</b> , 2, 1526-1532	240
1347	Accurate predictions of nonpolar solvation free energies require explicit consideration of binding-site hydration. <b>2011</b> , 133, 13081-92	53
1346	Active participation of Mg ion in the reaction coordinate of RNA self-cleavage catalyzed by the hammerhead ribozyme. <b>2011</b> , 7, 1-3	47
1345	Atomic-level characterization of the ensemble of the Aβ(1-42) monomer in water using unbiased molecular dynamics simulations and spectral algorithms. <b>2011</b> , 405, 570-83	179
1344	A Computational Investigation into the Suitability of Purely Siliceous Zeolites as Reverse Osmosis Membranes. <b>2011</b> , 115, 4063-4075	30
1343	Probing the Transport of Ionic Liquids in Aqueous Solution through Nanopores. <b>2011</b> , 2, 2331-2336	28
1342	Application of Molecular Dynamics Simulations in Molecular Property Prediction I: Density and Heat of Vaporization. <b>2011</b> , 7, 2151-2165	85
1341	Simulating water with rigid non-polarizable models: a general perspective. <b>2011</b> , 13, 19663-88	640
1340	Optimizing Protein-Solvent Force Fields to Reproduce Intrinsic Conformational Preferences of Model Peptides. <b>2011</b> , 7, 1220-30	127
1339	Towards a rational spacer design for bivalent inhibition of estrogen receptor. <b>2011</b> , 25, 253-62	13
1338	The Effects of Charge Transfer Interactions on the Properties of Ice Ih. <b>2011</b> , 145, 355-364	3
1337	Prediction of the viscosity of water confined in carbon nanotubes. <b>2011</b> , 10, 403-414	56
1336	Nanoconfinement induced anomalous water diffusion inside carbon nanotubes. <b>2011</b> , 10, 1359-1364	45
1335	Folding of EK peptide and its dependence on salt concentration and pH: A computational study. <b>2011</b> , 54, 1974-1981	7
1334	Size and temperature effects on the viscosity of water inside carbon nanotubes. <b>2011</b> , 6, 87	45
1333	Free-energy landscape of the GB1 hairpin in all-atom explicit solvent simulations with different force fields: Similarities and differences. <b>2011</b> , 79, 1318-28	103

1332	A comparison of different initialization protocols to obtain statistically independent molecular dynamics simulations. <b>2011</b> , 32, 187-95		54
1331	Multipole electrostatics in hydration free energy calculations. <b>2011</b> , 32, 967-77		60
1330	Optimal scaling factors for CM1 and CM3 atomic charges in RM1-based aqueous simulations. <b>2011</b> , 32, 2836-42		15
1329	Soft-core potentials in thermodynamic integration: comparing one- and two-step transformations. <b>2011</b> , 32, 3253-63		137
1328	Structural characteristics of hydration sites in lysozyme. <b>2011</b> , 156, 31-42		11
1327	Assessment of dynamic properties of water around a monovalent ion: A classical molecular dynamics simulation study. <b>2011</b> , 966, 26-30		11
1326	Partition coefficients of organic molecules in squalane and water/ethanol mixtures by molecular dynamics simulations. <b>2011</b> , 306, 162-170		2
1325	Path integral Monte Carlo simulations for rigid rotors and their application to water. <b>2011</b> , 109, 149-168		22
1324	Compressive dynamic scission of carbon nanotubes under sonication: fracture by atomic ejection. <b>2011</b> , 467, 1270-1289		22
1323	Optimization of linear and branched alkane interactions with water to simulate hydrophobic hydration. <i>Journal of Chemical Physics</i> , <b>2011</b> , 135, 054510	3.9	32
1322	Molecular dynamics simulation of the dielectric constant of water: the effect of bond flexibility. <i>Journal of Chemical Physics</i> , <b>2011</b> , 134, 234501	3.9	70
1321	Robust three-body water simulation model. <i>Journal of Chemical Physics</i> , <b>2011</b> , 134, 184501	3.9	105
1320	Molecular dynamics simulations of vapor/liquid coexistence using the nonpolarizable water models. <i>Journal of Chemical Physics</i> , <b>2011</b> , 134, 124708	3.9	50
1319	Accounting for water molecules in drug design. <b>2011</b> , 6, 65-74		75
1318	Computation of methodology-independent single-ion solvation properties from molecular simulations. IV. Optimized Lennard-Jones interaction parameter sets for the alkali and halide ions in water. <i>Journal of Chemical Physics</i> , <b>2011</b> , 134, 144104	3.9	117
1317	The importance of polarisability in the modelling of solubility: quantifying the effect of charged co-solutes on the solubility of small non-polar solutes. <b>2011</b> , 37, 299-309		4
1316	Sources of the deficiencies in the popular SPC/E and TIP3P models of water. <i>Journal of Chemical Physics</i> , <b>2011</b> , 134, 054106	3.9	27
1315	The large quadrupole of water molecules. <i>Journal of Chemical Physics</i> , <b>2011</b> , 134, 134501	3.9	41

1314	The effects of charge transfer on the properties of liquid water. <i>Journal of Chemical Physics</i> , <b>2011</b> , 134, 184507	3.9	89
1313	Comment on "Isotope effects in liquid water by infrared spectroscopy. IV. No free OH groups in liquid water" [J. Chem. Phys. 133, 164509 (2010)]. <i>Journal of Chemical Physics</i> , <b>2011</b> , 135, 117101; author reply 117102	3.9	6
1312	Testing recent charge-on-spring type polarizable water models. I. Melting temperature and ice properties. <i>Journal of Chemical Physics</i> , <b>2012</b> , 137, 194102	3.9	18
1311	Tracking all-vapor instant gas-hydrate formation and guest molecule populations: a possible probe for molecules trapped in water nanodroplets. <i>Journal of Chemical Physics</i> , <b>2012</b> , 137, 204501	3.9	10
1310	Grid inhomogeneous solvation theory: hydration structure and thermodynamics of the miniature receptor cucurbit[7]uril. <i>Journal of Chemical Physics</i> , <b>2012</b> , 137, 044101	3.9	214
1309	High-pressure effect on the dynamics of solvated peptides. <i>Journal of Chemical Physics</i> , <b>2012</b> , 136, 145103	3.9	3
1308	A set of molecular models for alkali and halide ions in aqueous solution. <i>Journal of Chemical Physics</i> , <b>2012</b> , 136, 084501	3.9	53
1307	Effect of nanopatterns on Kapitza resistance at a water-gold interface during boiling: A molecular dynamics study. <b>2012</b> , 112, 053508		66
1306	Ionic force field optimization based on single-ion and ion-pair solvation properties: going beyond standard mixing rules. <i>Journal of Chemical Physics</i> , <b>2012</b> , 136, 124103	3.9	108
1305	Testing the recent charge-on-spring type polarizable water models. II. Vapor-liquid equilibrium. <i>Journal of Chemical Physics</i> , <b>2012</b> , 137, 194103	3.9	16
1304	Simple Ion Transfer at Liquid Liquid Interfaces. <b>2012</b> , 2012, 1-34		19
1303	Prediction of the Temperature-Dependent Thermal Conductivity and Shear Viscosity for Rigid Water Models. <b>2012</b> , 3,		9
1302	Model Dependence of the Electrostatic Response to a Molecular-Sized Ion in Water. <b>2012</b> , 81, SA012		3
1301	Carbon nanotube-based charge-controlled speed-regulating nanoclutch. <b>2012</b> , 111, 114304		13
1300	Simple model of hydrophobic hydration. <b>2012</b> , 116, 6177-86		16
1299	The conformational ensembles of $\beta$ -synuclein and tau: combining single-molecule FRET and simulations. <b>2012</b> , 103, 1940-9		101
1298	Biomolecular electrostatics and solvation: a computational perspective. <b>2012</b> , 45, 427-91		132
1297	Uncertainty Quantification in MD Simulations. Part I: Forward Propagation. <b>2012</b> , 10, 1428-1459		50

1296	Uncertainty Quantification in MD Simulations. Part II: Bayesian Inference of Force-Field Parameters. <b>2012</b> , 10, 1460-1492		60
1295	Optimizing solute-water van der Waals interactions to reproduce solvation free energies. <b>2012</b> , 116, 4524-34		116
1294	Analytical model for three-dimensional Mercedes-Benz water molecules. <b>2012</b> , 85, 061503		12
1293	A comparison of the value of viscosity for several water models using Poiseuille flow in a nano-channel. <i>Journal of Chemical Physics</i> , <b>2012</b> , 136, 134104	3-9	77
1292	Molecular Simulation of a Zn <sup>II</sup> triazamacrocyle Metal-Organic Frameworks Family with Extraframework Anions. <b>2012</b> , 116, 2952-2959		5
1291	Molecular dynamics simulations of the interactions of potential foulant molecules and a reverse osmosis membrane. <b>2012</b> , 22, 175-184		46
1290	Water structure-forming capabilities are temperature shifted for different models. <b>2012</b> , 116, 7538-43		12
1289	Water Sheared by Charged Graphene Sheets. <b>2012</b> , 26, 1897-1908		9
1288	The road not taken: a theoretical view of an unexpected cryptochrome charge transfer path. <b>2012</b> , 14, 11518-24		17
1287	Revealing the ionization ability of binding site I of human serum albumin using 2-(2'-hydroxyphenyl)benzoxazole as a pH sensitive probe. <b>2012</b> , 14, 2832-9		39
1286	Force and Stress along Simulated Dissociation Pathways of Cucurbituril-Guest Systems. <b>2012</b> , 8, 966-976		13
1285	Crystal lattice properties fully determine short-range interaction parameters for alkali and halide ions. <i>Journal of Chemical Physics</i> , <b>2012</b> , 137, 064104	3-9	53
1284	Hydration-determined orientational preferences in aromatic association from benzene dimer free energy volumes. <b>2012</b> , 116, 324-31		10
1283	Definition and computation of intermolecular contact in liquids using additively weighted Voronoi tessellation. <b>2012</b> , 116, 4657-66		10
1282	Effects of Chain Grafting Positions and Surface Coverage on Conformations of Model Reversed-Phase Liquid Chromatography Stationary Phases. <b>2012</b> , 116, 8456-8464		10
1281	Molecular Dynamics Simulations of Star Polymeric Molecules with Diblock Arms, a Comparative Study. <b>2012</b> , 8, 3733-49		16
1280	Development of polarizable models for molecular mechanical calculations. 3. Polarizable water models conforming to Thole polarization screening schemes. <b>2012</b> , 116, 7999-8008		42
1279	A refined MS-EVB model for proton transport in aqueous environments. <b>2012</b> , 116, 343-52		72

1278	Investigation of methanol-peptide nuclear Overhauser effects through molecular dynamics simulations. <b>2012</b> , 116, 1965-73			11
1277	Ice Ih-Water Interfacial Free Energy of Simple Water Models with Full Electrostatic Interactions. <b>2012</b> , 8, 2383-90			36
1276	Properties of Heavy Water in the Temperature Range T = 223 K to 373 K from Molecular Dynamics Simulation Using the Simple Point Charge/Heavy Water (SPC/HW) Model. <b>2012</b> , 57, 1751-1758			4
1275	Water model tuning for improved reproduction of rotational diffusion and NMR spectral density. <b>2012</b> , 116, 6279-87			57
1274	Dependence of pyranose ring puckering on anomeric configuration: methyl idopyranosides. <b>2012</b> , 116, 6380-6			29
1273	Molecular simulation of aqueous electrolyte solubility. 3. Alkali-halide salts and their mixtures in water and in hydrochloric acid. <b>2012</b> , 116, 5468-78			59
1272	Development of ions-TIP4P-Ew force fields for molecular processes in bulk and at the aqueous interface using molecular simulations. <b>2012</b> , 173, 47-54			20
1271	Thermal conductivity, shear viscosity and specific heat of rigid water models. <b>2012</b> , 542, 37-41			92
1270	Are Protein Force Fields Getting Better? A Systematic Benchmark on 524 Diverse NMR Measurements. <b>2012</b> , 8, 1409-1414			307
1269	Structural Insight into the Prolyl Hydroxylase PHD2: A Molecular Dynamics and DFT Study. <b>2012</b> , 2012, 4973-4985			5
1268	On the absolute thermodynamics of water from computer simulations: a comparison of first-principles molecular dynamics, reactive and empirical force fields. <i>Journal of Chemical Physics</i> , <b>2012</b> , 137, 244507	3.9		51
1267	Simple liquid models with corrected dielectric constants. <b>2012</b> , 116, 6936-44			54
1266	A GROMOS Parameter Set for Vicinal Diether Functions: Properties of Polyethyleneoxide and Polyethyleneglycol. <b>2012</b> , 8, 3943-63			56
1265	Predicting the effect of ions on the conformation of the H-NS dimerization domain. <b>2012</b> , 103, 89-98			12
1264	9.6 New Technologies for Molecular Dynamics Simulations. <b>2012</b> , 86-104			3
1263	Simulation of Water Transport Through Functionalized Single-Walled Carbon Nanotubes (SWCNTs). <b>2012</b> , 116, 24943-24953			40
1262	Liquid-liquid transition in ST2 water. <i>Journal of Chemical Physics</i> , <b>2012</b> , 137, 214505	3.9		128
1261	Water participation in molecular recognition and protein-ligand association: Probing the drug binding site "Sudlow I" in human serum albumin. <b>2012</b> ,			

1260	Charge transfer in model peptides: obtaining Marcus parameters from molecular simulation. <b>2012</b> , 116, 2284-93		39
1259	Density maximum and polarizable models of water. <i>Journal of Chemical Physics</i> , <b>2012</b> , 137, 084506	3.9	29
1258	Activity Coefficients of Complex Molecules by Molecular Simulation and Gibbs-Duhem Integration. <b>2012</b> , 10, 26-41		18
1257	Correlations in liquid water for the TIP3P-Ewald, TIP4P-2005, TIP5P-Ewald, and SWM4-NDP models. <i>Journal of Chemical Physics</i> , <b>2012</b> , 136, 064518	3.9	37
1256	Molecular Modeling and Simulation of Vapor-Liquid Equilibria of Ethylene Oxide, Ethylene Glycol, and Water as Well as their Binary Mixtures. <b>2012</b> , 51, 7428-7440		24
1255	Practical Aspects of Computational Chemistry II. <b>2012</b> ,		2
1254	Release of high-energy water as an essential driving force for the high-affinity binding of cucurbit[n]urils. <b>2012</b> , 134, 15318-23		380
1253	Prediction of the Temperature-Dependent Thermal Conductivity and Shear Viscosity for Rigid Water Models. <b>2012</b> ,		
1252	The Molecular Structure and Conformational Dynamics of Chitosan Polymers: An Integrated Perspective from Experiments and Computational Simulations. <b>2012</b> ,		3
1251	Transferability of conformational dependent charges from protein simulations. <b>2012</b> , 112, 1768-1785		9
1250	Comparison of end-point continuum-solvation methods for the calculation of protein-ligand binding free energies. <b>2012</b> , 80, 1326-42		62
1249	Refinement of protein structure homology models via long, all-atom molecular dynamics simulations. <b>2012</b> , 80, 2071-9		193
1248	Attraction between like-charged monovalent ions. <i>Journal of Chemical Physics</i> , <b>2012</b> , 136, 184501	3.9	22
1247	Local structure evolution and its connection to thermodynamic and transport properties of 1-butyl-3-methylimidazolium tetrafluoroborate and water mixtures by molecular dynamics simulations. <b>2012</b> , 116, 3249-63		68
1246	Water diffusion inside carbon nanotubes: mutual effects of surface and confinement. <b>2012</b> , 14, 964-71		64
1245	Intrinsic disorder modulates protein self-assembly and aggregation. <b>2012</b> , 109, 6951-6		84
1244	Strength of hydrogen bonds of water depends on local environment. <i>Journal of Chemical Physics</i> , <b>2012</b> , 136, 144305	3.9	51
1243	Will molecular dynamics simulations of proteins ever reach equilibrium?. <b>2012</b> , 14, 8662-77		75

1242	Comparative study of flavins binding with human serum albumin: a fluorometric, thermodynamic, and molecular dynamics approach. <b>2012</b> , 13, 2142-53	28
1241	Adaptive Green-Kubo estimates of transport coefficients from molecular dynamics based on robust error analysis. <i>Journal of Chemical Physics</i> , <b>2012</b> , 136, 154102	3-9 35
1240	Digraphs in Chemistry: All Possible Structures and Temperature-Dependent Distribution of Water Clusters. <b>2012</b> , 49-68	2
1239	Alchemical prediction of hydration free energies for SAMPL. <b>2012</b> , 26, 551-62	60
1238	The polarizing forces of water. <b>2012</b> , 131, 1	5
1237	Computational approaches to the interpretation of NMR data for studying protein dynamics. <b>2012</b> , 396, 124-134	8
1236	Fluid phase behavior from molecular simulation: Hydrazine, Monomethylhydrazine, Dimethylhydrazine and binary mixtures containing these compounds. <b>2012</b> , 322-323, 79-91	8
1235	A multi-scale framework for multi-phase equilibrium flash. <b>2012</b> , 36, 79-98	20
1234	Molecular geometry effects and the Gibbs-Helmholtz Constrained equation of state. <b>2012</b> , 37, 1-14	10
1233	On the relation between hydrogen bonds, tetrahedral order and molecular mobility in model water. <b>2012</b> , 538, 35-38	14
1232	Free energy calculations on snake venom metalloproteinase BaP1. <b>2012</b> , 79, 990-1000	4
1231	A semiempirical approach to ligand-binding affinities: dependence on the Hamiltonian and corrections. <b>2012</b> , 33, 1179-89	26
1230	Sucrose in aqueous solution revisited, Part 2: adaptively biased molecular dynamics simulations and computational analysis of NMR relaxation. <b>2012</b> , 97, 289-302	11
1229	Sucrose in aqueous solution revisited, Part 1: molecular dynamics simulations and direct and indirect dipolar coupling analysis. <b>2012</b> , 97, 276-88	23
1228	Molecular dynamics simulations of the mechanisms of thermal conduction in methane hydrates. <b>2012</b> , 55, 167-174	5
1227	Mesoscale inhomogeneities in aqueous solutions of small amphiphilic molecules. <b>2013</b> , 167, 217-38	69
1226	The Influence of Water on the Solubility of Carbon Dioxide in Imidazolium Based Ionic Liquids. <b>2013</b> , 227, 167-176	16
1225	Comparison of force fields on the basis of various model approaches--how to design the best model for the [C <sub>n</sub> MIM][NTf <sub>2</sub> ] family of ionic liquids. <b>2013</b> , 14, 3368-74	30

1224	Binding of hydroxyquinoline probes to human serum albumin: combining molecular modeling and Förster's resonance energy transfer spectroscopy to understand flexible ligand binding. <b>2013</b> , 117, 1062-74	51
1223	Structural heterogeneity in familial Alzheimer's disease mutants of amyloid-beta peptides. <b>2013</b> , 9, 997-1003	32
1222	Characteristics of thermal conductivity in classical water models. <i>Journal of Chemical Physics</i> , <b>2013</b> , 138, 064505	3.9 94
1221	Conformational entropy of intrinsically disordered protein. <b>2013</b> , 117, 5503-9	25
1220	A coarse-grained model for polyethylene glycol in bulk water and at a water/air interface. <b>2013</b> , 15, 17093-104	46
1219	Correlation of structural order, anomalous density, and hydrogen bonding network of liquid water. <b>2013</b> , 117, 8831-43	36
1218	Flexibility of the bacterial chaperone trigger factor in microsecond-timescale molecular dynamics simulations. <b>2013</b> , 105, 732-44	14
1217	Systematic improvement of a classical molecular model of water. <b>2013</b> , 117, 9956-72	235
1216	The quest for self-consistency in hydrogen bond definitions. <i>Journal of Chemical Physics</i> , <b>2013</b> , 139, 084504	57
1215	Molecular dynamics simulations of highly crowded amino acid solutions: comparisons of eight different force field combinations with experiment and with each other. <b>2013</b> , 9,	31
1214	Adsorption in Metal-Organic Frameworks. <b>2013</b> , 989-1006	3
1213	Unraveling cellulose microfibrils: a twisted tale. <b>2013</b> , 99, 746-56	51
1212	Derivation of fixed partial charges for amino acids accommodating a specific water model and implicit polarization. <b>2013</b> , 117, 2328-38	79
1211	Polarizable water models from mixed computational and empirical optimization. <b>2013</b> , 117, 9486-500	23
1210	Wetting kinetics of water nano-droplet containing non-surfactant nanoparticles: A molecular dynamics study. <b>2013</b> , 103, 253104	32
1209	Assessing the influence of solvation models on structural characteristics of intrinsically disordered protein. <b>2013</b> , 1017, 194-199	7
1208	Cucurbit[8]uril and blue-box: high-energy water release overwhelms electrostatic interactions. <b>2013</b> , 135, 14879-88	136
1207	Molecular dynamics simulations of disjoining pressure effect in ultra-thin water film on a metal surface. <b>2013</b> , 103, 263110	24



1206	Overview of Medea-GIBBS capabilities for thermodynamic property calculation and VLE behaviour description of pure compounds and mixtures: application to polar compounds generated from ligno-cellulosic biomass. <b>2013</b> , 39, 1165-1211		14
1205	Lennard-Jones Lattice Summation in Bilayer Simulations Has Critical Effects on Surface Tension and Lipid Properties. <b>2013</b> , 9, 3527-37		89
1204	Effects of magnesium ions and water molecules on the structure of amorphous calcium carbonate: a molecular dynamics study. <b>2013</b> , 117, 14849-56		29
1203	Insights on hydrogen-bond lifetimes in liquid and supercooled water. <b>2013</b> , 117, 16188-95		42
1202	A systematic development of a polarizable potential of water. <i>Journal of Chemical Physics</i> , <b>2013</b> , 138, 204507	3.9	107
1201	Cooperative dynamic and diffusion behavior above and below the dynamical crossover of supercooled water. <i>Journal of Chemical Physics</i> , <b>2013</b> , 139, 044509	3.9	11
1200	Homogeneous ice nucleation at moderate supercooling from molecular simulation. <b>2013</b> , 135, 15008-17		214
1199	A transferable H2O interaction potential based on a single center multipole expansion: SCME. <b>2013</b> , 15, 16542-56		29
1198	Comparison of MM/GBSA calculations based on explicit and implicit solvent simulations. <b>2013</b> , 15, 7731-9		56
1197	Simulation optimization of spherical non-polar guest recognition by deep-cavity cavitands. <i>Journal of Chemical Physics</i> , <b>2013</b> , 139, 234502	3.9	12
1196	Effects of microcomplexity on hydrophobic hydration in amphiphiles. <b>2013</b> , 135, 4918-21		26
1195	Molecular determinants of inactivation of the resuscitation promoting factor B from <i>Mycobacterium tuberculosis</i> . <b>2013</b> , 31, 195-205		22
1194	Mass accommodation of water: bridging the gap between molecular dynamics simulations and kinetic condensation models. <b>2013</b> , 117, 410-20		65
1193	Influence of the long-range corrections on the interfacial properties of molecular models using Monte Carlo simulation. <i>Journal of Chemical Physics</i> , <b>2013</b> , 138, 034707	3.9	48
1192	Kinetic water stability of an isostructural family of zinc-based pillared metal-organic frameworks. <b>2013</b> , 29, 633-42		138
1191	Approaches to efficiently estimate solvation and explicit water energetics in ligand binding: the use of WaterMap. <b>2013</b> , 8, 277-87		41
1190	An overview of the Amber biomolecular simulation package. <b>2013</b> , 3, 198-210		1187
1189	Temperature dependence of the DNA double helix at the nanoscale: structure, elasticity, and fluctuations. <b>2013</b> , 105, 1904-14		26

1188	Free Energy Approaches for Modeling Atomic Force Microscopy in Liquids. <b>2013</b> , 9, 600-8		57
1187	Stable conformation of full-length amyloid- $\beta$ (1-42) monomer in water: Replica exchange molecular dynamics and ab initio molecular orbital simulations. <b>2013</b> , 577, 131-137		15
1186	Electrostatic properties of water models evaluated by a long-range potential based solely on the Wolf charge-neutral condition. <b>2013</b> , 556, 308-314		8
1185	Quantitative cw Overhauser effect dynamic nuclear polarization for the analysis of local water dynamics. <b>2013</b> , 74, 33-56		81
1184	Structure and thermodynamics of H <sub>3</sub> O <sup>+</sup> (H <sub>2</sub> O) <sub>8</sub> clusters: A combined molecular dynamics and quantum mechanics approach. <b>2013</b> , 1021, 240-248		12
1183	Six-site polarizable model of water based on the classical Drude oscillator. <i>Journal of Chemical Physics</i> , <b>2013</b> , 138, 034508	3.9	92
1182	Substrate dynamics in enzyme action: rotations of monosaccharide subunits in the binding groove are essential for pectin methylesterase processivity. <b>2013</b> , 104, 1731-9		22
1181	Understanding Adsorption of Highly Polar Vapors on Mesoporous MIL-100(Cr) and MIL-101(Cr): Experiments and Molecular Simulations. <b>2013</b> , 117, 7613-7622		60
1180	Simulating DNA by molecular dynamics: aims, methods, and validation. <b>2013</b> , 924, 445-68		8
1179	Rational Design of Particle Mesh Ewald Compatible Lennard-Jones Parameters for +2 Metal Cations in Explicit Solvent. <b>2013</b> , 9, 2733-2748		365
1178	Transient access to the protein interior: simulation versus NMR. <b>2013</b> , 135, 8735-48		46
1177	The intrinsic conformational features of amino acids from a protein coil library and their applications in force field development. <b>2013</b> , 15, 3413-28		49
1176	Super-resolution in solution X-ray scattering and its applications to structural systems biology. <b>2013</b> , 42, 415-41		157
1175	Computational IR spectroscopy of water: OH stretch frequencies, transition dipoles, and intermolecular vibrational coupling constants. <i>Journal of Chemical Physics</i> , <b>2013</b> , 138, 174108	3.9	52
1174	Differences in $\beta$ -strand populations of monomeric A $\beta$ 0 and A $\beta$ 2. <b>2013</b> , 104, 2714-24		114
1173	Finite-size scaling investigation of the liquid-liquid critical point in ST2 water and its stability with respect to crystallization. <i>Journal of Chemical Physics</i> , <b>2013</b> , 138, 244506	3.9	53
1172	Systematic Parametrization of Polarizable Force Fields from Quantum Chemistry Data. <b>2013</b> , 9, 452-60		124
1171	Water nanodroplets: predictions of five model potentials. <i>Journal of Chemical Physics</i> , <b>2013</b> , 138, 194303	3.9	38

1170	Understanding the Control of Mineralization by Polyelectrolyte Additives: Simulation of Preferential Binding to Calcite Surfaces. <b>2013</b> , 117, 6904-6913	47
1169	Matching of additive and polarizable force fields for multiscale condensed phase simulations. <b>2013</b> , 9, 2826-2837	23
1168	Is the Calcite-Water Interface Understood? Direct Comparisons of Molecular Dynamics Simulations with Specular X-ray Reflectivity Data. <b>2013</b> , 117, 5028-5042	127
1167	Free energy of solvated salt bridges: a simulation and experimental study. <b>2013</b> , 117, 7254-9	30
1166	Pressure reentrant assembly: direct simulation of volumes of micellization. <b>2013</b> , 29, 14743-7	9
1165	Entropy from state probabilities: hydration entropy of cations. <b>2013</b> , 117, 6466-72	22
1164	A New Maximum Likelihood Approach for Free Energy Profile Construction from Molecular Simulations. <b>2013</b> , 9, 153-164	59
1163	Molecular modeling of nucleic Acid structure: electrostatics and solvation. <b>2014</b> , 55, 7.9.1-27	4
1162	Molecular simulations of RNA 2'-O-transesterification reaction models in solution. <b>2013</b> , 117, 94-103	21
1161	Investigation of ethanol-peptide and water-peptide interactions through intermolecular nuclear overhauser effects and molecular dynamics simulations. <b>2013</b> , 117, 4880-92	15
1160	pH-Independence of trialanine and the effects of termini blocking in short peptides: a combined vibrational, NMR, UVCD, and molecular dynamics study. <b>2013</b> , 117, 3689-706	57
1159	Rotamer decomposition and protein dynamics: efficiently analyzing dihedral populations from molecular dynamics. <b>2013</b> , 34, 198-205	7
1158	Bridging the gap between theory and experiment to derive a detailed understanding of hammerhead ribozyme catalysis. <b>2013</b> , 120, 25-91	8
1157	Multistate reweighting and configuration mapping together accelerate the efficiency of thermodynamic calculations as a function of molecular geometry by orders of magnitude. <i>Journal of Chemical Physics</i> , <b>2013</b> , 138, 154108	3.9 9
1156	Ligand clouds around protein clouds: a scenario of ligand binding with intrinsically disordered proteins. <b>2013</b> , 9, e1003249	60
1155	Distal loop flexibility of a regulatory domain modulates dynamics and activity of C-terminal SRC kinase (csk). <b>2013</b> , 9, e1003188	9
1154	Experimental and computational analysis of the transition state for ribonuclease A-catalyzed RNA 2'-O-transphosphorylation. <b>2013</b> , 110, 13002-7	52
1153	Molecular Simulation of CO <sub>2</sub> - and CO <sub>3</sub> -Brine-Mineral Systems. <b>2013</b> , 77, 189-228	31

1152	Long-time mean-square displacements in proteins. <b>2013</b> , 88, 052706		17
1151	Global motions exhibited by proteins in micro- to milliseconds simulations concur with anisotropic network model predictions. <i>Journal of Chemical Physics</i> , <b>2013</b> , 139, 121912	3.9	56
1150	Development of accurate force fields for the simulation of biomineralization. <b>2013</b> , 532, 3-23		9
1149	The water supercooled regime as described by four common water models. <i>Journal of Chemical Physics</i> , <b>2013</b> , 139, 024506	3.9	15
1148	Determining the phase diagram of water from direct coexistence simulations: the phase diagram of the TIP4P/2005 model revisited. <i>Journal of Chemical Physics</i> , <b>2013</b> , 139, 154505	3.9	48
1147	6. Molecular Simulation of CO <sub>2</sub> - and CO <sub>3</sub> -Brine-Mineral Systems. <b>2013</b> , 189-228		
1146	A biophysical study with carbohydrate derivatives explains the molecular basis of monosaccharide selectivity of the <i>Pseudomonas aeruginosa</i> lectin LecB. <b>2014</b> , 9, e112822		24
1145	Encapsulation kinetics and dynamics of carbon monoxide in clathrate hydrate. <b>2014</b> , 5, 4128		49
1144	The molecular charge distribution, the hydration shell, and the unique properties of liquid water. <i>Journal of Chemical Physics</i> , <b>2014</b> , 141, 244504	3.9	11
1143	Simulating ion clustering in potassium thiocyanate aqueous solutions with various ion-water models. <b>2014</b> , 57, 1723-1730		2
1142	Conformation and dynamics of 8-Arg-vasopressin in solution. <b>2014</b> , 20, 2485		10
1141	Hydration free energies calculated using the AMBER ff03 charge model for natural and unnatural amino acids and multiple water models. <b>2014</b> , 71, 745-752		7
1140	Role of electrostatic interactions in binding of peptides and intrinsically disordered proteins to their folded targets. 1. NMR and MD characterization of the complex between the c-Crk N-SH3 domain and the peptide Sos. <b>2014</b> , 53, 6473-95		29
1139	Molecular dispersion energy parameters for alkali and halide ions in aqueous solution. <i>Journal of Chemical Physics</i> , <b>2014</b> , 140, 044504	3.9	32
1138	Local dynamics coupled to hydration water determines DNA-sequence-dependent deformability. <b>2014</b> , 90, 022723		12
1137	Molecular structures and solvation of free monomeric and dimeric ferriheme in aqueous solution: insights from molecular dynamics simulations and extended X-ray absorption fine structure spectroscopy. <b>2014</b> , 53, 10811-24		11
1136	Ab initio calculation of the electronic absorption spectrum of liquid water. <i>Journal of Chemical Physics</i> , <b>2014</b> , 140, 164511	3.9	6
1135	Homogeneous ice nucleation evaluated for several water models. <i>Journal of Chemical Physics</i> , <b>2014</b> , 141, 18C529	3.9	107

1134	Calibration of forcefields for molecular simulation: sequential design of computer experiments for building cost-efficient kriging metamodels. <b>2014</b> , 35, 130-49		19
1133	Diffusive and quantum effects of water properties in different states of matter. <i>Journal of Chemical Physics</i> , <b>2014</b> , 141, 044502	3-9	5
1132	The R-factor gap in macromolecular crystallography: an untapped potential for insights on accurate structures. <b>2014</b> , 281, 4046-60		45
1131	Surface Adsorption in Nonpolarizable Atomic Models. <b>2014</b> , 10, 5616-24		4
1130	Effect of nanostructures on the meniscus shape and disjoining pressure of ultrathin liquid film. <b>2014</b> , 14, 7131-7		31
1129	High strength, molecularly thin nanoparticle membranes. <b>2014</b> , 113, 258301		29
1128	Comparative assessment of the ELBA coarse-grained model for water. <b>2014</b> , 112, 1566-1576		64
1127	Mathematical and computational modeling in biology at multiple scales. <b>2014</b> , 11, 52		7
1126	On the Transferability of Three Water Models Developed by Adaptive Force Matching. <b>2014</b> , 10, 25-43		9
1125	Local order in the unfolded state: conformational biases and nearest neighbor interactions. <b>2014</b> , 4, 725-73		47
1124	Difference in dimer conformation between amyloid- $\beta$ (112) and (113) proteins: Replica exchange molecular dynamics simulations in water. <b>2014</b> , 595-596, 242-249		17
1123	Molecular processes of ion effects on aqueous nanofilm rupture. <b>2014</b> , 193, 139-151		7
1122	Phase equilibria of methane clathrate hydrates from Grand Canonical Monte Carlo simulations. <b>2014</b> , 369, 47-54		35
1121	Bayesian energy landscape tilting: towards concordant models of molecular ensembles. <b>2014</b> , 106, 1381-90		45
1120	Classical electrostatics for biomolecular simulations. <b>2014</b> , 114, 779-814		195
1119	Update to the general amber force field for small solutes with an emphasis on free energies of hydration. <b>2014</b> , 118, 3793-804		32
1118	Self-consistent field convergence for proteins: a comparison of full and localized-molecular-orbital schemes. <b>2014</b> , 20, 2159		12
1117	Quantum mechanical study of solvent effects in a prototype SN2 reaction in solution: Cl- attack on CH3Cl. <i>Journal of Chemical Physics</i> , <b>2014</b> , 140, 054109	3-9	15

1116	The marine cyanobacterial metabolite gallinamide A is a potent and selective inhibitor of human cathepsin L. <b>2014</b> , 77, 92-9		43
1115	Polar nanoregions in water: a study of the dielectric properties of TIP4P/2005, TIP4P/2005f and TTM3F. <i>Journal of Chemical Physics</i> , <b>2014</b> , 140, 124504	3-9	37
1114	Prediction of Small Molecule Hydration Thermodynamics with Grid Cell Theory. <b>2014</b> , 10, 35-48		49
1113	Evaluation of reduced point charge models of proteins through Molecular Dynamics simulations: application to the Vps27 UIM-1-Ubiquitin complex. <b>2014</b> , 47, 44-61		5
1112	The structural organization of N-methyl-2-pyrrolidone + water mixtures: a densitometry, x-ray diffraction, and molecular dynamics study. <i>Journal of Chemical Physics</i> , <b>2014</b> , 140, 124503	3-9	27
1111	Evidence for the role of active site residues in the hairpin ribozyme from molecular simulations along the reaction path. <b>2014</b> , 136, 7789-92		29
1110	Advanced potential energy surfaces for condensed phase simulation. <b>2014</b> , 65, 149-74		50
1109	Practical Aspects of Free-Energy Calculations: A Review. <b>2014</b> , 10, 2632-47		271
1108	Site-directed analysis on protein hydrophobicity. <b>2014</b> , 35, 1364-70		13
1107	Clusters of coarse-grained water molecules. <b>2014</b> , 118, 7338-48		4
1106	Ground state spectroscopy of hydroxyquinolines: evidence for the formation of protonated species in water-rich dioxane-water mixtures. <b>2014</b> , 16, 61-70		7
1105	Taking into Account the Ion-induced Dipole Interaction in the Nonbonded Model of Ions. <b>2014</b> , 10, 289-297		201
1104	Hydration control of the mechanical and dynamical properties of cellulose. <b>2014</b> , 15, 4152-9		36
1103	Dynamic architecture of a protein kinase. <b>2014</b> , 111, E4623-31		142
1102	Density and phase equilibrium for ice and structure I hydrates using the Gibbs-Helmholtz constrained equation of state. <b>2014</b> , 92, 2977-2991		11
1101	Principal component analysis of molecular dynamics: on the use of Cartesian vs. internal coordinates. <i>Journal of Chemical Physics</i> , <b>2014</b> , 141, 014111	3-9	97
1100	Intrinsic Helical and Sheet conformational preferences: a computational case study of alanine. <b>2014</b> , 23, 970-80		15
1099	Hydrogen bonding of water confined in zeolites and their zeolitic imidazolate framework counterparts. <b>2014</b> , 4, 29571		15

1098	Probing molecular interaction in ionic liquids by low frequency spectroscopy: Coulomb energy, hydrogen bonding and dispersion forces. <b>2014</b> , 16, 21903-29	172
1097	Are buckyballs hydrophobic?. <b>2014</b> , 118, 12263-70	17
1096	Balanced Protein-Water Interactions Improve Properties of Disordered Proteins and Non-Specific Protein Association. <b>2014</b> , 10, 5113-5124	409
1095	Effects of surface-active organic matter on carbon dioxide nucleation in atmospheric wet aerosols: a molecular dynamics study. <b>2014</b> , 16, 23723-34	5
1094	Intermolecular network analysis of the liquid and vapor interfaces of pentane and water: microsolvation does not trend with interfacial properties. <b>2014</b> , 16, 12475-87	13
1093	On the application of binary correction factors in lattice distortion calculations for methane clathrate hydrates. <b>2014</b> , 94, 974-990	6
1092	Building Water Models: A Different Approach. <b>2014</b> , 5, 3863-3871	321
1091	COFFDROP: A Coarse-Grained Nonbonded Force Field for Proteins Derived from All-Atom Explicit-Solvent Molecular Dynamics Simulations of Amino Acids. <b>2014</b> , 10, 5178-5194	12
1090	Parametrization of an Orbital-Based Linear-Scaling Quantum Force Field for Noncovalent Interactions. <b>2014</b> , 10, 1086-1098	27
1089	Effect of the Confinement and Presence of Cations on Hydrogen Bonding of Water in LTA-Type Zeolite. <b>2014</b> , 118, 9056-9065	23
1088	Fragment orbital based description of charge transfer in peptides including backbone orbitals. <b>2014</b> , 118, 4261-72	16
1087	Residue-specific force field based on the protein coil library. RSFF1: modification of OPLS-AA/L. <b>2014</b> , 118, 6983-98	73
1086	Charge transfer effects of ions at the liquid water/vapor interface. <i>Journal of Chemical Physics</i> , <b>2014</b> , 140, 184703	3,9 28
1085	ff14ipq: A Self-Consistent Force Field for Condensed-Phase Simulations of Proteins. <b>2014</b> , 10, 4515-4534	67
1084	Tribute to William C. Swope. <b>2014</b> , 118, 6357-9	
1083	Evaluation of Host-Guest Binding Thermodynamics of Model Cavities with Grid Cell Theory. <b>2014</b> , 10, 4055-68	20
1082	Non-polarizable force field of water based on the dielectric constant: TIP4P/ψ <b>2014</b> , 118, 1263-72	74
1081	POVME 2.0: An Enhanced Tool for Determining Pocket Shape and Volume Characteristics. <b>2014</b> , 10, 5047-5056	164

1080	Validating solution ensembles from molecular dynamics simulation by wide-angle X-ray scattering data. <b>2014</b> , 107, 435-447	82
1079	Comparison of reduced point charge models of proteins: Molecular Dynamics simulations of Ubiquitin. <b>2014</b> , 57, 1340-1354	4
1078	Parametrization of 2,2,2-trifluoroethanol based on the generalized AMBER force field provides realistic agreement between experimental and calculated properties of pure liquid as well as water-mixed solutions. <b>2014</b> , 118, 10390-404	15
1077	Evaluating the strength of salt bridges: a comparison of current biomolecular force fields. <b>2014</b> , 118, 6561-9	74
1076	Characterization of the glass transition of water predicted by molecular dynamics simulations using nonpolarizable intermolecular potentials. <b>2014</b> , 118, 1867-80	6
1075	Crystal structure and encapsulation dynamics of ice II-structured neon hydrate. <b>2014</b> , 111, 10456-61	28
1074	Optimizing Protein-Protein van der Waals Interactions for the AMBER ff9x/ff12 Force Field. <b>2014</b> , 10, 273-81	22
1073	Cooperative Contributions of the Intermolecular Charge Fluxes and Intramolecular Polarizations in the Far-Infrared Spectral Intensities of Liquid Water. <b>2014</b> , 10, 1219-27	29
1072	Hydration of porphyrin and Mg-porphyrin: ab initio quantum mechanical charge field molecular dynamics simulations. <b>2014</b> , 10, 117-27	12
1071	Toward a molecular dynamics force field for simulations of 40% trifluoroethanol-water. <b>2014</b> , 118, 1471-80	16
1070	Nanoconfined gases, liquids and liquid crystals in porous materials. <b>2014</b> , 40, 698-712	5
1069	Surface tension, viscosity, and rheology of water-based nanofluids: a microscopic interpretation on the molecular level. <b>2014</b> , 16, 1	52
1068	Bridging Calorimetry and Simulation through Precise Calculations of Cucurbituril-Guest Binding Enthalpies. <b>2014</b> , 10, 4069-4078	65
1067	The SAMPL4 host-guest blind prediction challenge: an overview. <b>2014</b> , 28, 305-17	142
1066	ZIBgridfree: efficient conformational analysis by partition-of-unity coupling. <b>2014</b> , 52, 781-804	4
1065	Structure and dynamics of potassium chloride in aqueous solution. <b>2014</b> , 118, 9404-13	13
1064	How short is too short for the interactions of a water potential? Exploring the parameter space of a coarse-grained water model using uncertainty quantification. <b>2014</b> , 118, 8190-202	51
1063	Coarse-Graining of TIP4P/2005, TIP4P-Ew, SPC/E, and TIP3P to Monatomic Anisotropic Water Models Using Relative Entropy Minimization. <b>2014</b> , 10, 4104-20	86



1062	Calculation of Lipid-Bilayer Permeabilities Using an Average Force. <b>2014</b> , 10, 554-64	50
1061	Pressure-Dependent Properties of Elementary Hydrophobic Interactions: Ramifications for Activation Properties of Protein Folding. <b>2014</b> , 118, 7488-7509	44
1060	Ion counting from explicit-solvent simulations and 3D-RISM. <b>2014</b> , 106, 883-94	77
1059	Force-Field Development from Electronic Structure Calculations with Periodic Boundary Conditions: Applications to Gaseous Adsorption and Transport in Metal-Organic Frameworks. <b>2014</b> , 10, 1477-88	97
1058	Direct Evaluation of Polypeptide Partial Molar Volumes in Water Using Molecular Dynamics Simulations. <b>2014</b> , 59, 3130-3135	8
1057	Ions increase strength of hydrogen bond in water. <b>2014</b> , 610-611, 159-162	12
1056	A fixed-charge model for alcohol polarization in the condensed phase, and its role in small molecule hydration. <b>2014</b> , 118, 6438-46	45
1055	Study of structure and spectroscopy of water-hydroxide ion clusters: A combined simulated annealing and DFT-based approach. <b>2014</b> , 126, 659-675	14
1054	Investigation of conformational mobility of insulin superfamily peptides: Use of SPC/E and TIP4P water models. <b>2014</b> , 48, 432-438	1
1053	Computer simulation study of the structure of LiCl aqueous solutions: test of non-standard mixing rules in the ion interaction. <b>2014</b> , 118, 7680-91	32
1052	Dipeptide Aggregation in Aqueous Solution from Fixed Point-Charge Force Fields. <b>2014</b> , 10, 1631-1637	8
1051	Interaction of charged amino-acid side chains with ions: an optimization strategy for classical force fields. <b>2014</b> , 118, 3960-72	33
1050	Difference in the Conformation and Dynamics of Aspartic Acid on the Flat Regions, Step Edges, and Kinks of a Calcite Surface: A Molecular Dynamics Study. <b>2014</b> , 118, 14335-14345	30
1049	Multiscale Modeling of Water in Mg-MOF-74: From Electronic Structure Calculations to Adsorption Isotherms. <b>2014</b> , 118, 16218-16227	21
1048	Polyelectrolyte decomplexation via addition of salt: charge correlation driven zipper. <b>2014</b> , 118, 3226-34	30
1047	Effects of the hydroxyl group on phenyl based ligand/ERRP protein binding. <b>2014</b> , 27, 1371-9	6
1046	Peptide Conformation Analysis Using an Integrated Bayesian Approach. <b>2014</b> , 10, 4152-4159	16
1045	Publications of William C. Swope. <b>2014</b> , 118, 6365-7	1

1044	Assembly of responsive-shape coated nanoparticles at water surfaces. <b>2014</b> , 6, 5132-7	27
1043	Multiple scale dynamics in proteins probed at multiple time scales through fluctuations of NMR chemical shifts. <b>2014</b> , 118, 3823-31	6
1042	Direct Mixing of Atomistic Solutes and Coarse-Grained Water. <b>2014</b> , 10, 4684-93	39
1041	Molecular dynamics study of the volumetric and hydrophobic properties of the amphiphilic molecule C8E6. <b>2014</b> , 189, 74-80	40
1040	Building Force Fields: An Automatic, Systematic, and Reproducible Approach. <b>2014</b> , 5, 1885-91	294
1039	Correlation as a determinant of configurational entropy in supramolecular and protein systems. <b>2014</b> , 118, 6447-55	33
1038	Diffusive Models of Membrane Permeation with Explicit Orientational Freedom. <b>2014</b> , 10, 2710-8	35
1037	The tunable mechanical property of water-filled carbon nanotubes under an electric field. <b>2014</b> , 47, 125302	4
1036	Water in the Liquid State: A Computational Viewpoint. <b>2014</b> , 161-200	6
1035	The crystal structure of the streptococcal collagen-like protein 2 globular domain from invasive M3-type group A Streptococcus shows significant similarity to immunomodulatory HIV protein gp41. <b>2014</b> , 289, 5122-33	20
1034	Effect of D23N mutation on the dimer conformation of amyloid $\beta$ proteins: ab initio molecular simulations in water. <b>2014</b> , 50, 113-24	6
1033	Structural dynamics and conformational equilibria of SERCA regulatory proteins in membranes by solid-state NMR restrained simulations. <b>2014</b> , 106, 2566-76	18
1032	Investigation of the Ergopeptide Epimerization Process. <b>2014</b> , 2, 102-111	8
1031	Water-air gas exchange of elemental mercury: An experimentally determined mercury diffusion coefficient for Hg <sup>0</sup> water-air flux calculations. <b>2014</b> , 59, 1461-1467	20
1030	Force-Field Representation of Biomolecular Systems. <b>2015</b> , 45-77	2
1029	Water filling and electric field-induced enhancement in the mechanical property of carbon nanotubes. <b>2015</b> , 5, 17537	7
1028	Motional displacements in proteins: The origin of wave-vector-dependent values. <b>2015</b> , 91, 052705	12
1027	Ligand structure and mechanical properties of single-nanoparticle-thick membranes. <b>2015</b> , 91, 062403	17

1026	Contact- and distance-based principal component analysis of protein dynamics. <i>Journal of Chemical Physics</i> , <b>2015</b> , 143, 244114	3.9	46
1025	Charge-dependent many-body exchange and dispersion interactions in combined QM/MM simulations. <i>Journal of Chemical Physics</i> , <b>2015</b> , 143, 234111	3.9	15
1024	The role of intermolecular interactions in the prediction of the phase equilibria of carbon dioxide hydrates. <i>Journal of Chemical Physics</i> , <b>2015</b> , 143, 094506	3.9	41
1023	A theoretical study of the dissociation of the sl methane hydrate induced by an external electric field. <i>Journal of Chemical Physics</i> , <b>2015</b> , 143, 204503	3.9	20
1022	The role of conformational selection in the molecular recognition of the wild type and mutants XPA67-80 peptides by ERCC1. <b>2015</b> , 83, 1341-51		2
1021	Structural fidelity and NMR relaxation analysis in a prototype RNA hairpin. <b>2015</b> , 21, 963-74		24
1020	Assessment of metal-assisted nucleophile activation in the hepatitis delta virus ribozyme from molecular simulation and 3D-RISM. <b>2015</b> , 21, 1566-77		16
1019	References. 359-378		
1018	Peptide-polymer ligands for a tandem WW-domain, an adaptive multivalent protein-protein interaction: lessons on the thermodynamic fitness of flexible ligands. <b>2015</b> , 11, 837-47		9
1017	Chemistry specificity of DNA-polycation complex salt response: a simulation study of DNA, polylysine and polyethyleneimine. <b>2015</b> , 17, 5279-89		32
1016	Mean ionic activity coefficients in aqueous NaCl solutions from molecular dynamics simulations. <i>Journal of Chemical Physics</i> , <b>2015</b> , 142, 044507	3.9	93
1015	Reparametrized E3B (Explicit Three-Body) Water Model Using the TIP4P/2005 Model as a Reference. <b>2015</b> , 11, 2268-77		38
1014	Accurate evaluation of charge asymmetry in aqueous solvation. <b>2015</b> , 119, 6092-100		12
1013	Kirkwood-Buff Approach Rescues Overcollapse of a Disordered Protein in Canonical Protein Force Fields. <b>2015</b> , 119, 7975-84		61
1012	Prediction of the phase equilibria of methane hydrates using the direct phase coexistence methodology. <i>Journal of Chemical Physics</i> , <b>2015</b> , 142, 044501	3.9	81
1011	Temperature effects on nanostructure and mechanical properties of single-nanoparticle thick membranes. <b>2015</b> , 181, 339-54		10
1010	Exploiting Transient Protein States for the Design of Small-Molecule Stabilizers of Mutant p53. <b>2015</b> , 23, 2246-2255		33
1009	Binding enthalpy calculations for a neutral host-guest pair yield widely divergent salt effects across water models. <b>2015</b> , 11, 4555-64		27

1008	On the calculation of x-ray scattering signals from pairwise radial distribution functions. <b>2015</b> , 48, 244010	22
1007	Molecular Dynamics Study on the Equilibrium and Kinetic Properties of Tetrahydrofuran Clathrate Hydrates. <b>2015</b> , 119, 1400-1409	27
1006	All-atom crystal simulations of DNA and RNA duplexes. <b>2015</b> , 1850, 1059-1071	17
1005	Water: one molecule, two surfaces, one mistake. <b>2015</b> , 113, 1145-1163	39
1004	A LAMMPS implementation of volume-temperature replica exchange molecular dynamics. <b>2015</b> , 189, 119-127	3
1003	Role of hydrophilicity and length of diblock arms for determining star polymer physical properties. <b>2015</b> , 119, 944-57	9
1002	Multipolar Ewald methods, 2: applications using a quantum mechanical force field. <b>2015</b> , 11, 451-61	17
1001	Revised Parameters for the AMOEBA Polarizable Atomic Multipole Water Model. <b>2015</b> , 119, 9423-9437	149
1000	Disordered structural ensembles of vasopressin and oxytocin and their mutants. <b>2015</b> , 119, 896-905	28
999	KECSA-Movable Type Implicit Solvation Model (KMTISM). <b>2015</b> , 11, 667-82	16
998	Interpretation of pH-activity profiles for acid-base catalysis from molecular simulations. <b>2015</b> , 54, 1307-13	27
997	Molecular Dynamics Simulations of 441 Two-Residue Peptides in Aqueous Solution: Conformational Preferences and Neighboring Residue Effects with the Amber ff99SB-ildn-NMR Force Field. <b>2015</b> , 11, 1315-29	9
996	Multipolar Ewald methods, 1: theory, accuracy, and performance. <b>2015</b> , 11, 436-50	30
995	Characterization of the three-dimensional free energy manifold for the uracil ribonucleoside from asynchronous replica exchange simulations. <b>2015</b> , 11, 373-7	9
994	Evaluation of water displacement energetics in protein binding sites with grid cell theory. <b>2015</b> , 17, 8416-26	22
993	Understanding the binding of inhibitors of matrix metalloproteinases by molecular docking, quantum mechanical calculations, molecular dynamics simulations, and a MMGBSA/MMBappl study. <b>2015</b> , 11, 1041-51	28
992	A review of methods for the calculation of solution free energies and the modelling of systems in solution. <b>2015</b> , 17, 6174-91	269
991	Conformational changes and allosteric communications in human serum albumin due to ligand binding. <b>2015</b> , 33, 2192-204	9

990	High Affinity Fluorescent Ligands for the Estrogen Receptor. <b>2015</b> , 2015, 2157-2166	13
989	Ion hydration and associated defects in hydrogen bond network of water: observation of reorientationally slow water molecules beyond first hydration shell in aqueous solutions of MgCl <sub>2</sub> . <b>2015</b> , 91, 012114	13
988	Reversible stretching of pre-strained water-filled carbon nanotubes under electric fields. <b>2015</b> , 18, 1201-1207	5
987	The Surface Potential of the Water-Vapor Interface from Classical Simulations. <b>2015</b> , 119, 9114-22	27
986	Comparison of structural, thermodynamic, kinetic and mass transport properties of Mg(2+) ion models commonly used in biomolecular simulations. <b>2015</b> , 36, 970-82	52
985	Remarkable conformational flexibility of aqueous 18-crown-6 and its strontium(II) complex-ab initio molecular dynamics simulations. <b>2015</b> , 17, 16359-66	5
984	Microscopic structure of methanol/water mixtures: Synchrotron X-ray diffraction experiments and molecular dynamics simulations over the entire composition range. <b>2015</b> , 209, 586-595	20
983	Toward Improved Force-Field Accuracy through Sensitivity Analysis of Host-Guest Binding Thermodynamics. <b>2015</b> , 119, 10145-55	25
982	The interplay between dynamic heterogeneities and structure of bulk liquid water: A molecular dynamics simulation study. <i>Journal of Chemical Physics</i> , <b>2015</b> , 142, 244507	3-9 4
981	Surface-active organic matter induces salt morphology transitions during new atmospheric particle formation and growth. <b>2015</b> , 5, 63240-63251	3
980	Assessing the potential of atomistic molecular dynamics simulations to probe reversible protein-protein recognition and binding. <b>2015</b> , 5, 10549	39
979	Bridged bicyclic peptides as potential drug scaffolds: synthesis, structure, protein binding and stability. <b>2015</b> , 6, 5473-5490	26
978	Thermophysical properties of supercritical water and bond flexibility. <b>2015</b> , 92, 012124	15
977	Thermodynamic and Transport Properties of H <sub>2</sub> O + NaCl from Polarizable Force Fields. <b>2015</b> , 11, 3802-10	49
976	Constant pressure Gibbs ensemble Monte Carlo simulations for the prediction of structure I gas hydrate occupancy. <b>2015</b> , 26, 446-452	17
975	Direct Coexistence Methods to Determine the Solubility of Salts in Water from Numerical Simulations. Test Case NaCl. <b>2015</b> , 119, 8389-96	32
974	Molecular Dynamics Simulations of Intrinsically Disordered Proteins: Force Field Evaluation and Comparison with Experiment. <b>2015</b> , 11, 3420-31	174
973	Significant Refinement of Protein Structure Models Using a Residue-Specific Force Field. <b>2015</b> , 11, 1949-56	20

972	Effect of hydrostatic pressure on gas solubilization in micelles. <b>2015</b> , 31, 3318-25		6
971	Water dispersion interactions strongly influence simulated structural properties of disordered protein states. <b>2015</b> , 119, 5113-23		468
970	Hydrophobic Ambivalence: Teetering on the Edge of Randomness. <b>2015</b> , 6, 1696-701		46
969	Hydrophobic hydration and the anomalous partial molar volumes in ethanol-water mixtures. <i>Journal of Chemical Physics</i> , <b>2015</b> , 142, 064501	3.9	25
968	Stacking Free Energies of All DNA and RNA Nucleoside Pairs and Dinucleoside-Monophosphates Computed Using Recently Revised AMBER Parameters and Compared with Experiment. <b>2015</b> , 11, 2315-28		60
967	Parametrization of Backbone Flexibility in a Coarse-Grained Force Field for Proteins (COFFDROP) Derived from All-Atom Explicit-Solvent Molecular Dynamics Simulations of All Possible Two-Residue Peptides. <b>2015</b> , 11, 2341-54		10
966	Signature properties of water: Their molecular electronic origins. <b>2015</b> , 112, 6341-6		38
965	Systematic evaluation of bundled SPC water for biomolecular simulations. <b>2015</b> , 17, 8393-406		19
964	Amyloid $\beta$ Protein and Alzheimer's Disease: When Computer Simulations Complement Experimental Studies. <b>2015</b> , 115, 3518-63		426
963	Composition dependence of thermodynamic, dynamic and dielectric properties of water-methanol model mixtures. Molecular dynamics simulation results with the OPLS-AA model for methanol. <b>2015</b> , 212, 70-78		21
962	Modulating RNA Alignment Using Directional Dynamic Kinks: Application in Determining an Atomic-Resolution Ensemble for a Hairpin using NMR Residual Dipolar Couplings. <b>2015</b> , 137, 12954-65		21
961	Ab initio investigation of the aqueous solvation of the nitrate ion. <b>2015</b> , 17, 27027-34		13
960	Dynamical role of phosphorylation on serine/threonine-proline Pin1 substrates from constant force molecular dynamics simulations. <i>Journal of Chemical Physics</i> , <b>2015</b> , 142, 075102	3.9	9
959	Ion mixing, hydration, and transport in aqueous ionic systems. <i>Journal of Chemical Physics</i> , <b>2015</b> , 142, 184905	3.9	13
958	United polarizable multipole water model for molecular mechanics simulation. <i>Journal of Chemical Physics</i> , <b>2015</b> , 143, 014504	3.9	30
957	Is the Hexacyanoferrate(II) Anion Stable in Aqueous Solution? A Combined Theoretical and Experimental Study. <b>2015</b> , 54, 10335-41		13
956	Open challenges in structure-based virtual screening: Receptor modeling, target flexibility consideration and active site water molecules description. <b>2015</b> , 583, 105-19		78
955	Protein-Ligand Electrostatic Binding Free Energies from Explicit and Implicit Solvation. <b>2015</b> , 11, 4450-9		24

954	Water diffusion in zeolite membranes: Molecular dynamics studies on effects of water loading and thermostat. <b>2015</b> , 495, 322-333	13
953	Improved Force Field Parameters Lead to a Better Description of RNA Structure. <b>2015</b> , 11, 3969-72	81
952	Folding and binding energy of a calmodulin-binding cell antiproliferative peptide. <b>2015</b> , 61, 281-9	
951	Conformation and Dynamics of the Troponin I C-Terminal Domain: Combining Single-Molecule and Computational Approaches for a Disordered Protein Region. <b>2015</b> , 137, 11962-9	40
950	SAFT-Force field for the simulation of molecular fluids: 4. A single-site coarse-grained model of water applicable over a wide temperature range. <b>2015</b> , 113, 1228-1249	63
949	Hydrophobicity: effect of density and order on water's rotational slowing down. <b>2015</b> , 11, 7977-85	12
948	Investigation of graphene oxide nanosheets dispersion in water based on solubility parameters: a molecular dynamics simulation study. <b>2015</b> , 5, 106421-106430	26
947	Cosolvent Effects on Solute-Solvent Hydrogen-Bond Dynamics: Ultrafast 2D IR Investigations. <b>2015</b> , 119, 15334-43	25
946	Toward Automated Benchmarking of Atomistic Force Fields: Neat Liquid Densities and Static Dielectric Constants from the ThermoML Data Archive. <b>2015</b> , 119, 12912-20	24
945	Force Field for Mg(2+), Mn(2+), Zn(2+), and Cd(2+) Ions That Have Balanced Interactions with Nucleic Acids. <b>2015</b> , 119, 15460-70	66
944	Large-Scale Analysis of 48 DNA and 48 RNA Tetranucleotides Studied by 1 $\mu$ s Explicit-Solvent Molecular Dynamics Simulations. <b>2015</b> , 11, 5906-17	16
943	Biocatalytic route to chiral acyloins: P450-catalyzed regio- and enantioselective hydroxylation of ketones. <b>2015</b> , 80, 950-6	27
942	Systematic procedure to parametrize force fields for molecular fluids. <b>2015</b> , 11, 683-93	37
941	Coulomb repulsion in short polypeptides. <b>2015</b> , 119, 33-43	15
940	Toward structure prediction of cyclic peptides. <b>2015</b> , 17, 4210-9	39
939	Stacking disorder in ice I. <b>2015</b> , 17, 60-76	169
938	Improved SPC force field of water based on the dielectric constant: SPC/. <b>2015</b> , 420, 116-123	28
937	Molecular Modeling of Proteins. <b>2015</b> ,	6

936	Automatic GROMACS topology generation and comparisons of force fields for solvation free energy calculations. <b>2015</b> , 119, 810-23		65
935	Parameterization of highly charged metal ions using the 12-6-4 LJ-type nonbonded model in explicit water. <b>2015</b> , 119, 883-95		150
934	Binding Mechanisms of Intrinsically Disordered Proteins: Theory, Simulation, and Experiment. <b>2016</b> , 3, 52		80
933	The Mutational Landscape of the Oncogenic MZF1 SCAN Domain in Cancer. <b>2016</b> , 3, 78		24
932	Free energies of solvation in the context of protein folding: Implications for implicit and explicit solvent models. <b>2016</b> , 37, 629-40		17
931	Molecular Dynamics Simulation Study of Parallel Telomeric DNA Quadruplexes at Different Ionic Strengths: Evaluation of Water and Ion Models. <b>2016</b> , 120, 7380-91		26
930	A polarizable, charge transfer model of water using the drude oscillator. <b>2016</b> , 37, 2060-6		13
929	Minimal Basis Iterative Stockholder: Atoms in Molecules for Force-Field Development. <b>2016</b> , 12, 3894-912		81
928	Effect of simple solutes on the long range dipolar correlations in liquid water. <i>Journal of Chemical Physics</i> , <b>2016</b> , 144, 104502	3.9	6
927	Anisotropy in geometrically rough structure of ice prismatic plane interface during growth: Development of a modified six-site model of HO and a molecular dynamics simulation. <i>Journal of Chemical Physics</i> , <b>2016</b> , 145, 244706	3.9	8
926	A single-site multipole model for liquid water. <i>Journal of Chemical Physics</i> , <b>2016</b> , 145, 034501	3.9	12
925	A comprehensive scenario of the thermodynamic anomalies of water using the TIP4P/2005 model. <i>Journal of Chemical Physics</i> , <b>2016</b> , 145, 054505	3.9	39
924	Simulated conduction rates of water through a (6,6) carbon nanotube strongly depend on bulk properties of the model employed. <i>Journal of Chemical Physics</i> , <b>2016</b> , 144, 184502	3.9	36
923	Intrinsic instability of thin liquid films on nanostructured surfaces. <b>2016</b> , 109, 111601		3
922	Comparing generalized ensemble methods for sampling of systems with many degrees of freedom. <i>Journal of Chemical Physics</i> , <b>2016</b> , 145, 174107	3.9	10
921	High-Resolution Mapping of a Repeat Protein Folding Free Energy Landscape. <b>2016</b> , 111, 2368-2376		29
920	Structural Ensembles of Membrane-bound $\beta$ -Synuclein Reveal the Molecular Determinants of Synaptic Vesicle Affinity. <b>2016</b> , 6, 27125		62
919	Relationship between the line of density anomaly and the lines of melting, crystallization, cavitation, and liquid spinodal in coarse-grained water models. <i>Journal of Chemical Physics</i> , <b>2016</b> , 144, 234507	3.9	28



918	On the accuracy of the MB-pol many-body potential for water: Interaction energies, vibrational frequencies, and classical thermodynamic and dynamical properties from clusters to liquid water and ice. <i>Journal of Chemical Physics</i> , <b>2016</b> , 145, 194504	3.9	146
917	Understanding the large solubility of lidocaine in 1-n-butyl-3-methylimidazolium based ionic liquids using molecular simulation. <i>Journal of Chemical Physics</i> , <b>2016</b> , 144, 084501	3.9	11
916	Accuracy limit of rigid 3-point water models. <i>Journal of Chemical Physics</i> , <b>2016</b> , 145, 074501	3.9	106
915	Consensus on the solubility of NaCl in water from computer simulations using the chemical potential route. <i>Journal of Chemical Physics</i> , <b>2016</b> , 144, 124504	3.9	79
914	Insights into How Cyclic Peptides Switch Conformations. <b>2016</b> , 12, 2480-8		34
913	Molecular dynamics simulation of triclinic lysozyme in a crystal lattice. <b>2016</b> , 25, 87-102		29
912	Ambient-Potential Composite Ewald Method for ab Initio Quantum Mechanical/Molecular Mechanical Molecular Dynamics Simulation. <b>2016</b> , 12, 2611-32		26
911	Force Field Development from Periodic Density Functional Theory Calculations for Gas Separation Applications Using Metal-Organic Frameworks. <b>2016</b> , 120, 12590-12604		71
910	Modeling Molecular Interactions in Water: From Pairwise to Many-Body Potential Energy Functions. <b>2016</b> , 116, 7501-28		234
909	Correlation between Surface Tension and the Bulk Dynamics in Salty Atmospheric Aquatic Droplets. <b>2016</b> , 120, 11508-11518		4
908	Slide-and-exchange mechanism for rapid and selective transport through the nuclear pore complex. <b>2016</b> , 113, E2489-97		63
907	Recent progress in molecular simulation of aqueous electrolytes: force fields, chemical potentials and solubility. <b>2016</b> , 114, 1665-1690		81
906	Predicting Octanol/Water Partition Coefficients of Alcohol Ethoxylate Surfactants Using a Combination of Molecular Dynamics and the Conductor-like Screening Model for Realistic Solvents. <b>2016</b> , 55, 4782-4789		8
905	Knowledge-Based Methods To Train and Optimize Virtual Screening Ensembles. <b>2016</b> , 56, 830-42		16
904	Zinc- and copper-porphyrins in aqueous solution - two similar complexes with strongly contrasting hydration. <b>2016</b> , 12, 2288-2295		4
903	Multiscale Modeling of Thin Liquid Films. <b>2016</b> , 507-536		2
902	Fast and slow dynamics and the local structure of liquid and supercooled water next to a hydrophobic amino acid. <b>2016</b> , 18, 27639-27647		10
901	Ultrafast anisotropic protein quake propagation after CO photodissociation in myoglobin. <b>2016</b> , 113, 10565-70		35

900	Role of donor-acceptor macrocycles in sequence specific peptide recognition and their optoelectronic properties: a detailed computational insight. <b>2016</b> , 18, 20682-90	3
899	Free-standing graphene slit membrane for enhanced desalination. <b>2016</b> , 110, 350-355	33
898	Enhancing Virtual Screening Performance of Protein Kinases with Molecular Dynamics Simulations. <b>2016</b> , 56, 1923-1935	14
897	Molecular Dynamics Simulations of Hydration Effects on Solvation, Diffusivity, and Permeability in Chitosan/Chitin Films. <b>2016</b> , 120, 8997-9010	22
896	Multiscale Materials Modeling for Nanomechanics. <b>2016</b> ,	11
895	Predicting the Chemical Potential and Osmotic Pressure of Polysaccharide Solutions by Molecular Simulations. <b>2016</b> , 12, 4375-84	33
894	Status of the Gaussian Electrostatic Model, a Density-Based Polarizable Force Field. <b>2016</b> , 287-318	1
893	Unexpected inhibition of CO <sub>2</sub> gas hydrate formation in dilute TBAB solutions and the critical role of interfacial water structure. <b>2016</b> , 185, 517-523	36
892	Monte Carlo Simulation of Adsorption of Polar and Nonpolar Gases in (FP)YEu Metal-Organic Framework. <b>2016</b> , 61, 4209-4214	6
891	A MoS <sub>2</sub> -Based Capacitive Displacement Sensor for DNA Sequencing. <b>2016</b> , 10, 9009-16	35
890	Succession of Alkane Conformational Motifs Bound within Hydrophobic Supramolecular Capsular Assemblies. <b>2016</b> , 120, 10394-10402	18
889	Femtosecond X-Ray Scattering Study of Ultrafast Photoinduced Structural Dynamics in Solvated [Co(terpy) <sub>2</sub> ] <sup>2+</sup> . <b>2016</b> , 117, 013002	65
888	Biological evaluation and molecular docking studies of AA3052, a compound containing a selective opioid peptide agonist DALDA and d-Phe-Phe-d-Phe-Leu-Leu-NH <sub>2</sub> , a substance P analogue. <b>2016</b> , 93, 11-20	6
887	Further along the Road Less Traveled: AMBER ff15ipq, an Original Protein Force Field Built on a Self-Consistent Physical Model. <b>2016</b> , 12, 3926-47	108
886	Assessment of Hydration Thermodynamics at Protein Interfaces with Grid Cell Theory. <b>2016</b> , 120, 10442-10452	10
885	Are AMBER Force Fields and Implicit Solvation Models Additive? A Folding Study with a Balanced Peptide Test Set. <b>2016</b> , 12, 5631-5642	14
884	Side-chain dynamics analysis of KE07 series. <b>2016</b> , 65, 148-153	1
883	Structure-based Inhibitor Design for the Intrinsically Disordered Protein c-Myc. <b>2016</b> , 6, 22298	61

882	Comparison of hydration behavior and conformational preferences of the Trp-cage mini-protein in different rigid-body water models. <b>2016</b> , 18, 32796-32813	14
881	Adsorption and desorption behavior of ionic and nonionic surfactants on polymer surfaces. <b>2016</b> , 12, 9692-9704	24
880	Implicit Solvent Model for Million-Atom Atomistic Simulations: Insights into the Organization of 30-nm Chromatin Fiber. <b>2016</b> , 12, 5946-5959	20
879	Mechanism of Nucleation and Growth of A $\beta$ 0 Fibrils from All-Atom and Coarse-Grained Simulations. <b>2016</b> , 120, 12088-12097	16
878	Optimized atomistic force fields for aqueous solutions of Magnesium and Calcium Chloride: Analysis, achievements and limitations. <b>2016</b> , 225, 1391-1409	7
877	Sensitivity of Protein Glass Transition to the Choice of Water Model. <b>2016</b> , 12, 5643-5655	12
876	Refining Disordered Peptide Ensembles with Computational Amide I Spectroscopy: Application to Elastin-Like Peptides. <b>2016</b> , 120, 11395-11404	18
875	Ice VII from aqueous salt solutions: From a glass to a crystal with broken H-bonds. <b>2016</b> , 6, 32040	23
874	Structural and physical properties of condensed H <sub>2</sub> O systems up to 2 GPa: A brief review. <b>2016</b> , 71, 36-42	
873	Osmotic Pressure Simulations of Amino Acids and Peptides Highlight Potential Routes to Protein Force Field Parameterization. <b>2016</b> , 120, 8217-29	19
872	A Weeks-Chandler-Andersen based potential fitting procedure for molecular dynamics simulations of the calcite-water interface. <b>2016</b> , 418, 62-73	
871	Assessing the Current State of Amber Force Field Modifications for DNA. <b>2016</b> , 12, 4114-27	203
870	Release of Entropic Spring Reveals Conformational Coupling Mechanism in the ABC Transporter BtuCD-F. <b>2016</b> , 110, 2407-2418	8
869	Controllable deformation of salt water-filled carbon nanotubes using an electric field with application to molecular sieving. <b>2016</b> , 27, 315702	10
868	Multilayer Nanoporous Graphene Membranes for Water Desalination. <b>2016</b> , 16, 1027-33	242
867	Characterization of A $\beta$ Monomers through the Convergence of Ensemble Properties among Simulations with Multiple Force Fields. <b>2016</b> , 120, 259-77	66
866	Spatial Decomposition of Translational Water-Water Correlation Entropy in Binding Pockets. <b>2016</b> , 12, 414-29	29
865	Understanding the Thermodynamics of Hydrogen Bonding in Alcohol-Containing Mixtures: Cross-Association. <b>2016</b> , 120, 3388-402	34

864	Stress testing the ELBA water model. <b>2016</b> , 42, 337-346	18
863	Ribozyme Catalysis with a Twist: Active State of the Twister Ribozyme in Solution Predicted from Molecular Simulation. <b>2016</b> , 138, 3058-65	46
862	Impact of Surface Water Layers on Protein--Ligand Binding: How Well Are Experimental Data Reproduced by Molecular Dynamics Simulations in a Thermolysin Test Case?. <b>2016</b> , 56, 223-33	23
861	Understanding the Solubility of Acetaminophen in 1-n-Alkyl-3-methylimidazolium-Based Ionic Liquids Using Molecular Simulation. <b>2016</b> , 120, 3360-9	12
860	Cellulose Nanofibrils and Mechanism of their Mineralization in Biomimetic Synthesis of Hydroxyapatite/Native Bacterial Cellulose Nanocomposites: Molecular Dynamics Simulations. <b>2016</b> , 32, 125-34	19
859	Challenges in modelling nanoparticles for drug delivery. <b>2016</b> , 28, 023002	13
858	Nucleobase-functionalized graphene nanoribbons for accurate high-speed DNA sequencing. <b>2016</b> , 8, 1861-7	43
857	Adsorbed water on iron surface by molecular dynamics. <b>2016</b> , 362, 70-78	9
856	Molecular Multipole Potential Energy Functions for Water. <b>2016</b> , 120, 1833-42	9
855	On the linear approximation of mixture internal energies of departure. <b>2016</b> , 85, 72-75	4
854	Local Dissipation in Nanofluid Dynamic Wetting: Effects of Structural Disjoining Pressure. <b>2016</b> , 41-58	
853	Bulk Dissipation in Nanofluid Dynamic Wetting: Wettability-Related Parameters. <b>2016</b> , 59-76	
852	Dynamic Wetting by Nanofluids. <b>2016</b> ,	2
851	Torsional failure of water-filled carbon nanotubes. <b>2016</b> , 25, 87-97	3
850	Reduced point charge models of proteins: assessment based on molecular dynamics simulations. <b>2016</b> , 42, 289-304	3
849	Mapping intermolecular interactions and active site conformations: from human MMP-1 crystal structure to molecular dynamics free energy calculations. <b>2017</b> , 35, 564-573	11
848	Interfacial Gas Enrichment at Hydrophobic Surfaces and the Origin of Promotion of Gas Hydrate Formation by Hydrophobic Solid Particles. <b>2017</b> , 121, 3830-3840	62
847	Toward accurately modeling N-methylated cyclic peptides. <b>2017</b> , 19, 5377-5388	16

846	Elucidation of Single Hydrogen Bonds in GTPases via Experimental and Theoretical Infrared Spectroscopy. <b>2017</b> , 112, 66-77		8
845	Extreme biophysics: Enzymes under pressure. <b>2017</b> , 38, 1174-1182		21
844	Epigallocatechin-3-gallate preferentially induces aggregation of amyloidogenic immunoglobulin light chains. <b>2017</b> , 7, 41515		20
843	Computer Simulations of Intrinsically Disordered Proteins. <b>2017</b> , 68, 117-134		51
842	A molecular dynamics investigation of the influence of water structure on ion conduction through a carbon nanotube. <i>Journal of Chemical Physics</i> , <b>2017</b> , 146, 074502	3.9	22
841	SEEK: Simulation Enabled Estimation of Kinetic Rates, A Computational Tool to Estimate Molecular Kinetics and Its Application to Trypsin-Benzamidine Binding. <b>2017</b> , 121, 3597-3606		49
840	A corresponding-states analysis of the liquid-vapor equilibrium properties of common water models. <i>Journal of Chemical Physics</i> , <b>2017</b> , 146, 064505	3.9	8
839	Size and shape effects on the thermodynamic properties of nanoscale volumes of water. <b>2017</b> , 19, 9016-9027		19
838	Estimating the solubility of 1:1 electrolyte aqueous solutions: the chemical potential difference rule. <b>2017</b> , 115, 1301-1308		14
837	The inhibition of methane hydrate formation by water alignment underneath surface adsorption of surfactants. <b>2017</b> , 197, 488-496		23
836	molecular dynamics simulations of liquid water using high quality meta-GGA functionals. <b>2017</b> , 8, 3554-3565		60
835	Coarse-Grained Simulation of Rodlike Higher-Order Quadruplex Structures at Different Salt Concentrations. <b>2017</b> , 2, 386-396		7
834	A nontoxic pain killer designed by modeling of pathological receptor conformations. <b>2017</b> , 355, 966-969		133
833	Beyond histograms: efficiently estimating radial distribution functions via spectral Monte Carlo. <i>Journal of Chemical Physics</i> , <b>2017</b> , 146,	3.9	3
832	Spectroscopic (FT-IR, FT-Raman, UV, NMR, NLO) investigation, molecular docking and molecular simulation dynamics on 1-Methyl-3-Phenylpiperazine. <b>2017</b> , 1143, 328-343		3
831	Developing and Validating a Set of All-Atom Potential Models for Sodium Dodecyl Sulfate. <b>2017</b> , 13, 2742-2750		16
830	Swelling and Tensile Properties of Tetra-Polyethylene glycol via Coarse-Grained Molecular Models. <b>2017</b> , 26, 1600098		3
829	V67L Mutation Fills an Internal Cavity To Stabilize RecA Mtu Intein. <b>2017</b> , 56, 2715-2722		8

828	Revisiting Hydrogen Bond Thermodynamics in Molecular Simulations. <b>2017</b> , 13, 2851-2857	16
827	The IDP-Specific Force Field ff14IDPSFF Improves the Conformer Sampling of Intrinsically Disordered Proteins. <b>2017</b> , 57, 1166-1178	108
826	Approaches for calculating solvation free energies and enthalpies demonstrated with an update of the FreeSolv database. <b>2017</b> , 62, 1559-1569	114
825	Reparameterization of Solute-Solute Interactions for Amino Acid-Sugar Systems Using Isopiestic Osmotic Pressure Molecular Dynamics Simulations. <b>2017</b> , 13, 1874-1882	18
824	Conformation Dynamics of the Intrinsically Disordered Protein c-Myb with the Force Field. <b>2017</b> , 7, 29713-29721	12
823	Hidden electrostatic basis of dynamic allostery in a PDZ domain. <b>2017</b> , 114, E5825-E5834	58
822	Divalent Metal Ion Activation of a Guanine General Base in the Hammerhead Ribozyme: Insights from Molecular Simulations. <b>2017</b> , 56, 2985-2994	35
821	Nanoscale Fluid Mechanics Working Principles of Transverse Flow Carbon Nanotube Membrane for Enhanced Desalination. <b>2017</b> , 09, 1750034	12
820	Free-Energy Calculations of Ionic Hydration Consistent with the Experimental Hydration Free Energy of the Proton. <b>2017</b> , 8, 2705-2712	30
819	The transient manifold structure of the p53 extreme C-terminal domain: insight into disorder, recognition, and binding promiscuity by molecular dynamics simulations. <b>2017</b> , 19, 21287-21296	11
818	Engineering the expression of an anti-interleukin-13 antibody through rational design and mutagenesis. <b>2017</b> , 30, 303-311	6
817	Dispersion Interactions in Water Clusters. <b>2017</b> , 121, 3736-3745	8
816	Effect of Hydrophobic Core Topology and Composition on the Structure and Kinetics of Star Polymers: A Molecular Dynamics Study. <b>2017</b> , 121, 2902-2918	5
815	Direct Comparison of Amino Acid and Salt Interactions with Double-Stranded and Single-Stranded DNA from Explicit-Solvent Molecular Dynamics Simulations. <b>2017</b> , 13, 1794-1811	15
814	Matrix Metalloproteases. <b>2017</b> ,	
813	Reparameterization of Protein Force Field Nonbonded Interactions Guided by Osmotic Coefficient Measurements from Molecular Dynamics Simulations. <b>2017</b> , 13, 1812-1826	31
812	Building a More Predictive Protein Force Field: A Systematic and Reproducible Route to AMBER-FB15. <b>2017</b> , 121, 4023-4039	147
811	Computational Approaches to Matrix Metalloprotease Drug Design. <b>2017</b> , 1579, 273-285	2

810	The Abundance of Atmospheric CO <sub>2</sub> in Ocean Exoplanets: a Novel CO <sub>2</sub> Deposition Mechanism. <b>2017</b> , 838, 24	19
809	Predicting hydrophobic solvation by molecular simulation: 1. Testing united-atom alkane models. <b>2017</b> , 38, 346-358	8
808	Predicting RNA Structures via a Simple van der Waals Correction to an All-Atom Force Field. <b>2017</b> , 13, 395-399	29
807	On the Role of Nonspherical Cavities in Short Length-Scale Density Fluctuations in Water. <b>2017</b> , 121, 370-380	18
806	Metal Ion Modeling Using Classical Mechanics. <b>2017</b> , 117, 1564-1686	189
805	Molecular Dynamics Simulation of Tau Peptides for the Investigation of Conformational Changes Induced by Specific Phosphorylation Patterns. <b>2017</b> , 1523, 33-59	4
804	Water Structure and Transport in Zeolites with Pores in One or Three Dimensions from Molecular Dynamics Simulations. <b>2017</b> , 121, 381-391	9
803	Benchmark Free Energies and Entropies for Saturated and Compressed Water. <b>2017</b> , 62, 4032-4040	6
802	Grid-Based Projector Augmented Wave (GPAW) Implementation of Quantum Mechanics/Molecular Mechanics (QM/MM) Electrostatic Embedding and Application to a Solvated Diplatinum Complex. <b>2017</b> , 13, 6010-6022	24
801	Multiscale Modeling of the Three-Dimensional Meniscus Shape of a Wetting Liquid Film on Micro-/Nanostructured Surfaces. <b>2017</b> , 33, 12028-12037	7
800	Observations on AMBER Force Field Performance under the Conditions of Low pH and High Salt Concentrations. <b>2017</b> , 121, 9838-9847	4
799	Effect of solvation on the ionization of guanine nucleotide: A hybrid QM/EFP study. <b>2017</b> , 38, 2528-2537	8
798	Reduced Point Charge Models of Proteins: Effect of Protein-Water Interactions in Molecular Dynamics Simulations of Ubiquitin Systems. <b>2017</b> , 121, 9771-9784	4
797	Size-Matching Ligand Insertion in MOF-74 for Enhanced CO <sub>2</sub> Capture under Humid Conditions. <b>2017</b> , 121, 24444-24451	24
796	A review on simulation of methane production from gas hydrate reservoirs: Molecular dynamics prospective. <b>2017</b> , 159, 754-772	48
795	How Water's Properties Are Encoded in Its Molecular Structure and Energies. <b>2017</b> , 117, 12385-12414	182
794	The Multiple Origins of the Hydrophobicity of Fluorinated Apolar Amino Acids. <b>2017</b> , 3, 881-897	21
793	Quantum mechanical force fields for condensed phase molecular simulations. <b>2017</b> , 29, 383002	18

792	Thermal characterization assessment of rigid and flexible water models in a nanogap using molecular dynamics. <b>2017</b> , 687, 270-275		2
791	Thermodynamic properties of the 1-butyl-3-methylimidazolium mesilate ionic liquid [C4mim][OMs] in condensed phase, using molecular simulations. <b>2017</b> , 244, 422-432		6
790	High-Throughput Computational Screening of MetalOrganic Frameworks for Thiol Capture. <b>2017</b> , 121, 22208-22215		25
789	Liquid part of the phase diagram and percolation line for two-dimensional Mercedes-Benz water. <b>2017</b> , 96, 032122		6
788	Effect of a Paramagnetic Spin Label on the Intrinsically Disordered Peptide Ensemble of Amyloid- $\beta$ . <b>2017</b> , 113, 1002-1011		13
787	Comparison of simulation and experimental results for a model aqueous tert-butanol solution. <i>Journal of Chemical Physics</i> , <b>2017</b> , 147, 024503	3.9	11
786	Decreasing temperature enhances the formation of sixfold hydrogen bonded rings in water-rich water-methanol mixtures. <b>2017</b> , 7, 1073		18
785	A Multidimensional B-Spline Correction for Accurate Modeling Sugar Puckering in QM/MM Simulations. <b>2017</b> , 13, 3975-3984		9
784	A comparison of classical interatomic potentials applied to highly concentrated aqueous lithium chloride solutions. <b>2017</b> , 242, 845-858		19
783	An interaction energy driven biased sampling technique: A faster route to ionization spectra in condensed phase. <b>2017</b> , 38, 2248-2257		9
782	Signatures of Solvation Thermodynamics in Spectra of Intermolecular Vibrations. <b>2017</b> , 13, 4467-4481		31
781	Calculation of the Nucleation Barrier and Interfacial Free Energy of New-Phase nuclei by the thermodynamic integration method using molecular dynamics simulation data. <b>2017</b> , 11, 473-480		4
780	Perspective: Surface freezing in water: A nexus of experiments and simulations. <i>Journal of Chemical Physics</i> , <b>2017</b> , 147, 060901	3.9	19
779	Accurate Modeling of Water Clusters with Density-Functional Theory Using Atom-Centered Potentials. <b>2017</b> , 13, 4205-4215		7
778	Structure-Based Insights into the Dynamics and Function of Two-Domain SlpA from Escherichia coli. <b>2017</b> , 56, 6533-6543		2
777	Spatial Distribution of Hydrophobic Drugs in Model Nanogel-Core Star Polymers. <b>2017</b> , 50, 9702-9712		5
776	On phonons and water flow enhancement in carbon nanotubes. <b>2017</b> , 12, 1106-1108		14
775	Homology Modeling and Molecular Dynamics Simulation Combined with X-ray Solution Scattering Defining Protein Structures of Thromboxane and Prostacyclin Synthases. <b>2017</b> , 121, 11229-11240		6



774	Ionic Solution: What Goes Right and Wrong with Continuum Solvation Modeling. <b>2017</b> , 121, 11169-11179	9
773	Building better water models using the shape of the charge distribution of a water molecule. <i>Journal of Chemical Physics</i> , <b>2017</b> , 147, 194103	3-9 3
772	Evaluating Force-Field London Dispersion Coefficients Using the Exchange-Hole Dipole Moment Model. <b>2017</b> , 13, 6146-6157	29
771	Influences of lone-pair electrons on directionality of hydrogen bonds formed by hydrophilic amino acid side chains in molecular dynamics simulation. <b>2017</b> , 7, 15859	13
770	Comparison of RESP and IPolQ-Mod Partial Charges for Solvation Free Energy Calculations of Various Solute/Solvent Pairs. <b>2017</b> , 13, 6266-6274	12
769	Shedding light on the different behavior of ionic and nonionic surfactants in emulsion polymerization: from atomistic simulations to experimental observations. <b>2017</b> , 19, 31692-31705	5
768	Guest Controlled Nonmonotonic Deep Cavity Cavitand Assembly State Switching. <b>2017</b> , 121, 10717-10725	10
767	Hydration of iron-porphyrins: ab initio quantum mechanical charge field molecular dynamics simulation study. <b>2017</b> , 19, 30822-30833	1
766	Evaluating Force Field Performance in Thermodynamic Calculations of Cyclodextrin Host-Guest Binding: Water Models, Partial Charges, and Host Force Field Parameters. <b>2017</b> , 13, 4253-4269	33
765	Dual Action of Hydrotropes at the Water/Oil Interface. <b>2017</b> , 121, 16423-16431	17
764	Significantly Improved Protein Folding Thermodynamics Using a Dispersion-Corrected Water Model and a New Residue-Specific Force Field. <b>2017</b> , 8, 3199-3205	28
763	Crowding in Cellular Environments at an Atomistic Level from Computer Simulations. <b>2017</b> , 121, 8009-8025	89
762	Effect of solvent model when probing protein dynamics with molecular dynamics. <b>2017</b> , 71, 80-87	2
761	Multipole moments of water molecules and the aqueous solvation of monovalent ions. <b>2017</b> , 228, 54-62	9
760	On the hydrogen-bond network and the non-Arrhenius transport properties of water. <b>2017</b> , 29, 015101	25
759	Binding free energies in the SAMPL5 octa-acid host-guest challenge calculated with DFT-D3 and CCSD(T). <b>2017</b> , 31, 87-106	18
758	Understanding decoupling mechanisms of liquid-mixture transport properties through regression analysis with structural perturbation. <b>2017</b> , 105, 12-17	1
757	Fully renewable polyesters via polycondensation catalyzed by <i>Thermobifida cellulolytica</i> cutinase 1: an integrated approach. <b>2017</b> , 19, 490-502	25

756	Comparison of force fields for Alzheimer's A $\beta$ 2: A case study for intrinsically disordered proteins. <b>2017</b> , 26, 174-185		92
755	Fully compositional multi-scale reservoir simulation of various CO2 sequestration mechanisms. <b>2017</b> , 96, 183-195		12
754	Advances in RNA molecular dynamics: a simulator's guide to RNA force fields. <b>2017</b> , 8, e1396		31
753	Structure and dynamics of the multi-domain resuscitation promoting factor RpfB from <i>Mycobacterium tuberculosis</i> . <b>2017</b> , 35, 1322-1330		14
752	Molecular simulations of polyamide membrane materials used in desalination and water reuse applications: Recent developments and future prospects. <b>2017</b> , 524, 436-448		72
751	Synthesis and evaluation of C9 alkoxy analogues of (-)-stepholidine as dopamine receptor ligands. <b>2017</b> , 125, 255-268		7
750	High precision determination of the melting points of water TIP4P/2005 and water TIP4P/Ice models by the direct coexistence technique. <i>Journal of Chemical Physics</i> , <b>2017</b> , 147, 244506	3-9	39
749	Structural Insight into Interaction between C20 Phenylalanyl Derivative of Tylosin and Ribosomal Tunnel. <b>2017</b> , 82, 925-932		5
748	Seeing real-space dynamics of liquid water through inelastic x-ray scattering. <b>2017</b> , 3, e1603079		41
747	Fullerene-water nanofluid confined in graphene nanochannel. <b>2017</b> , 7, 125208		
746	Insilico direct folding of thrombin-binding aptamer G-quadruplex at all-atom level. <b>2017</b> , 45, 12648-12656		29
745	Comparison of the Melting Temperatures of Classical and Quantum Water Potential Models. <b>2017</b> , 5,		3
744	3.14 Molecular Simulation Methods to Investigate Protein Adsorption Behavior at the Atomic Level. <b>2017</b> , 268-294		1
743	A structural explanation for the low effectiveness of the seasonal influenza H3N2 vaccine. <b>2017</b> , 13, e1006682	143	
742	A Non-Polarizable Three-Site Water Model Reproduces the Density Anomaly of the Liquid. <b>2018</b> , 3, 2017-2020	1	
741	Role of Structural Defects in the Water Adsorption Properties of MOF-801. <b>2018</b> , 122, 5545-5552		37
740	Structural principles that enable oligomeric small heat-shock protein paralogs to evolve distinct functions. <b>2018</b> , 359, 930-935		29
739	Surface chemical heterogeneity modulates silica surface hydration. <b>2018</b> , 115, 2890-2895		57

738	An efficient method for computing excess free energy of liquid. <b>2018</b> , 61, 135-140		13
737	The influence of polarizability and charge transfer on specific ion effects in the dynamics of aqueous salt solutions. <i>Journal of Chemical Physics</i> , <b>2018</b> , 148, 222803	3.9	20
736	Specific Cation Effects on SCN in Bulk Solution and at the Air-Water Interface. <b>2018</b> , 122, 5094-5105		16
735	Effects of CNT size on the desalination performance of an outer-wall CNT slit membrane. <b>2018</b> , 20, 13896-13902		12
734	Diffusion of aqueous solutions of ionic, zwitterionic, and polar solutes. <i>Journal of Chemical Physics</i> , <b>2018</b> , 148, 222827	3.9	6
733	Comparing Classical Water Models Using Molecular Dynamics To Find Bulk Properties. <b>2018</b> , 95, 888-894		12
732	A Four-Site Molecular Model for Simulations of Liquid Methanol and Water-Methanol Mixtures: MeOH-4P. <b>2018</b> , 14, 2526-2537		9
731	Comparison of permutationally invariant polynomials, neural networks, and Gaussian approximation potentials in representing water interactions through many-body expansions. <i>Journal of Chemical Physics</i> , <b>2018</b> , 148, 241725	3.9	104
730	Biomolecular Simulations under Realistic Macroscopic Salt Conditions. <b>2018</b> , 122, 5466-5486		28
729	DNP-Enhanced MAS NMR: A Tool to Snapshot Conformational Ensembles of $\beta$ -Synuclein in Different States. <b>2018</b> , 114, 1614-1623		25
728	Force Field Benchmark of Amino Acids: I. Hydration and Diffusion in Different Water Models. <b>2018</b> , 58, 1037-1052		56
727	Interaction of Na, K, Mg and Ca counter cations with RNA. <b>2018</b> , 10, 659-678		23
726	Effect of the Dielectric Constant on the Solubility of Acetone in Water. <b>2018</b> , 63, 1170-1179		7
725	Examination of ethanol interactions with Trp-cage peptide through MD simulations and intermolecular nuclear Overhauser effects. <b>2018</b> , 31, e3809		
724	Learning about Biomolecular Solvation from Water in Protein Crystals. <b>2018</b> , 122, 2475-2486		10
723	Pressure control in interfacial systems: Atomistic simulations of vapor nucleation. <i>Journal of Chemical Physics</i> , <b>2018</b> , 148, 064706	3.9	10
722	Quasiharmonic Analysis of the Energy Landscapes of Dihydrofolate Reductase from Piezophiles and Mesophiles. <b>2018</b> , 122, 5527-5533		6
721	Accuracy Comparison of Generalized Born Models in the Calculation of Electrostatic Binding Free Energies. <b>2018</b> , 14, 1656-1670		13

720	Influence of Solvent on the Drug-Loading Process of Amphiphilic Nanogel Star Polymers. <b>2018</b> , 122, 5356-53674	
719	Divergent effect of electric fields on the mechanical property of water-filled carbon nanotubes with an application as a nanoscale trigger. <b>2018</b> , 29, 025707	2
718	A GPU-Accelerated Parameter Interpolation Thermodynamic Integration Free Energy Method. <b>2018</b> , 14, 1564-1582	26
717	A zeolite-like aluminophosphate membrane with molecular-sieving property for water desalination. <b>2018</b> , 9, 2533-2539	18
716	First Principles Calculation of the Reaction Rates for Ligand Binding to Myoglobin: The Cases of NO and CO. <b>2018</b> , 24, 5350-5358	5
715	In Silico Study of Recognition between Alpha and Alpha Fibril Surfaces: An N-Terminal Helical Recognition Motif and Its Implications for Inhibitor Design. <b>2018</b> , 9, 935-944	10
714	A Minimum Variance Clustering Approach Produces Robust and Interpretable Coarse-Grained Models. <b>2018</b> , 14, 1071-1082	12
713	Exploring the Rich Potential Energy Surface of (HO) and Its Physical Implications. <b>2018</b> , 14, 1141-1153	15
712	Consensus Conformations of Dinucleoside Monophosphates Described with Well-Converged Molecular Dynamics Simulations. <b>2018</b> , 14, 1456-1470	9
711	Impact of intracellular ionic strength on dimer binding in the NF-kB inducing kinase. <b>2018</b> , 202, 183-190	
710	Force Field Benchmark of the TraPPE-UA for Polar Liquids: Density, Heat of Vaporization, Dielectric Constant, Surface Tension, Volumetric Expansion Coefficient, and Isothermal Compressibility. <b>2018</b> , 122, 1669-1678	15
709	RNA Structural Dynamics As Captured by Molecular Simulations: A Comprehensive Overview. <b>2018</b> , 118, 4177-4338	235
708	Calculation of Thermodynamic Properties of Bound Water Molecules. <b>2018</b> , 1762, 389-402	3
707	Molecular Dynamics Characterization of Temperature and Pressure Effects on the Water-Methane Interface. <b>2018</b> , 24, 75-81	10
706	Potential of metal-organic frameworks for adsorptive separation of industrially and environmentally relevant liquid mixtures. <b>2018</b> , 367, 82-126	73
705	Analysis of the influence of simulation parameters on biomolecule-linked water networks. <b>2018</b> , 82, 117-128	1
704	Neuraminidase A from Streptococcus pneumoniae has a modular organization of catalytic and lectin domains separated by a flexible linker. <b>2018</b> , 285, 2428-2445	14
703	Force Field for Water over Pt(111): Development, Assessment, and Comparison. <b>2018</b> , 14, 3238-3251	28

702	Macromolecular crowding effects in flexible polymer solutions. <b>2018</b> , 17, 1840006		3
701	Investigation of the Water Adsorption Properties and Structural Stability of MIL-100(Fe) with Different Anions. <b>2018</b> , 34, 4180-4187		25
700	The coexistence temperature of hydrogen clathrates: A molecular dynamics study. <i>Journal of Chemical Physics</i> , <b>2018</b> , 148, 114503	3.9	9
699	Determination of Dynamical Heterogeneity from Dynamic Neutron Scattering of Proteins. <b>2018</b> , 114, 2397-2407		5
698	Absolute proton hydration free energy, surface potential of water, and redox potential of the hydrogen electrode from first principles: QM/MM MD free-energy simulations of sodium and potassium hydration. <i>Journal of Chemical Physics</i> , <b>2018</b> , 148, 222814	3.9	55
697	Validierung von molekularen Simulationen: eine Übersicht verschiedener Aspekte. <b>2018</b> , 130, 894-915		3
696	Validation of Molecular Simulation: An Overview of Issues. <b>2018</b> , 57, 884-902		74
695	Molecular dynamics simulation strategies for designing carbon-nanotube-based targeted drug delivery. <b>2018</b> , 23, 235-250		58
694	Binding affinities of the farnesoid X receptor in the D3R Grand Challenge 2 estimated by free-energy perturbation and docking. <b>2018</b> , 32, 211-224		9
693	Advanced models for water simulations. <b>2018</b> , 8, e1355		30
692	Dynamical behavior of molecular partial charges implied by the far-infrared spectral profile of liquid water. <b>2018</b> , 512, 165-170		3
691	Self-Recovery Superhydrophobic Surfaces: Modular Design. <b>2018</b> , 12, 359-367		23
690	High-temperature dynamic behavior in bulk liquid water: A molecular dynamics simulation study using the OPC and TIP4P-Ew potentials. <b>2018</b> , 13, 1		6
689	Role of electrostatic interactions in determining the G-quadruplex structures. <b>2018</b> , 693, 216-221		2
688	Coexistence of Multilayered Phases of Confined Water: The Importance of Flexible Confining Surfaces. <b>2018</b> , 12, 448-454		33
687	Simulating the free energy of passive membrane permeation for small molecules. <b>2018</b> , 44, 1147-1157		7
686	A- to B-DNA Transition in AMBER Force Fields and Its Coupling to Sugar Pucker. <b>2018</b> , 14, 319-328		13
685	Force field development and simulations of intrinsically disordered proteins. <b>2018</b> , 48, 40-48		98

684	Amber-Compatible Parametrization Procedure for Peptide-like Compounds: Application to 1,4- and 1,5-Substituted Triazole-Based Peptidomimetics. <b>2018</b> , 58, 90-110	7
683	1,5-Disubstituted 1,2,3-Triazole-Containing Peptidotriazolamers: Design Principles for a Class of Versatile Peptidomimetics. <b>2018</b> , 24, 953-961	16
682	Molecular dynamics simulation of liquid water and ice nanoclusters using a new effective HFD-like model. <b>2018</b> , 39, 269-278	1
681	Water models for biomolecular simulations. <b>2018</b> , 8, e1347	84
680	Overview of the SAMPL6 host-guest binding affinity prediction challenge. <b>2018</b> , 32, 937-963	77
679	Intrinsically Disordered Landscapes for Human CD4 Receptor Peptide. <b>2018</b> , 122, 11906-11921	7
678	Molecular Dynamics Simulations of Water-Mediated Cholesterol Capture within an Open-Ended Single-Walled Carbon Nanotube. <b>2019</b> , 20, 142-147	0
677	Targeting the Pentose Phosphate Pathway: Characterization of a New 6PGL Inhibitor. <b>2018</b> , 115, 2114-2126	2
676	Dynamic and Electronic Polarization Corrections to the Dielectric Constant of Water. <b>2018</b> , 122, 9243-9250	6
675	What Drives N Spin Relaxation in Disordered Proteins? Combined NMR/MD Study of the H4 Histone Tail. <b>2018</b> , 115, 2348-2367	13
674	Theoretical Approaches to Describing the Oxygen Reduction Reaction Activity of Single-Atom Catalysts. <b>2018</b> , 122, 29307-29318	39
673	A QM/MM Derived Polarizable Water Model for Molecular Simulation. <b>2018</b> , 23,	6
672	High and low density patches in simulated liquid water. <i>Journal of Chemical Physics</i> , <b>2018</b> , 149, 204507	3,9 22
671	Interfacing CRYSTAL/AMBER to Optimize QM/MM Lennard-Jones Parameters for Water and to Study Solvation of TiO <sub>2</sub> Nanoparticles. <b>2018</b> , 23,	5
670	Oriental Distribution of Free O-H Groups of Interfacial Water is Exponential. <b>2018</b> , 121, 246101	35
669	Molecular Insights into the Unusual Structure of an Antifreeze Protein with a Hydrated Core. <b>2018</b> , 122, 9827-9839	12
668	Molecular Mechanism of ATP Hydrolysis in an ABC Transporter. <b>2018</b> , 4, 1334-1343	38
667	Intramolecular Diffusion in $\beta$ Synuclein: It Depends on How You Measure It. <b>2018</b> , 115, 1190-1199	5

666	Biporous Metal-Organic Framework with Tunable CO/CH Separation Performance Facilitated by Intrinsic Flexibility. <b>2018</b> , 10, 36144-36156	26
665	Grand Canonical Monte Carlo Simulations on Phase Equilibria of Methane, Carbon Dioxide, and Their Mixture Hydrates. <b>2018</b> , 122, 9724-9737	5
664	Recent Advances in Clathrate Hydrates Research using Molecular Simulations. <b>2018</b> , 28, 102-112	
663	Dispersion Correction Alleviates Dye Stacking of Single-Stranded DNA and RNA in Simulations of Single-Molecule Fluorescence Experiments. <b>2018</b> , 122, 11626-11639	13
662	Molecular Dynamics Study on the Reverse Osmosis Using Multilayer Porous Graphene Membranes. <b>2018</b> , 8,	6
661	Molecular enhanced sampling with autoencoders: On-the-fly collective variable discovery and accelerated free energy landscape exploration. <b>2018</b> , 39, 2079-2102	83
660	Structure, Dynamics, and Hydration Free Energy of Carbon Dioxide in Aqueous Solution: A Quantum Mechanical/Molecular Mechanics Molecular Dynamics Thermodynamic Integration (QM/MM MD TI) Simulation Study. <b>2018</b> , 14, 6472-6483	13
659	On the Applicability of Force Fields To Study the Aggregation of Amyloidogenic Peptides Using Molecular Dynamics Simulations. <b>2018</b> , 14, 6063-6075	51
658	Correlation effects and many-body interactions in water clusters. <b>2018</b> , 14, 979-991	9
657	SAMPL6 host-guest challenge: binding free energies via a multistep approach. <b>2018</b> , 32, 1097-1115	12
656	Computational screening of hydrophobic metal-organic frameworks for the separation of H <sub>2</sub> S and CO <sub>2</sub> from natural gas. <b>2018</b> , 6, 18898-18905	52
655	Structural accommodations accompanying splicing of a group II intron RNP. <b>2018</b> , 46, 8542-8556	6
654	Structural Stability of Peptidic His-Containing Proton Wire in Solution and in the Adsorbed State. <b>2018</b> , 34, 6997-7005	4
653	A New Methodology for Evaluating the Structural Similarity between Different Phases Using a Dimensionality Reduction Technique. <b>2018</b> , 3, 5789-5798	2
652	The structure of aqueous lithium chloride solutions at high concentrations as revealed by a comparison of classical interatomic potential models. <b>2018</b> , 264, 179-197	19
651	Low-voltage electrostatic modulation of ion diffusion through layered graphene-based nanoporous membranes. <b>2018</b> , 13, 685-690	134
650	The spatial range of protein hydration. <i>Journal of Chemical Physics</i> , <b>2018</b> , 148, 215104	3.9 20
649	Simulations of 1-Butyl-3-methylimidazolium Tetrafluoroborate + Acetonitrile Mixtures: Force-Field Validation and Frictional Characteristics. <b>2018</b> , 122, 7385-7393	8

648	Compressibility of the protein-water interface. <i>Journal of Chemical Physics</i> , <b>2018</b> , 148, 215102	3.9	11
647	Aqueous Ion Trapping and Transport in Graphene-Embedded 18-Crown-6 Ether Pores. <b>2018</b> , 12, 6677-6684		31
646	Partition coefficients of methylated DNA bases obtained from free energy calculations with molecular electron density derived atomic charges. <b>2018</b> , 39, 1728-1737		3
645	A Grand Canonical Monte Carlo Study of the N <sub>2</sub> , CO, and Mixed N <sub>2</sub> /O Clathrate Hydrates. <b>2018</b> , 122, 18432-18444		17
644	Force Field Benchmark of Amino Acids. 2. Partition Coefficients between Water and Organic Solvents. <b>2018</b> , 58, 1669-1681		28
643	Modeling Soft Supramolecular Nanostructures by Molecular Simulations. <b>2018</b> ,		
642	Computational discovery of chemically patterned surfaces that effect unique hydration water dynamics. <b>2018</b> , 115, 8093-8098		30
641	A new approach for the prediction of partition functions using machine learning techniques. <i>Journal of Chemical Physics</i> , <b>2018</b> , 149, 044118	3.9	15
640	Complex Behavior of Ordered and Icelike Water in Carbon Nanotubes near Its Bulk Boiling Point. <b>2018</b> , 9, 4746-4752		6
639	Properties of Hydrogen Bonds in Water and Monohydric Alcohols. <b>2018</b> , 92, 1516-1522		6
638	Explicit ions/implicit water generalized Born model for nucleic acids. <i>Journal of Chemical Physics</i> , <b>2018</b> , 148, 195101	3.9	3
637	Systematic molecular model development with reliable charge distributions for gaseous adsorption in nanoporous materials. <b>2018</b> , 6, 16029-16042		8
636	Coarse-Grained Simulations of Aqueous Thermoresponsive Polyethers. <b>2018</b> , 10,		9
635	Developing a molecular dynamics force field for both folded and disordered protein states. <b>2018</b> , 115, E4758-E4766		434
634	Crowding Stabilizes DMSO-Water Hydrogen-Bonding Interactions. <b>2018</b> , 122, 5984-5990		16
633	Assimilating Radial Distribution Functions To Build Water Models with Improved Structural Properties. <b>2018</b> , 58, 1766-1778		12
632	Structures, dynamics, and hydrogen-bond interactions of antifreeze proteins in TIP4P/Ice water and their dependence on force fields. <b>2018</b> , 13, e0198887		11
631	Water-mediated curvature change in graphene by single-walled carbon nanotubes. <b>2018</b> , 20, 22359-22367		2



630	Validating Molecular Dynamics Simulations against Experimental Observables in Light of Underlying Conformational Ensembles. <b>2018</b> , 122, 6673-6689		41
629	How proteins modify water dynamics. <i>Journal of Chemical Physics</i> , <b>2018</b> , 148, 215103	3.9	23
628	Analysis of three-phase equilibrium conditions for methane hydrate by isometric-isothermal molecular dynamics simulations. <i>Journal of Chemical Physics</i> , <b>2018</b> , 148, 184501	3.9	6
627	The geometry of protein hydration. <i>Journal of Chemical Physics</i> , <b>2018</b> , 148, 215101	3.9	24
626	Folding free energy landscapes of $\alpha$ -sheets with non-polarizable and polarizable CHARMM force fields. <i>Journal of Chemical Physics</i> , <b>2018</b> , 149, 072317	3.9	20
625	Bind3P: Optimization of a Water Model Based on Host-Guest Binding Data. <b>2018</b> , 14, 3621-3632		15
624	Gradual Crossover from Subdiffusion to Normal Diffusion: A Many-Body Effect in Protein Surface Water. <b>2018</b> , 120, 248101		45
623	Human p38 $\beta$ mitogen-activated protein kinase in the Asp168-Phe169-Gly170-in (DFG-in) state can bind allosteric inhibitor Doramapimod. <b>2019</b> , 37, 2049-2060		10
622	Modelling water with simple Mercedes-Benz models. <b>2019</b> , 45, 279-294		3
621	A comparison of different water models for melting point calculation of methane hydrate using molecular dynamics simulations. <b>2019</b> , 516, 6-14		18
620	Functional UiO-66 for the removal of sulfur-containing compounds in gas and liquid mixtures: A molecular simulation study. <b>2019</b> , 356, 737-745		10
619	Calculation of the surface tension of water: 40 years of molecular simulations. <b>2019</b> , 45, 295-303		12
618	Thermodynamics of Helix formation in small peptides of varying length in vacuo, implicit solvent and explicit solvent: Comparison between AMBER force fields. <b>2019</b> , 18, 1950015		6
617	Synthesis, Biological Evaluation and In Silico Computational Studies of 7-Chloro-4-(1-1,2,3-triazol-1-yl)quinoline Derivatives: Search for New Controlling Agents against (Lepidoptera: Noctuidae) Larvae. <b>2019</b> , 67, 9210-9219		7
616	Are crystallographic B-factors suitable for calculating protein conformational entropy?. <b>2019</b> , 21, 18149-18160		12
615	Development of an Advanced Force Field for Water Using Variational Energy Decomposition Analysis. <b>2019</b> , 15, 5001-5013		27
614	Effects of Large Guest Molecular Structure on Thermal Expansion Behaviors in Binary (C <sub>4</sub> H <sub>8</sub> O + CH <sub>4</sub> ) Clathrate Hydrates. <b>2019</b> , 123, 20705-20714		5
613	Binding Free Energies of Conformationally Disordered Peptides Through Extensive Sampling and End-Point Methods. <b>2019</b> , 2039, 229-242		1

612	A new topological descriptor for water network structure. <b>2019</b> , 11, 48	6
611	Using Small-Angle Scattering Data and Parametric Machine Learning to Optimize Force Field Parameters for Intrinsically Disordered Proteins. <b>2019</b> , 6, 64	11
610	Development of Nonbonded Models for Metal Cations Using the Electronic Continuum Correction. <b>2019</b> , 40, 2464-2472	10
609	Cyclization of RGD Peptides by Suzuki-Miyaura Cross-Coupling. <b>2019</b> , 62, 7417-7430	21
608	Accuracy of MD solvent models in RNA structure refinement assessed via liquid-crystal NMR and spin relaxation data. <b>2019</b> , 207, 250-259	3
607	Glycine Substitution Effects on the Supramolecular Morphology and Rigidity of Cell-Adhesive Amphiphilic Peptides. <b>2019</b> , 25, 13523-13530	16
606	Dynamic allostery-based molecular workings of kinase:peptide complexes. <b>2019</b> , 116, 15052-15061	19
605	Ab Initio Molecular Dynamics Simulations of the Influence of Lithium Bromide Salt on the Deprotonation of Formic Acid in Aqueous Solution. <b>2019</b> , 123, 6823-6829	6
604	Systematic Optimization of Water Models Using Liquid/Vapor Surface Tension Data. <b>2019</b> , 123, 7061-7073	18
603	Chemical accuracy in modeling halide ion hydration from many-body representations. <b>2019</b> , 4, 1631212	21
602	Multiscale Modeling and Simulation of Water and Methane Hydrate Crystal Interface. <b>2019</b> , 19, 5142-5151	9
601	Rare Angiogenin and Ribonuclease 4 variants associated with amyotrophic lateral sclerosis exhibit loss-of-function: a comprehensive in silico study. <b>2019</b> , 34, 1661-1677	4
600	Modification of messenger RNA by 2'-O-methylation regulates gene expression in vivo. <b>2019</b> , 10, 3401	50
599	Molecular simulations of the pistol ribozyme: unifying the interpretation of experimental data and establishing functional links with the hammerhead ribozyme. <b>2019</b> , 25, 1439-1456	12
598	The effects of charge density distributions of metal ions on single water molecule dissociation of $[M(H_2O)_6]^{3+}$ systems. <b>2019</b> , 3, 085016	
597	How Sugars Modify Caffeine Self-Association and Solubility: Resolving a Mechanism of Selective Hydrotrophy. <b>2019</b> , 141, 18056-18063	11
596	Polarizable Embedding with a Transferable HO Potential Function I: Formulation and Tests on Dimer. <b>2019</b> , 15, 6562-6577	6
595	Well-Balanced Force Field 03 for Folded and Disordered Proteins. <b>2019</b> , 15, 6769-6780	27

594	Temperature-Dependent Interactions Explain Normal and Inverted Solubility in a D-Crystallin Mutant. <b>2019</b> , 117, 930-937	2
593	Strategies for Late-Stage Optimization: Profiling Thermodynamics by Preorganization and Salt Bridge Shielding. <b>2019</b> , 62, 9753-9771	10
592	Dynamic Curvature Nanochannel-Based Membrane with Anomalous Ionic Transport Behaviors and Reversible Rectification Switch. <b>2019</b> , 31, e1805130	84
591	Anisotropic interfacial properties between monolayered black phosphorus and water. <b>2019</b> , 475, 857-862	6
590	Solubility of Water in Hydrogen at High Pressures: A Molecular Simulation Study. <b>2019</b> , 64, 4103-4115	16
589	Unraveling the Water Adsorption Mechanism in the Mesoporous MIL-100(Fe) Metal-Organic Framework. <b>2019</b> , 123, 23014-23025	20
588	Spontaneously Forming Dendritic Voids in Liquid Water Can Host Small Polymers. <b>2019</b> , 10, 5585-5591	11
587	Water Runs Deep. <b>2019</b> , 1-33	3
586	Aggregation dynamics of charged peptides in water: Effect of salt concentration. <i>Journal of Chemical Physics</i> , <b>2019</b> , 151, 074901	3.9 1
585	Photochemically Induced Water Harvesting in Metal-Organic Framework. <b>2019</b> , 7, 15854-15859	15
584	Development of a Robust Indirect Approach for MM-gQM Free Energy Calculations That Combines Force-Matched Reference Potential and Bennett's Acceptance Ratio Methods. <b>2019</b> , 15, 5543-5562	31
583	Hydrophobic but Water-Friendly: Favorable Water-Perfluoromethyl Interactions Promote Hydration Shell Defects. <b>2019</b> , 141, 15856-15868	11
582	Systematically improved melting point prediction: a detailed physical simulation model is required. <b>2019</b> , 55, 12044-12047	7
581	Dynamical ensemble of the active state and transition state mimic for the RNA-cleaving 8-17 DNAzyme in solution. <b>2019</b> , 47, 10282-10295	15
580	Persistent homology analysis of osmolyte molecular aggregation and their hydrogen-bonding networks. <b>2019</b> , 21, 21038-21048	6
579	Locating Minimum Energy Crossings of Different Spin States Using the Fragment Molecular Orbital Method. <b>2019</b> , 15, 6074-6084	8
578	Solubility of Polar and Nonpolar Aromatic Molecules in Subcritical Water: The Role of the Dielectric Constant. <b>2019</b> , 15, 6277-6293	9
577	Glass polymorphism and liquid-liquid phase transition in aqueous solutions: experiments and computer simulations. <b>2019</b> , 21, 23238-23268	22

576	A force field of Li, Na, K, Mg, Ca, Cl, and SO in aqueous solution based on the TIP4P/2005 water model and scaled charges for the ions. <i>Journal of Chemical Physics</i> , <b>2019</b> , 151, 134504	3.9	78
575	Characterization of nucleation of methane hydrate crystals: Interfacial theory and molecular simulation. <b>2019</b> , 557, 556-567		7
574	Optimization of Protein-Ligand Electrostatic Interactions Using an Alchemical Free-Energy Method. <b>2019</b> , 15, 6504-6512		5
573	Ultrahigh Permeable CN-Inspired Graphene Nanomesh Membranes versus Highly Strained CN for Reverse Osmosis Desalination. <b>2019</b> , 123, 8740-8752		6
572	Decoding signatures of structure, bulk thermodynamics, and solvation in three-body angle distributions of rigid water models. <i>Journal of Chemical Physics</i> , <b>2019</b> , 151, 094501	3.9	6
571	Thermodynamics of helix formation in small peptides of varying length in vacuo, in implicit solvent, and in explicit solvent. <b>2018</b> , 25, 3		24
570	Encapsulation driven conformational changes in n-alkanes inside a hydrogen-bonded supramolecular cavitand assembly. <b>2019</b> , 521, 100-107		7
569	Molecular simulation of peptides coming of age: Accurate prediction of folding, dynamics and structures. <b>2019</b> , 664, 76-88		14
568	Unexpected trends in the hydrophobicity of fluorinated amino acids reflect competing changes in polarity and conformation. <b>2019</b> , 21, 2029-2038		12
567	An adjustable permeation membrane up to the separation for multicomponent gas mixture. <b>2019</b> , 9, 7380		8
566	Structures and Dynamics of Interfacial Water. <b>2019</b> ,		
565	Oriental Distribution of Free OH Groups of Interfacial Water. <b>2019</b> , 41-56		
564	AMOEBa+ Classical Potential for Modeling Molecular Interactions. <b>2019</b> , 15, 4122-4139		53
563	Cleaning Up Mechanistic Debris Generated by Twister Ribozymes Using Computational RNA Enzymology. <b>2019</b> , 9, 5803-5815		15
562	The interplay between molecular flexibility and RNA chemical probing reactivities analyzed at the nucleotide level via an extensive molecular dynamics study. <b>2019</b> , 162-163, 108-127		5
561	Cage Occupancies in Nitrogen Clathrate Hydrates from Monte Carlo Simulations. <b>2019</b> , 123, 16757-16765		7
560	Seven-Site Effective Pair Potential for Simulating Liquid Water. <b>2019</b> , 123, 4594-4603		9
559	All-atom molecular dynamics study on the non-solvent induced phase separation: Thermodynamics of adding water to poly(vinylidene fluoride)/N-methyl-2-pyrrolidone solution. <i>Journal of Chemical Physics</i> , <b>2019</b> , 150, 184505	3.9	2

558	Mass accommodation at a high-velocity water liquid-vapor interface. <i>Journal of Chemical Physics</i> , <b>2019</b> , 150, 154705	3.9	4
557	Electronic coarse graining: Predictive atomistic modeling of condensed matter. <b>2019</b> , 91,		4
556	Adsorption and dissociation of water molecules at the $\alpha$ -Al <sub>2</sub> O <sub>3</sub> (0001) surface: A 2-dimensional hybrid self-consistent charge density functional based tight-binding/molecular mechanics molecular dynamics (2D SCC-DFTB/MM MD) simulation study. <b>2019</b> , 164, 195-204		5
555	Studying surfactants adsorption on heterogeneous substrates. <b>2019</b> , 23, 115-122		11
554	Predicting the Impact of Aqueous Ions on Fate and Transport of Munition Compounds in the Environment. <b>2019</b> , 123, 4973-4979		3
553	Structural insights into DNA-stabilized silver clusters. <b>2019</b> , 15, 4284-4293		6
552	Interactions of Water and Alkanes: Modifying Additive Force Fields to Account for Polarization Effects. <b>2019</b> , 15, 3854-3867		19
551	Framework for Conducting and Analyzing Crystal Simulations of Nucleic Acids to Aid in Modern Force Field Evaluation. <b>2019</b> , 123, 4611-4624		3
550	Effects of Pressure and Temperature on the Atomic Fluctuations of Dihydrofolate Reductase from a Psychropiezophile and a Mesophile. <b>2019</b> , 20,		7
549	A two-dimensional replica-exchange molecular dynamics method for simulating RNA folding using sparse experimental restraints. <b>2019</b> , 162-163, 96-107		5
548	Computational Fluorine Scanning Using Free-Energy Perturbation. <b>2019</b> , 59, 2776-2784		9
547	Maximizing accuracy of RNA structure in refinement against residual dipolar couplings. <b>2019</b> , 73, 117-139		3
546	Understanding Water Structure in an Ion-Pair Solvation Shell in the Vicinity of a Water/Membrane Interface. <b>2019</b> , 123, 3945-3954		5
545	Evolution of All-Atom Protein Force Fields to Improve Local and Global Properties. <b>2019</b> , 10, 2227-2234		39
544	Ultrafast Propulsion of Water Nanodroplets on Patterned Graphene. <b>2019</b> , 13, 5465-5472		27
543	Decoupling pH Dependence of Flat Band Potential in Aqueous Dye-Sensitized Electrodes. <b>2019</b> , 123, 8681-8687		12
542	The combined force field-sampling problem in simulations of disordered amyloid- $\beta$ peptides. <i>Journal of Chemical Physics</i> , <b>2019</b> , 150, 104108	3.9	25
541	Automated Markov state models for molecular dynamics simulations of aggregation and self-assembly. <i>Journal of Chemical Physics</i> , <b>2019</b> , 150, 115101	3.9	28

540	Thermophysical properties of glyceline-water mixtures investigated by molecular modelling. <b>2019</b> , 21, 6467-6476	30
539	Molecular Dynamics Simulations Combined with Nuclear Magnetic Resonance and/or Small-Angle X-ray Scattering Data for Characterizing Intrinsically Disordered Protein Conformational Ensembles. <b>2019</b> , 59, 1743-1758	22
538	Directing self-assembly in solution towards improved cooperativity in Fe(iii) complexes with amphiphilic tridentate ligands. <b>2019</b> , 48, 4239-4247	4
537	1,4-Disubstituted 1-1,2,3-Triazole Containing Peptidotriazolamers: A New Class of Peptidomimetics With Interesting Foldamer Properties. <b>2019</b> , 7, 155	14
536	Functionalization of Enzymatically Synthesized Rigid Poly(itaconate)s via Post-Polymerization Aza-Michael Addition of Primary Amines. <b>2019</b> , 361, 2559	12
535	Significantly enhanced convective heat transfer through surface modification in nanochannels. <b>2019</b> , 136, 702-708	21
534	Adaptations for Pressure and Temperature Effects on Loop Motion in and Dihydrofolate Reductase. <b>2019</b> , 39, 225-237	4
533	General Purpose Water Model Can Improve Atomistic Simulations of Intrinsically Disordered Proteins. <b>2019</b> , 15, 2620-2634	52
532	Temperature Dependence of Intrinsically Disordered Proteins in Simulations: What are We Missing?. <b>2019</b> , 15, 2672-2683	33
531	Statistical properties for diffusive motion of hydration water on protein surface. <b>2019</b> , 562, 1-5	2
530	Infinite Dilution Activity Coefficients as Constraints for Force Field Parametrization and Method Development. <b>2019</b> , 15, 3066-3074	7
529	Force Field Development and Nanoreactor Chemistry. <b>2019</b> , 127-159	
528	Systematic parameterization procedure to develop force fields for molecular fluids using explicit water. <b>2019</b> , 490, 1-12	8
527	Molecular dynamics characterization of the water-methane, ethane, and propane gas mixture interfaces. <b>2019</b> , 208, 114769	10
526	Characterizing the structural and thermodynamic properties of $A_{\#}2$ and $A_{\#}0$ . <b>2019</b> , 510, 442-448	11
525	Mechanosensitive Ion Permeation across Subnanoporous MoS <sub>2</sub> Monolayers. <b>2019</b> , 123, 3588-3593	5
524	The dielectric constant: Reconciling simulation and experiment. <i>Journal of Chemical Physics</i> , <b>2019</b> , 150, 084108	3.9 18
523	Globally correlated conformational entropy underlies positive and negative cooperativity in a kinase's enzymatic cycle. <b>2019</b> , 10, 799	20

522	Developing and Testing of Lipid Force Fields with Applications to Modeling Cellular Membranes. <b>2019</b> , 119, 6227-6269	48
521	Modeling and simulation of adsorption of methane, ethane, hydrogen sulfide and water from natural gas in (FP)YEu MetalOrganic Framework. <b>2019</b> , 579, 012020	
520	3. In Silico methods to predict solubility. <b>2019</b> , 71-112	
519	Association of functional variants and protein-to-protein physical interactions of human MutY homolog linked with familial adenomatous polyposis and colorectal cancer syndrome. <b>2019</b> , 4, 155-173	1
518	Effect of substrate wettability and flexibility on the initial stage of water vapor condensation. <b>2019</b> , 15, 10055-10064	1
517	Molecular Dynamics model of peptide-protein conjugation: case study of covalent complex between Sos1 peptide and N-terminal SH3 domain from Grb2. <b>2019</b> , 9, 20219	1
516	Empirical S=O stretch vibrational frequency map. <i>Journal of Chemical Physics</i> , <b>2019</b> , 151, 234107	3.9 6
515	Computationally Modeling Electrostatic Binding Energetics in a Crowded, Dynamic Environment: Physical Insights from a Peptide-DNA System. <b>2019</b> , 123, 10718-10734	2
514	Hydration of Closely Related Manganese and Magnesium Porphyrins in Aqueous Solutions: Ab Initio Quantum Mechanical Charge Field Molecular Dynamics Simulation Study. <b>2019</b> , 123, 10769-10779	0
513	Combining molecular dynamics simulations and experimental analyses in protein misfolding. <b>2019</b> , 118, 33-110	6
512	Opening dynamics of HIV-1 gp120 upon receptor binding is dictated by a key hydrophobic core. <b>2019</b> , 21, 26003-26016	3
511	Self-diffusion coefficient of bulk and confined water: a critical review of classical molecular simulation studies. <b>2019</b> , 45, 425-453	69
510	Perspective on computational simulations of glycosaminoglycans. <b>2019</b> , 9, e1388	12
509	Effect of truncating electrostatic interactions on predicting thermodynamic properties of waterethanol systems. <b>2019</b> , 45, 336-350	10
508	Polarization Corrections and the Hydration Free Energy of Water. <b>2019</b> , 15, 1065-1078	16
507	Temperature dependent network stability in simple alcohols and pure water: The evolution of Laplace spectra. <b>2019</b> , 273, 670-675	4
506	Challenges and advances in atomistic simulations of potassium and sodium ion channel gating and permeation. <b>2019</b> , 597, 679-698	20
505	Highly mechanosensitive ion channels from graphene-embedded crown ethers. <b>2019</b> , 18, 76-81	52



504	Pore Morphology Determines Spontaneous Liquid Extrusion from Nanopores. <b>2019</b> , 13, 1728-1738	15
503	Transport properties of bulk water at 243B50 K: a Comparative molecular dynamics simulation study using SPC/E, TIP4P, and TIP4P/2005 water models. <b>2019</b> , 117, 1926-1933	10
502	Mechanisms for Benzene Dissociation through the Excited State of T4 Lysozyme L99A Mutant. <b>2019</b> , 116, 205-214	11
501	Dynamical Effects of Trimethylamine N-Oxide on Aqueous Solutions of Urea. <b>2019</b> , 123, 1108-1115	7
500	Ab Initio Molecular Dynamics Simulations of the Influence of Lithium Bromide on the Structure of the Aqueous Solution-Air Interface. <b>2019</b> , 123, 729-737	3
499	Many-Body Effects Determine the Local Hydration Structure of Cs in Solution. <b>2019</b> , 10, 406-412	28
498	Interplay between Conformational Entropy and Solvation Entropy in Protein-Ligand Binding. <b>2019</b> , 141, 2012-2026	51
497	Assessing the Predictive Power of Relative Binding Free Energy Calculations for Test Cases Involving Displacement of Binding Site Water Molecules. <b>2019</b> , 59, 754-765	16
496	Conformational rearrangements in n-alkanes encapsulated within capsular self-assembly of capped carbon nanotubes. <b>2019</b> , 517, 198-207	2
495	Modeling, Simulations, and Bioinformatics at the Service of RNA Structure. <b>2019</b> , 5, 51-73	20
494	Adsorption Behaviors and Phase Equilibria for Clathrate Hydrates of Sulfur- and Nitrogen-Containing Small Molecules. <b>2019</b> , 123, 2691-2702	2
493	Why Computed Protein Folding Landscapes Are Sensitive to the Water Model. <b>2019</b> , 15, 625-636	22
492	Biomolecular force fields: where have we been, where are we now, where do we need to go and how do we get there?. <b>2019</b> , 33, 133-203	35
491	Force field development phase II: Relaxation of physics-based criteria for inclusion of more rigorous physics into the representation of molecular energetics. <b>2019</b> , 33, 205-264	26
490	Effects of oscillating pressure on desalination performance of transverse flow CNT membrane. <b>2019</b> , 451, 35-44	9
489	Structural and dynamic studies provide insights into specificity and allosteric regulation of ribonuclease as, a key enzyme in mycobacterial virulence. <b>2020</b> , 38, 2455-2467	1
488	The numerical modeling of the vapor bubble growth on the silicon substrate inside the flat plate heat pipe. <b>2020</b> , 147, 118945	7
487	MDMS: Software Facilitating Performing Molecular Dynamics Simulations. <b>2020</b> , 41, 266-271	1



486	Molecular simulation of equal density temperature in CCS under geological sequestration conditions. <b>2020</b> , 10, 90-102		2
485	Properties of Aqueous Trehalose Mixtures: Glass Transition and Hydrogen Bonding. <b>2020</b> , 16, 1249-1262		12
484	Revisiting OPLS-AA Force Field for the Simulation of Anionic Surfactants in Concentrated Electrolyte Solutions. <b>2020</b> , 16, 1136-1145		12
483	Emergence of non-monotonic deep cavity cavitand assembly with increasing portal methylation. <b>2020</b> , 5, 656-665		2
482	On the transferability of ion parameters to the TIP4P/2005 water model using molecular dynamics simulations. <i>Journal of Chemical Physics</i> , <b>2020</b> , 152, 024501	3.9	28
481	Temperature-dependence of the dielectric relaxation of water using non-polarizable water models. <b>2020</b> , 22, 1011-1018		16
480	Structure and Thermodynamic Stability of Zeolitic Imidazolate Framework Surfaces. <b>2020</b> , 124, 1458-1468		0
479	A computational study on the role of water and conformational fluctuations in Hsp90 in response to inhibitors. <b>2020</b> , 96, 107510		8
478	Investigations on different two-dimensional materials as slit membranes for enhanced desalination. <b>2020</b> , 598, 117653		13
477	ff19SB: Amino-Acid-Specific Protein Backbone Parameters Trained against Quantum Mechanics Energy Surfaces in Solution. <b>2020</b> , 16, 528-552		197
476	Transformation of hydrogen bond network during CO2 clathrate hydrate dissociation. <b>2020</b> , 499, 143644		6
475	Prediction of plasticization in a real biopolymer system (starch) using molecular dynamics simulations. <b>2020</b> , 187, 108387		11
474	Assessing salt-surfactant synergistic effects on interfacial tension from molecular dynamics simulations. <b>2020</b> , 299, 112223		13
473	Non-zero Lennard-Jones parameters for the Toukan-Rahman water model: more accurate calculations of the solvation free energy of organic substances. <b>2020</b> , 34, 437-441		5
472	Base pairing, structural and functional insights into N4-methylcytidine (m4C) and N4,N4-dimethylcytidine (m42C) modified RNA. <b>2020</b> , 48, 10087-10100		5
471	Phase Behavior of Two-Dimensional Water Confined in Graphene Nanocapillaries. <b>2020</b> ,		
470	An investigation on the effects of nanoplastic particles on nanoporous graphene membrane desalination. <b>2020</b> , 496, 114765		2
469	Biomolecular Binding at Aqueous Interfaces of Langmuir Monolayers of Bioconjugated Amphiphilic Mesogenic Molecules: A Molecular Dynamics Study. <b>2020</b> , 36, 12281-12287		6

468	Reaction-field electrostatics in molecular dynamics simulations: development of a conservative scheme compatible with an atomic cutoff. <b>2020</b> , 22, 26419-26437		8
467	Probing the temperature profile across a liquid-vapor interface upon phase change. <i>Journal of Chemical Physics</i> , <b>2020</b> , 153, 144706	3.9	3
466	Quantifying how step-wise fluorination tunes local solute hydrophobicity, hydration shell thermodynamics and the quantum mechanical contributions of solute-water interactions. <b>2020</b> , 22, 22997-23008		1
465	Simulation of Liquids with the Tight-Binding Density-Functional Approach and Improved Atomic Charges. <b>2020</b> , 124, 7421-7432		1
464	Protein Denaturation, Zero Entropy Temperature, and the Structure of Water around Hydrophobic and Amphiphilic Solutes. <b>2020</b> , 124, 10994-11006		6
463	Effect of pH on the Supramolecular Structure of Urease by Molecular Dynamics Simulations. <b>2020</b> , 12,		3
462	Polarizable Multipolar Molecular Dynamics Using Distributed Point Charges. <b>2020</b> , 16, 7267-7280		2
461	Adsorption of CO and N molecules at the surface of solid water. A grand canonical Monte Carlo study. <i>Journal of Chemical Physics</i> , <b>2020</b> , 153, 204502	3.9	2
460	Precipitant ions influence on lysozyme oligomers stability investigated by molecular dynamics simulation at different temperatures. <b>2021</b> , 39, 7223-7230		4
459	Computer-aided engineering of adipyl-CoA synthetase for enhancing adipic acid synthesis. <b>2020</b> , 42, 2693-2701		1
458	Integrated Structural Modeling of Full-Length LRH-1 Reveals Inter-domain Interactions Contribute to Receptor Structure and Function. <b>2020</b> , 28, 830-846.e9		7
457	Do Internal and External Surfaces of Metal-Organic Frameworks Have the Same Hydrophobicity? Insights from Molecular Simulations. <b>2020</b> , 36, 13070-13078		4
456	Dissecting Dynamic and Hydration Contributions to Sequence-Dependent DNA Minor Groove Recognition. <b>2020</b> , 119, 1402-1415		0
455	A Reactive Force Field with Coarse-Grained Electrons for Liquid Water. <b>2020</b> , 11, 9240-9247		9
454	Carbon Dioxide Hydrate Growth Dynamics and Crystallography in Pure and Saline Water. <b>2020</b> , 20, 7129-7140		7
453	Understanding how water models affect the anomalous pressure dependence of their diffusion coefficients. <i>Journal of Chemical Physics</i> , <b>2020</b> , 153, 104510	3.9	0
452	Water in Nanopores and Biological Channels: A Molecular Simulation Perspective. <b>2020</b> , 120, 10298-10335		42
451	Charge distributions for molecular dynamics simulations from self-consistent polarization method. <b>2020</b> , 41, 2591-2597		2

450	Nucleotide Loading Modes of Human RNA Polymerase II as Deciphered by Molecular Simulations. <b>2020</b> , 10,		0
449	How good are polarizable and flexible models for water: Insights from a many-body perspective.. <i>Journal of Chemical Physics</i> , <b>2020</b> , 153, 060901	3.9	14
448	Dynamical Accuracy of Water Models on Supercooling. <b>2020</b> , 11, 7469-7475		1
447	Surface slip on rotating graphene membrane enables the temporal selectivity that breaks the permeability-selectivity trade-off. <b>2020</b> , 6, eaba9471		26
446	The conformational and mutational landscape of the ubiquitin-like marker for autophagosome formation in cancer. <b>2021</b> , 17, 2818-2841		4
445	Bottom-up derived flexible water model with dipole and quadrupole moments for coarse-grained molecular simulations. <b>2020</b> , 22, 27394-27412		2
444	Actin R256 Mono-methylation Is a Conserved Post-translational Modification Involved in Transcription. <b>2020</b> , 32, 108172		4
443	Microscopic Molecular Insights into Hydrate Formation and Growth in Pure and Saline Water Environments. <b>2020</b> , 124, 4241-4252		13
442	Molecular Selectivity of CO <sub>2</sub> Mixed Hydrates: Raman Spectroscopy and GCMC Studies. <b>2020</b> , 124, 11886-11891		5
441	Spontaneous drying of non-polar deep-cavity cavitand pockets in aqueous solution. <b>2020</b> , 12, 589-594		22
440	Modeling and Simulation of Concentrated Aqueous Solutions of LiTFSI for Battery Applications. <b>2020</b> , 124, 11790-11799		18
439	Pressure Induced Wetting and Dewetting of the Nonpolar Pocket of Deep-Cavity Cavitands in Water. <b>2020</b> , 124, 4781-4792		3
438	Base-pair conformational switch modulates miR-34a targeting of Sirt1 mRNA. <b>2020</b> , 583, 139-144		22
437	Molecular Structure, Binding Affinity, and Biological Activity in the Epigenome. <b>2020</b> , 21,		3
436	Effect of hydrophilicity on water transport through sub-nanometer pores. <b>2020</b> , 611, 118297		11
435	Systematic Parametrization of Divalent Metal Ions for the OPC3, OPC, TIP3P-FB, and TIP4P-FB Water Models. <b>2020</b> , 16, 4429-4442		18
434	Weighted persistent homology for osmolyte molecular aggregation and hydrogen-bonding network analysis. <b>2020</b> , 10, 9685		8
433	Fragment Screening Hit Draws Attention to a Novel Transient Pocket Adjacent to the Recognition Site of the tRNA-Modifying Enzyme TGT. <b>2020</b> , 63, 6802-6820		2

432	Three Popular Force Fields Predict Consensus Mechanism of Amyloid $\beta$ Peptide Binding to the Dimyristoylglycerophosphocholine Bilayer. <b>2020</b> , 60, 2282-2293		7
431	Proximal charge effects on guest binding to a non-polar pocket. <b>2020</b> , 11, 3656-3663		11
430	Structure and mechanism of monoclonal antibody binding to the junctional epitope of Plasmodium falciparum circumsporozoite protein. <b>2020</b> , 16, e1008373		15
429	Scaled charges at work: Salting out and interfacial tension of methane with electrolyte solutions from computer simulations. <b>2020</b> , 513, 112548		15
428	Interfacial properties of aqueous solutions of butanol isomers and cyclohexane. <b>2020</b> , 513, 112551		1
427	Power generation by reverse electro dialysis in a single-layer nanoporous membrane made from core-rim polycyclic aromatic hydrocarbons. <b>2020</b> , 15, 307-312		57
426	Dynamics of water trapped in transition metal oxide-graphene nano-confinement. <b>2020</b> , 32, 325101		2
425	Restructuring a Deep Eutectic Solvent by Water: The Nanostructure of Hydrated Choline Chloride/Urea. <b>2020</b> , 16, 3335-3342		36
424	Environment-Specific Force Field for Intrinsically Disordered and Ordered Proteins. <b>2020</b> , 60, 2257-2267		32
423	Polarizable TIP7P Water Model with Perturbation Charges Evaluated from ABEEM. <b>2020</b> , 124, 2450-2464		4
422	Liquid-phase mega-electron-volt ultrafast electron diffraction. <b>2020</b> , 7, 024301		20
421	AMBER-DYES in AMBER: Implementation of fluorophore and linker parameters into AmberTools. <i>Journal of Chemical Physics</i> , <b>2020</b> , 152, 221103	3.9	7
420	Simulations of activities, solubilities, transport properties, and nucleation rates for aqueous electrolyte solutions. <i>Journal of Chemical Physics</i> , <b>2020</b> , 153, 010903	3.9	16
419	Study of synergistic effect mechanism of compound polymer inhibitors adsorption on the surface of beta-dicalcium silicate based on molecular dynamics simulation. <b>2020</b> , 314, 113665		2
418	EasyAmber: A comprehensive toolbox to automate the molecular dynamics simulation of proteins. <b>2020</b> , 18, 2040011		6
417	Efficient calculation of excess free energy of pure and mixed alcohol solutions. <b>2020</b> , 749, 137397		1
416	In Silico Exploration of Conformational Dynamics and Novel Inhibitors for Targeting MEF2-Associated Transcriptional Activity. <b>2020</b> , 60, 1892-1909		2
415	Carbon dioxide in liquid ammonia: An ab initio Quantum Mechanical/Molecular Mechanical Molecular Dynamics Thermodynamic Integration (QM/MM MD TI) simulation study on structure, dynamics and thermodynamics of solvation. <b>2020</b> , 304, 112667		3

414	Three-site and five-site fixed-charge water models compatible with AMOEBA force field. <b>2020</b> , 41, 1034-1044	2
413	Lipase mediated enzymatic kinetic resolution of phenylethyl halohydrins acetates: A case of study and rationalization. <b>2020</b> , 485, 110819	1
412	Role of Water Molecules in Protein-Ligand Dissociation and Selectivity Discrimination: Analysis of the Mechanisms and Kinetics of Biomolecular Solvation Using Molecular Dynamics. <b>2020</b> , 60, 1818-1832	4
411	Osmotic pressure as driving force for recovering ionic liquids from aqueous solutions. <b>2020</b> , 599, 117835	6
410	Nanopumping of water via rotation of graphene nanoribbons. <b>2020</b> , 31, 175704	1
409	Insights into the Effect of Lowe Syndrome-Causing Mutation p.Asn591Lys of OCRL-1 through Protein-Protein Interaction Networks and Molecular Dynamics Simulations. <b>2020</b> , 60, 1019-1027	4
408	Mechanical Unfolding of Spectrin Repeats Induces Water-Molecule Ordering. <b>2020</b> , 118, 1076-1089	2
407	Force-field coefficient optimization of coarse-grained molecular dynamics models with a small computational budget. <b>2020</b> , 176, 109518	4
406	Pairwise-additive and polarizable atomistic force fields for molecular dynamics simulations of proteins. <b>2020</b> , 170, 1-71	5
405	A Polarization-Consistent Model for Alcohols to Predict Solvation Free Energies. <b>2020</b> , 60, 1352-1367	8
404	Water structure in solution and crystal molecular dynamics simulations compared to protein crystal structures.. <b>2020</b> , 10, 8435-8443	2
403	Ultrafast spontaneous driving of water droplets on monolayer graphene-covered gradient nanopillared surfaces. <b>2020</b> , 515, 145976	5
402	Configuration-Controlled Crystal and/or Gel Formation of Protected d-Glucosamines Supported by Promiscuous Interaction Surfaces and a Conformationally Heterogeneous Solution State. <b>2020</b> , 26, 11643-11655	1
401	Competitive Interactions at Electrolyte/Octanol Interfaces: A Molecular Perspective. <b>2020</b> , 124, 10924-10934	8
400	Differences between calcium rich and depleted alpha-lactalbumin investigated by molecular dynamics simulations and incoherent neutron scattering. <b>2020</b> , 101, 032415	3
399	Bayesian calibration of force fields for molecular simulations. <b>2020</b> , 169-227	2
398	Electron Paramagnetic Resonance Measurements of Four Nitroxide Probes in Supercooled Water Explained by Molecular Dynamics Simulations. <b>2020</b> , 124, 3962-3972	1
397	Support Vector Regression-Based Monte Carlo Simulation of Flexible Water Clusters. <b>2020</b> , 5, 7065-7073	2

396	Non-bonded force field model with advanced restrained electrostatic potential charges (RESP2). <b>2020</b> , 3,		33
395	Dielectric constant and density of aqueous alkali halide solutions by molecular dynamics: A force field assessment. <i>Journal of Chemical Physics</i> , <b>2020</b> , 152, 164502	3.9	11
394	Experimental study of water thermodynamics up to 1.2 GPa and 473 K. <i>Journal of Chemical Physics</i> , <b>2020</b> , 152, 154501	3.9	3
393	An in-silico approach: identification of PPAR-agonists from seaweeds for the management of Alzheimer's Disease. <b>2021</b> , 39, 2210-2229		5
392	Systematic Design-of-Experiments, factorial-design approaches for tuning simple empirical water models. <b>2021</b> , 47, 119-130		1
391	Molecular simulation of adsorption and diffusion of CH <sub>4</sub> and H <sub>2</sub> O in flexible metal-organic framework ZIF-8. <b>2021</b> , 286, 119342		10
390	Molecular dynamics simulations of the colloidal interaction between smectite clay nanoparticles in liquid water. <b>2021</b> , 584, 610-621		21
389	Understanding the relationship between the structural properties of three corrosion inhibitors and their surface protectiveness ability in different environments. <b>2021</b> , 542, 148600		9
388	Analysis of Atomistic Potentials for Poly(ethylene glycol) Ethers. <b>2021</b> , 17, 315-321		2
387	SAMPL7: Host-guest binding prediction by molecular dynamics and quantum mechanics. <b>2021</b> , 35, 63-77		3
386	Probing coupled motions of peptides in solution with fluorescence anisotropy and molecular dynamics simulation. <b>2021</b> , 541, 111018		3
385	Green and low-cost acetate-based electrolytes for the highly reversible zinc anode. <b>2021</b> , 485, 229329		11
384	A force field for bio-polymers in ionic liquids (BILFF) - part 1: [EMIm][OAc]/water mixtures. <b>2021</b> , 23, 1242-1253		5
383	Fluorinated metal organic frameworks, MFFIVE-Ni-L (M = Fe/Al, L = pyr), with coordinatively unsaturated metal site for CO separation from flue gas in the presence of humidity by computational methods. <b>2021</b> , 50, 466-471		6
382	Elucidation the binding mechanism of -derived isoquinoline alkaloids as Rho-kinase 1 inhibitors by molecular docking and dynamic simulation. <b>2021</b> , 39, 379-394		3
381	Reverse osmotic characteristics and mechanism of pillared graphene membranes for water desalination. <b>2021</b> , 0-0		1
380	Bulk supercooled water adsorbed films on silica surfaces: specific heat by Monte Carlo simulation. <b>2021</b> , 23, 2275-2285		1
379	Refinement of Bynuclein ensembles against SAXS data: Comparison of force fields and methods.		1

378	A high-throughput screening of metal-organic framework based membranes for biogas upgrading. <b>2021</b> , 231, 235-257	2
377	Molecular-scale origins of solution nanostructure and excess thermodynamic properties in a water/amphiphile mixture. <b>2021</b> , 23, 8880-8890	3
376	Study on the relationship between hydrogen bond network dynamics of water and its terahertz spectrum. <b>2021</b> , 0-0	1
375	Molecular Dynamics Investigation of Phenolic Oxidative Coupling Protein Hyp-1 Derived from <i>Hypericum perforatum</i> . <b>2021</b> , 11, 43	0
374	Thermal Transportation Behavior Prediction of Water Molecules by Different Rigid Water Models: A Molecular Dynamics Study. <b>2021</b> , 497-508	
373	Design, synthesis, antibacterial activity evaluation and molecular modeling studies of new sulfonamides containing a sulfathiazole moiety. <b>2021</b> , 45, 8166-8177	8
372	Thermodynamics and kinetics of the amyloid- $\beta$ peptide revealed by Markov state models based on MD data in agreement with experiment. <b>2021</b> , 12, 6652-6669	17
371	Automation of absolute protein-ligand binding free energy calculations for docking refinement and compound evaluation. <b>2021</b> , 11, 1116	15
370	The role of water in host-guest interaction. <b>2021</b> , 12, 93	11
369	Elucidating Solution Structures of Cyclic Peptides Using Molecular Dynamics Simulations. <b>2021</b> , 121, 2292-2324	11
368	In silico screening of drug candidates for thermoresponsive liposome formulations. <b>2021</b> , 6, 368-380	1
367	Free Energy Landscape and Rate Estimation of the Aromatic Ring Flips in Basic Pancreatic Trypsin Inhibitor Using Metadynamics.	1
366	Effect of the Water Model in Simulations of Protein-Protein Recognition and Association. <b>2021</b> , 13,	2
365	The impact of framework flexibility and defects on the water adsorption in CAU-10-H. <b>2021</b> , 23, 21329-21337	4
364	study of the inhibition of SARS-COV-2 viral cell entry by neem tree extracts.. <b>2021</b> , 11, 26524-26533	4
363	Organoselenium Compounds as Acetylcholinesterase Inhibitors: Evidence and Mechanism of Mixed Inhibition. <b>2021</b> , 125, 1531-1541	3
362	Improving Computational Assessment of Porous Materials for Water Adsorption Applications via Flat Histogram Methods. <b>2021</b> , 125, 4253-4266	5
361	Histone H4 Tails in Nucleosomes: a Fuzzy Interaction with DNA. <b>2021</b> , 133, 6554-6561	0

360	Parameterization of Monovalent Ions for the OPC3, OPC, TIP3P-FB, and TIP4P-FB Water Models. <b>2021</b> , 61, 869-880	19
359	Histone H4 Tails in Nucleosomes: a Fuzzy Interaction with DNA. <b>2021</b> , 60, 6480-6487	8
358	Hydrogen Bonding and Its Effect on the Orientational Dynamics of Water Molecules inside Polyelectrolyte Brush-Induced Soft and Active Nanoconfinement. <b>2021</b> , 54, 2011-2021	5
357	Evaluating the Performance of Water Models with Host-Guest Force Fields in Binding Enthalpy Calculations for Cucurbit[7]uril-Guest Systems. <b>2021</b> , 125, 1558-1567	1
356	Solar Desalination Using Thermally Responsive Ionic Liquids Regenerated with a Photonic Heater. <b>2021</b> , 55, 3260-3269	4
355	Computationally reconstructing cotranscriptional RNA folding from experimental data reveals rearrangement of non-native folding intermediates. <b>2021</b> , 81, 870-883.e10	16
354	Recent Force Field Strategies for Intrinsically Disordered Proteins. <b>2021</b> , 61, 1037-1047	24
353	Water-Salt Oligomers Enable Supersoluble Electrolytes for High-Performance Aqueous Batteries. <b>2021</b> , 33, e2007470	25
352	Direct observation of coherent femtosecond solvent reorganization coupled to intramolecular electron transfer. <b>2021</b> , 13, 343-349	21
351	Interfacial Response and Structural Adaptation of Structured Polyelectrolyte Thin Films. <b>2021</b> , 54, 2892-2898	
350	Configurational Entropy of Folded Proteins and Its Importance for Intrinsically Disordered Proteins. <b>2021</b> , 22,	2
349	Extension of the Variational Free Energy Profile and Multistate Bennett Acceptance Ratio Methods for High-Dimensional Potential of Mean Force Profile Analysis. <b>2021</b> , 125, 4216-4232	4
348	Time-lagged Independent Component Analysis of Random Walks and Protein Dynamics.	
347	The high stability of the three-helix bundle UBA domain of p62 protein as revealed by molecular dynamics simulations. <b>2021</b> , 27, 102	
346	Kirkwood-Buff-Derived Force Field for Peptides and Proteins: Applications of KBFF20. <b>2021</b> , 17, 2991-3009	1
345	Testing the Limitations of MD-Based Local Electric Fields Using the Vibrational Stark Effect in Solution: Penicillin G as a Test Case. <b>2021</b> , 125, 4415-4427	3
344	Parametrization of Trivalent and Tetravalent Metal Ions for the OPC3, OPC, TIP3P-FB, and TIP4P-FB Water Models. <b>2021</b> , 17, 2342-2354	10
343	Examining the Role of Different Molecular Interactions on Activation Energies and Activation Volumes in Liquid Water. <b>2021</b> , 17, 2659-2671	3



342	Synthesis and Phase Behavior of Methane Hydrate in a Layered Double Hydroxide: An Experimental and Molecular Dynamics Simulation Study. <b>2021</b> , 125, 7889-7897		4
341	Toward In Silico Prediction of CO Diffusion in Champagne Wines. <b>2021</b> , 6, 11231-11239		1
340	How adding a single methylene to dihydrofolate reductase can change its conformational dynamics. <i>Journal of Chemical Physics</i> , <b>2021</b> , 154, 165103	3.9	2
339	Triphenylphosphonium Analogs of Chloramphenicol as Dual-Acting Antimicrobial and Antiproliferating Agents. <b>2021</b> , 10,		3
338	Molecular dynamics study of water confined in MIL-101 metal-organic frameworks. <i>Journal of Chemical Physics</i> , <b>2021</b> , 154, 144503	3.9	5
337	On the role of the quadrupole moment of carbon atom on water adsorption on graphite and in graphitic pores. <b>2021</b> , 409, 128236		2
336	Entropy-Entropy Compensation between the Protein, Ligand, and Solvent Degrees of Freedom Fine-Tunes Affinity in Ligand Binding to Galectin-3C. <b>2021</b> , 1, 484-500		5
335	Refinement of Ξynuclein Ensembles Against SAXS Data: Comparison of Force Fields and Methods. <b>2021</b> , 8, 654333		14
334	Molecular dynamics investigation of the slip flow liquid-solid interfacial thermal conductance. <b>2021</b> , 11, 055204		
333	3.Al-Based Metal-Organic Framework MFM-300 and MIL-160 for SO <sub>2</sub> Capture: A Molecular Simulation Study. <b>2021</b> , 536, 112963		7
332	Topology and complexity of the hydrogen bond network in classical models of water. <b>2021</b> , 329, 115530		7
331	Structure and Dynamics of Meprin $\alpha$ Complex with a Hydroxamate-Based Inhibitor. <b>2021</b> , 22,		3
330	Analysis of the relative stability of lithium halide crystal structures: Density functional theory and classical models. <i>Journal of Chemical Physics</i> , <b>2021</b> , 154, 184507	3.9	1
329	Effect of the Simulation Box Size and Precipitant Concentration on the Behavior of Tetragonal Lysozyme Dimer. <b>2021</b> , 66, 525-528		
328	Fabrication and evaluation of effective zeolite membranes for water desalination. <b>2021</b> , 504, 114974		12
327	Field-Dependent Dehydration and Optimal Ionic Escape Paths for CN Membranes. <b>2021</b> , 125, 7044-7059		1
326	Force Field Benchmark of Amino Acids. 3. Hydration with Scaled Lennard-Jones Interactions. <b>2021</b> , 61, 3571-3582		3
325	Vapor-liquid equilibrium of water with the MB-pol many-body potential. <i>Journal of Chemical Physics</i> , <b>2021</b> , 154, 211103	3.9	11


324	Cyclodextrin solubilization in hydrated reline: Resolving the unique stabilization mechanism in a deep eutectic solvent. <i>Journal of Chemical Physics</i> , <b>2021</b> , 154, 224505	3.9	2
323	Molecular Selectivity of CH <sub>4</sub> /C <sub>2</sub> H <sub>6</sub> Mixed Hydrates: A GCMC Study. <b>2021</b> , 5, 1782-1791		1
322	Solid-Like Nano-Anion Cluster Constructs a Free Lithium-Ion-Conducting Superfluid Framework in a Water-in-Salt Electrolyte. <b>2021</b> , 125, 11838-11847		8
321	Investigation of radezolid interaction with non-canonical chloramphenicol binding site by molecular dynamics simulations. <b>2021</b> , 105, 107902		3
320	Evolution of the Free Energy Landscapes of <i>n</i> -Alkane Guests Bound within Supramolecular Complexes. <b>2021</b> , 125, 7299-7310		0
319	The effect of electron correlation in unraveling the hydration properties of Sc <sup>3+</sup> in aqueous solution: A rigid body quantum mechanics/molecular mechanics simulation study. <b>2021</b> , 331, 115735		1
318	Overview of Molecular Dynamics Simulation of Natural Gas Hydrate at Nanoscale. <b>2021</b> , 2021, 1-17		2
317	Molecular dynamics simulations on formation of CO <sub>2</sub> hydrate in the presence of metal particles. <b>2021</b> , 331, 115793		4
316	Markovian Weighted Ensemble Milestoning (M-WEM): Long-time Kinetics from Short Trajectories.		0
315	Effect of water models on structure and dynamics of lignin in solution. <b>2021</b> , 11, 065024		0
314	Ensemble-based screening of natural products and FDA-approved drugs identified potent inhibitors of SARS-CoV-2 that work with two distinct mechanisms. <b>2021</b> , 105, 107871		6
313	Energy-entropy prediction of octanol-water logP of SAMPL7 N-acyl sulfonamide bioisosters. <b>2021</b> , 35, 831-840		1
312	A novel hybrid method for the calculation of methane hydrate-water interfacial tension along the three-phase (hydrate-liquid water-vapor) equilibrium line. <i>Journal of Chemical Physics</i> , <b>2021</b> , 155, 024702 <sup>3,9</sup>	3.9	2
311	Calculation of CYP450 protein-ligand binding and dissociation free energy paths. <i>Journal of Chemical Physics</i> , <b>2021</b> , 155, 025101	3.9	
310	On the Use of Interaction Entropy and Related Methods to Estimate Binding Entropies. <b>2021</b> , 17, 5379-5391		4
309	Rational Design of Nonbonded Point Charge Models for Divalent Metal Cations with Lennard-Jones 12-6 Potential. <b>2021</b> , 61, 4031-4044		2
308	Exploring ligand dynamics in protein crystal structures with ensemble refinement. <b>2021</b> , 77, 1099-1115		0
307	Machine Learning and Enhanced Sampling Simulations for Computing the Potential of Mean Force and Standard Binding Free Energy. <b>2021</b> , 17, 5287-5300		4

306	Atomic Level Investigations of Early Aggregation of Tau43 in Water I. Conformational Propensity of Monomeric Tau43. <b>2021</b> , 42, 1134-1142	
305	Mechanistic Investigation of Electrostatic Field-Enhanced Water Evaporation. <b>2021</b> , 8, e2100875	5
304	Observing reorientation dynamics with Time-Resolved fluorescence and molecular dynamics in varying periodic boundary conditions. <b>2021</b> , 1-15	
303	Prediction of local thermodynamics of water in and around endo-functionalized molecular tube receptors: An approach using grid inhomogeneous solvation theory. <b>2021</b> , 334, 116338	3
302	Application of Molecular Dynamics Simulations in the Analysis of Cyclodextrin Complexes. <b>2021</b> , 22,	8
301	Systematic Comparison of the Structural and Dynamic Properties of Commonly Used Water Models for Molecular Dynamics Simulations. <b>2021</b> , 61, 4521-4536	14
300	Adaptations for Pressure and Temperature in Dihydrofolate Reductases. <b>2021</b> , 9,	1
299	Direct observation of ultrafast hydrogen bond strengthening in liquid water. <b>2021</b> , 596, 531-535	13
298	Ion transfer electrochemistry of the alkaloids berberine and palmatine: Sensing and physicochemical characterization. <b>2021</b> , 895, 115506	
297	A distant angiogenin variant causes amyotrophic lateral sclerosis through loss-of-function mechanisms: Insights from long-timescale atomistic simulations and conformational dynamics. <b>2021</b> , 135, 104602	1
296	Highly selective carbon capture by novel graphene-carbon nanotube hybrids. 1-9	1
295	Molecular dynamics of dissolution of a 36-chain cellulose I <sub>II</sub> microfibril at different temperatures above the critical pressure of water. <b>2021</b> , 336, 116271	0
294	Molecular dynamics simulation of the effect of wax molecules on methane hydrate formation. <b>2021</b> , 297, 120778	8
293	Time-Lagged Independent Component Analysis of Random Walks and Protein Dynamics. <b>2021</b> , 17, 5766-5776	3
292	Data-driven many-body models enable a quantitative description of chloride hydration from clusters to bulk. <i>Journal of Chemical Physics</i> , <b>2021</b> , 155, 064502	3-9 7
291	Nanopores in Atomically Thin 2D Nanosheets Limit Aqueous Single-Stranded DNA Transport. <b>2021</b> , 127, 138103	3
290	Probing the Internal Dynamics and Shape of Simple Peptides in Urea, Guanidinium Hydrochloride, and Proline Solutions with Time-Resolved Fluorescence Anisotropy and Atomistic Cosolvent Simulations. <b>2021</b> , 125, 10972-10984	0
289	High-throughput computational screening of porous polymer networks for natural gas sweetening based on a neural network. e17433	1

288	Cold denaturation induced helix-to-helix transition and its implication to activity of helical antifreeze protein. <b>2021</b> , 338, 116627		3
287	Thermophysical properties of water using reactive force fields. <i>Journal of Chemical Physics</i> , <b>2021</b> , 155, 114501	3.9	0
286	CHARMM-GUI Free Energy Calculator for Practical Ligand Binding Free Energy Simulations with AMBER. <b>2021</b> , 61, 4145-4151		4
285	Carbon Dioxide Capture Enhanced by Pre-Adsorption of Water and Methanol in UiO-66. <b>2021</b> , 27, 14653-14659		3
284	Two helices control the dynamic crosstalk between the catalytic domains of LRRK2.		0
283	Protein hydration shell formation: Dynamics of water in biological systems exhibiting nanoscopic cavities. <b>2021</b> , 337, 116584		2
282	Rational Design of Nonbonded Point Charge Models for Highly Charged Metal Cations with Lennard-Jones 12-6 Potential. <b>2021</b> , 61, 4613-4629		1
281	Balanced Solvent Model for Intrinsically Disordered and Ordered Proteins. <b>2021</b> , 61, 5141-5151		2
280	Mass Spectrometric and Bio-Computational Binding Strength Analysis of Multiply Charged RNase S Gas-Phase Complexes Obtained by Electrospray Ionization from Varying In-Solution Equilibrium Conditions. <b>2021</b> , 22,		1
279	Ultrafast self-propelled water droplet transport on a graphene-covered nanocone. <b>2021</b> , 54, 505307		1
278	Monte Carlo simulations for water adsorption in porous materials: Best practices and new insights. <b>2021</b> , 67, e17447		5
277	Free Energy Change during the Formation of Crystalline Contact between Lysozyme Monomers under Different Physical and Chemical Conditions. <b>2021</b> , 11, 1121		1
276	The shape of water in zeolites and its impact on epoxidation catalysis. <b>2021</b> , 4, 797-808		14
275	Properties of aqueous 1,4-dioxane solution via molecular dynamics. <i>Journal of Chemical Physics</i> , <b>2021</b> , 155, 154501	3.9	1
274	Cluster analysis on conformational changes of the GDP/KRAS complex induced by A59G and D33E. <b>2021</b> , 781, 138995		2
273	Molecular-level insights into the structure stability of CH <sub>4</sub> -C <sub>2</sub> H <sub>6</sub> hydrates. <b>2022</b> , 247, 117039		2
272	Determining Partial Atomic Charges for Liquid Water: Assessing Electronic Structure and Charge Models. <b>2021</b> , 17, 889-901		7
271	Machine learning for reparameterization of four-site water models: TIP4P-BG and TIP4P-BGT. <b>2021</b> , 23, 10164-10173		4

270	Structure retrieval in liquid-phase electron scattering. <b>2021</b> , 23, 1308-1316	6
269	Molecular Simulation of Protein-Surface Interactions. <b>2009</b> , 69-95	2
268	Molecular docking to flexible targets. <b>2015</b> , 1215, 445-69	15
267	WATsite2.0 with PyMOL Plugin: Hydration Site Prediction and Visualization. <b>2017</b> , 1611, 123-134	9
266	Atomistic Force Fields for Proteins. <b>2019</b> , 2022, 3-19	8
265	Molecular dynamics simulations as a complement to nuclear magnetic resonance and X-ray diffraction measurements. <b>2007</b> , 400, 89-102	8
264	Interatomic Potentials. <b>2010</b> , 33-49	1
263	CO <sub>2</sub> (aq) Parameterization Through Free Energy Perturbation/Monte Carlo Simulations for Use in CO <sub>2</sub> Sequestration. <b>2009</b> , 337-357	1
262	Explicit and Implicit Water Models for Biomolecular Simulations. <b>2019</b> ,	1
261	Charge Anisotropy of Nitrogen: Where Chemical Intuition Fails. <b>2020</b> , 16, 4443-4453	5
260	Attach-Pull-Release Calculations of Ligand Binding and Conformational Changes on the First BRD4 Bromodomain. <b>2017</b> , 13, 3260-3275	26
259	Influence of Ionic Strength on Hydrophobic Interactions in Water: Dependence on Solute Size and Shape. <b>2020</b> , 124, 10326-10336	8
258	Chapter 20:Computer Simulation Studies of Heat Capacity Effects Associated with Hydrophobic Effects. <b>2010</b> , 436-456	6
257	Desolvation of the substrate-binding protein TauA dictates ligand specificity for the alkanesulfonate ABC importer TauABC. <b>2019</b> , 476, 3649-3660	3
256	Mirror-image antiparallel sheets organize water molecules into superstructures of opposite chirality. <b>2020</b> , 117, 32902-32909	7
255	Affinity of small-molecule solutes to hydrophobic, hydrophilic, and chemically patterned interfaces in aqueous solution. <b>2021</b> , 118,	4
254	Automated docking refinement and virtual compound screening with absolute binding free energy calculations.	5
253	Thermodynamics and kinetics of the amyloid- $\beta$ peptide revealed by Markov state models based on MD data in agreement with experiment.	5

252	Overview of the SAMPL6 host-guest binding affinity prediction challenge.	5
251	The conformational and mutational landscape of the ubiquitin-like marker for the autophagosome formation in cancer.	3
250	Ensembler: Enabling High-Throughput Molecular Simulations at the Superfamily Scale. <b>2016</b> , 12, e1004728	14
249	Fascaplysin as a specific inhibitor for CDK4: insights from molecular modelling. <b>2012</b> , 7, e42612	39
248	An accurate coarse-grained model for chitosan polysaccharides in aqueous solution. <b>2017</b> , 12, e0180938	18
247	Uni-directional self-driving of water droplets on monolayer graphene-covered wedge-shaped copper substrate. <b>2021</b> , 70, 200202-200202	0
246	Structural Characteristics in Local Hydration. <b>2021</b> , 105-138	
245	Metastable Zr/Hf-MOFs: the hexagonal family of EHU-30 and their water-sorption induced structural transformation.	1
244	Neat Water. <b>2021</b> , 121-181	
243	Biophysical Methods to Investigate Hydration Structures of Proteins. <b>2021</b> , 25-59	
242	Development of Range-Corrected Deep Learning Potentials for Fast, Accurate Quantum Mechanical/Molecular Mechanical Simulations of Chemical Reactions in Solution. <b>2021</b> , 17, 6993-7009	14
241	How to strike a conformational balance in protein force fields for molecular dynamics simulations?. e1578	0
240	Unlocking the Allometric Growth and Dissolution of Zn Anodes at Initial Nucleation and an Early Stage with Atomic Force Microscopy. <b>2021</b> ,	1
239	Nanopumps without Pressure Gradients: Ultrafast Transport of Water in Patterned Nanotubes.. <b>2022</b> , 126, 660-669	0
238	Ion Transport in Super-Concentrated Aqueous Electrolytes for Lithium-Ion Batteries.	2
237	Simulation of the Chiral Sum Frequency Generation Response of Supramolecular Structures Requires Vibrational Couplings. <b>2021</b> , 125, 12072-12081	4
236	Free Energy Perturbation Monte Carlo Simulations of Salt Influences on Aqueous Freezing Point Depression. <b>2009</b> , 359-370	
235	An Introduction to Water. <b>2014</b> , 1-58	

- 234 Topological microstructure analysis of the TIP4P-EW water model. **2014**, 6, 415-426 0
- 233 X-Ray Scattering from Purely Classical MD. **2015**, 37-54
- 232 Molecular Dynamics Simulation of Membrane Free Energy Profiles Using Accurate Force Field for Ionic Liquids. **2017**, 265-284
- 231 Approaches for calculating solvation free energies and enthalpies demonstrated with an update of the FreeSolv database.
- 230 Biomolecular Simulations under Realistic Macroscopic Salt Conditions.
- 229 Molecular dynamics study on permeability of water in graphene-carbon nanotube hybrid structure. **2018**, 67, 056102 1
- 228  ~~2018~~-**2018**, 1268-1274
- 227 Computationally Reconstructing Cotranscriptional RNA Folding Pathways from Experimental Data Reveals Rearrangement of Non-Native Folding Intermediates. 1
- 226 Microscopic Study of Solid/Fluid Interface with Molecular Dynamics. **2019**, 73-89 1
- 225 Pressure-driven fluid flow characteristics in black phosphorus nanochannels. **2019**, 68, 170202 1
- 224 Association of Functional Variants and Protein-to-Protein Physical Interactions of Human MutY homolog linked with Familial Adenomatous Polyposis and colorectal cancer Syndrome.
- 223 Axial driving characteristics of water in rotating black phosphorus nanotubes. **2020**, 69, 110201
- 222 In-silico screening of drug candidates for thermoresponsive liposome formulations.
- 221 One-dimensional nature of protein low-energy vibrations. **2020**, 2, 0
- 220 Polarizable Water Potential Derived from a Model Electron Density. **2021**, 17, 7056-7084 5
- 219 Conformations and stability of capsaicin in bulk solvents: A molecular dynamics study. **2022**, 345, 117794
- 218 Modeling nanoscale cellular structures using molecular dynamics. **2022**, 53-76
- 217 Methods and Models. **2020**, 25-33

216	Reverse osmotic characteristics and mechanism of hydrogenated porous graphene. <b>2020</b> , 69, 098201	1
215	Synthesis of Extra-Large Pore, Large Pore and Medium Pore Zeolites Using a Small Imidazolium Cation as the Organic Structure-Directing Agent. <b>2021</b> ,	0
214	Using Activation Energies to Elucidate Mechanisms of Water Dynamics. <b>2021</b> , 125, 9941-9952	3
213	Conformation and dynamics of the kinase domain drive subcellular location and activation of LRRK2.	
212	Exploiting the glycan receptor-binding site of PltB subunit in salmonella typhi toxin for novel inhibitors: An in-silico approach. <b>2021</b> , 111, 108082	
211	X-ray emission spectroscopy: a genetic algorithm to disentangle corehole-induced dynamics. <b>2021</b> , 140, 1	3
210	Gaussian-Accelerated Molecular Dynamics with the Weighted Ensemble Method: A Hybrid Method Improves Thermodynamic and Kinetic Sampling. <b>2021</b> ,	1
209	Theoretical and computational approaches for prediction of liquids viscosity.	
208	Structural Features of the [C4mim][Cl] Ionic Liquid and Its Mixtures with Water: Insight from a H NMR Experimental and QM/MD Study. <b>2021</b> , 125, 13255-13266	1
207	Water adsorption in ideal and defective UiO-66 structures. <b>2021</b> , 111555	2
206	Pressure Adaptations in Deep-Sea Dihydrofolate Reductases: Compressibility versus Stability. <b>2021</b> , 10,	1
205	Machine Learning-Assisted Computational Screening of Metal-Organic Frameworks for Atmospheric Water Harvesting.. <b>2022</b> , 12,	0
204	Calculation of centralities in protein kinase A.	
203	Mycobactin Analogues with Excellent Pharmacokinetic Profile Demonstrate Potent Antitubercular Specific Activity and Exceptional Efflux Pump Inhibition.. <b>2022</b> ,	1
202	A systematic and critical review of application of molecular dynamics simulation in low salinity water injection.. <b>2021</b> , 300, 102594	5
201	Boron removal by water molecules inside covalent organic framework (COF) multilayers. <b>2022</b> , 526, 115548	3
200	Volumetric Properties for the Binding of 1,4-Dioxane to Amide Naphthotubes in Water. <b>2020</b> , 124, 9175-9181	4
199	An allosteric regulation mechanism of Arabidopsis Serine/Threonine kinase 1 (SIK1) through phosphorylation.. <b>2022</b> , 20, 368-379	0



198	Do molecular dynamics force fields accurately model Ramachandran distributions of amino acid residues in water?. <b>2022,</b>		2
197	Evidence for Entropically Controlled Interfacial Hydration in Mesoporous Organosilicas.. <b>2022,</b>		0
196	Cryo-EM demonstrates the in vitro proliferation of an ex vivo amyloid fibril morphology by seeding.. <b>2022,</b> 13, 85		0
195	Molecular dynamics of liquid-liquid equilibrium and interfacial properties of aqueous solutions of methyl esters.. <b>2022,</b>		1
194	Thymosin $\beta$ Is an Endogenous Iron Chelator and Molecular Switcher of Ferroptosis.. <b>2022,</b> 23,		0
193	Interfacial dynamics in inverted-headgroup lipid membranes.. <i>Journal of Chemical Physics</i> , <b>2022,</b> 156, 075102	3.9	1
192	The Madrid-2019 force field for electrolytes in water using TIP4P/2005 and scaled charges: Extension to the ions F, Br, I, Rb, and Cs.. <i>Journal of Chemical Physics</i> , <b>2022,</b> 156, 044505	3.9	3
191	Evaporation of Water Nanodroplets on Heated Surfaces: Does Nano Matter?. <b>2022,</b>		0
190	Molecular dynamics simulations of structural and dynamical aspects of DNA hydration water.. <b>2022,</b>		
189	Lability of the first solvation shell of silver cations in liquid ammonia: A quantum mechanical charge field molecular dynamics simulation study. <b>2022,</b> 350, 118517		0
188	Preferential self-interaction of DNA methyltransferase DNMT3A subunits containing the R882H cancer mutation leads to dominant changes of flanking sequence preferences.. <b>2022,</b> 167482		1
187	Water transport through a two-dimensional nanoporous material: is there a relationship between water flux and surface tension?.		
186	A Step in Carbon Capture from Wet Gases: Understanding the Effect of Water on CO <sub>2</sub> Adsorption and Diffusion in UiO-66.		1
185	Novel and Potential Small Molecule Scaffolds as DYRK1A Inhibitors by Integrated Molecular Docking-Based Virtual Screening and Dynamics Simulation Study.. <b>2022,</b> 27,		1
184	Model Folded Hydrophobic Polymers Reside in Highly Branched Voids.. <b>2021,</b> 183-189		1
183	Markovian Weighted Ensemble Milestoning (M-WEM): Long-Time Kinetics from Short Trajectories.. <b>2021,</b>		0
182	A scalable metal-organic framework as a durable physisorbent for carbon dioxide capture.. <b>2021,</b> 374, 1464-1469		32
181	Computational Models for the Study of Protein Aggregation.. <b>2022,</b> 2340, 51-78		

180	Investigation of the pH-dependent aggregation mechanisms of GCSF using low resolution protein characterization techniques and advanced molecular dynamics simulations.. <b>2022</b> , 20, 1439-1455			0
179	Characterization of Amyloidogenic Peptide Aggregability in Helical Subspace.. <b>2022</b> , 2340, 401-448			0
178	Cavitation nucleation in pure water using Molecular dynamics simulation.			0
177	Flexible actuator by electric bending of saline solution-filled carbon nanotubes. <b>2022</b> , 55, 215301			0
176	Microsecond molecular dynamics of methane-carbon dioxide swapping in pure and saline water environment.. <b>2022</b> , 12, 2634			
175	Interpretation of the X-Ray Emission Spectra of Liquid Water through Temperature and Isotope Dependence.. <b>2022</b> , 128, 086002			1
174	Magnesium force fields for OPC water with accurate solvation, ion-binding, and water-exchange properties: Successful transfer from SPC/E.. <i>Journal of Chemical Physics</i> , <b>2022</b> , 156, 114501	3.9		1
173	Temperature dependence of thermodynamic, dynamical, and dielectric properties of water models.. <i>Journal of Chemical Physics</i> , <b>2022</b> , 156, 126101	3.9		5
172	Comparing the Performance of Different AMBER Protein Forcefields, Partial Charge Assignments, and Water Models for Absolute Binding Free Energy Calculations.. <b>2022</b> ,			1
171	Data-informed reparameterization of modified RNA and the effect of explicit water models: application to pseudouridine and derivatives.. <b>2022</b> , 36, 205			0
170	Raman Optical Activity of N-Acetyl-L-Cysteine in water and in methanol: the "clusters-in-a-liquid" model and ab initio molecular dynamics simulations.. <b>2022</b> ,			0
169	Identification of the Precursor Cluster in the Crystallization Solution of Proteinase K Protein by Molecular Dynamics Methods. <b>2022</b> , 12, 484			0
168	State-averaged CASSCF with polarizable continuum model for studying photoreactions in solvents: Energies, analytical nuclear gradients, and non-adiabatic couplings.. <i>Journal of Chemical Physics</i> , <b>2022</b> , 156, 104102	3.9		2
167	Many-body effect renders universal subdiffusion to water on different proteins. <b>2022</b> , 4,			0
166	Freestanding non-covalent thin films of the propeller-shaped polycyclic aromatic hydrocarbon decacyclene.. <b>2022</b> , 13, 1920			
165	DOC2b Enhances $\beta$ Cell Function Via A Novel Tyrosine Phosphorylation-Dependent Mechanism.. <b>2022</b> ,			1
164	The lung surfactant activity probed with molecular dynamics simulations.. <b>2022</b> , 304, 102659			0
163	Freezing point depression of salt aqueous solutions using the Madrid-2019 model.. <i>Journal of Chemical Physics</i> , <b>2022</b> , 156, 134503	3.9		3

162	Theoretical analysis toward better description of the wavenumber shifts of the OH stretch of hydrogen-bonded water.		0
161	Concentration Dependence of Dynamics and Hydrogen Bonding in Aqueous Solutions of Urea, Methyl-substituted Ureas, and Trimethylamine N-Oxide. <b>2022</b> , 119120		
160	Molecular dynamics simulations of the effects of metal nanoparticles on methane hydrate formation. <b>2022</b> , 356, 118962		0
159	Designing sub-nanometer pores for efficient boron removal. <b>2022</b> , 533, 115755		1
158	Electric resonance-induced hydrate dissociation acceleration to extract methane gas. <b>2022</b> , 321, 124014		0
157	Influence of Methylene Fluorination and Chain Length on the Hydration Shell Structure and Thermodynamics of Linear Diols. <b>2021</b> ,		0
156	The pervasive impact of critical fluctuations in liquid-liquid extraction organic phases.. <i>Journal of Chemical Physics</i> , <b>2021</b> , 155, 244506	3.9	0
155	Magnesium Force Fields for OPC Water with Accurate Solvation, Ion-Binding, and Water-Exchange Properties: Successful Transfer from SPC/E.		
154	Modeling a unit cell: crystallographic refinement procedure using the biomolecular MD simulation platform .. <b>2022</b> , 9, 114-133		
153	Optimized Magnesium Force Field Parameters for Biomolecular Simulations with Accurate Solvation, Ion-Binding, and Water-Exchange Properties in SPC/E, TIP3P-fb, TIP4P/2005, TIP4P-Ew, and TIP4P-D. <b>2021</b> ,		3
152	The Role of Cations of the Precipitant in the Interaction of Protein Molecules in the Lysozyme Oligomers in Crystallization Solutions. <b>2021</b> , 11, 1534		0
151	An investigation of some H2S thermodynamical properties at the water interface under pressurised conditions through molecular dynamics.		1
150	Rational Design of Nonbonded Point Charge Models for Monovalent Ions with Lennard-Jones 12-6 Potential. <b>2021</b> ,		2
149	Suspect general base guanine found with a smoking gun in the pistol ribozyme.. <b>2022</b> ,		0
148	Thermal conductivity temperature dependance of water confined in nanoporous silicon.. <b>2022</b> ,		0
147	On the Nature of Guest Complexation in Water: Triggered Wetting-Water-Mediated Binding.. <b>2022</b> ,		0
146	Estimating ruggedness of free-energy landscapes of small globular proteins from principal component analysis of molecular dynamics trajectories.. <b>2022</b> , 105, 044404		1
145	Maximum in density of electrolyte solutions: Learning about ion-water interactions and testing the Madrid-2019 force field.. <i>Journal of Chemical Physics</i> , <b>2022</b> , 156, 154502	3.9	1

- 144 Graph neural networks accelerated molecular dynamics.. *Journal of Chemical Physics*, **2022**, 156, 144103 3.9 5
- 143 Rational design by structural biology of industrializable, long-acting antihyperglycemic GLP-1 receptor agonists.
- 142 Enhancement of the solubility of organic dyes in aqueous ionic solvents doped with surfactants. **2022**, 357, 118958 0
- 141 Data\_Sheet\_1.PDF. **2019**,
- 140 Data\_Sheet\_2.zip. **2019**,
- 139 Data\_Sheet\_1.PDF. **2019**,
- 138 LRRK2 dynamics analysis identifies allosteric control of the crosstalk between its catalytic domains.. **2022**, 20, e3001427 4
- 137 Multiscale computational investigations of the translesion synthesis bypass of tobacco-derived DNA adducts: critical insights that complement experimental biochemical studies.. **2022**, 0
- 136 Viscous peeling of a nanosheet.. **2022**,
- 135 Computational Modeling of Conformer Stability in Benenodin-1, a Thermally Actuated Lasso Peptide Switch.. **2022**, 0
- 134 Prediction of H Singlet Relaxation via Intermolecular Dipolar Couplings Using the Molecular Dynamics Method.. **2022**, 126, 3530-3538
- 133 Open Force Field Evaluator: An Automated, Efficient, and Scalable Framework for the Estimation of Physical Properties from Molecular Simulation.. **2022**, 1
- 132 Force Field Parameterization of Actinyl Molecular Cations Using the 12-6-4 Model.. **2022**, 0
- 131 Ephemeral Ice-Like Local Environments in Classical Rigid Models of Liquid Water. *Journal of Chemical Physics*, 3.9 1
- 130 Conformational dynamics of the hepatitis B virus pre-genomic RNA on multiple time scales: implications for viral replication. **2022**, 167633 1
- 129 Highly Ion-Permeable Porous Organic Cage Membranes with Hierarchical Channels.. **2022**, 4
- 128 Effects of Familial Alzheimer's Disease Mutations on the Folding Free Energy and Dipole-Dipole Interactions of the Amyloid  $\beta$  Peptide.
- 127 Spontaneous and Selective Potassium Transport through a Suspended Tailor-Cut Ti<sub>3</sub>C<sub>2</sub>T<sub>x</sub> MXene Film. 3

126	Aggregation of a Parkinson's Disease-Related Peptide: When Does Urea Weaken Hydrophobic Interactions?.			
125	Effect of Synthesis Temperature on Water Adsorption in UiO-66 Derivatives: Experiment, DFT+D Modeling, and Monte Carlo Simulations. <b>2022</b> , 126, 9185-9194			0
124	The Role of Cations and Anions in the Formation of Crystallization Oligomers in Protein Solutions as Revealed by Combination of Small-Angle X-ray Scattering and Molecular Dynamics. <b>2022</b> , 12, 751			0
123	Patched 1 regulates Smoothed by controlling sterol binding to its extracellular cysteine-rich domain. <b>2022</b> , 8,			1
122	Mechanical Stability of Fluorinated-Methane Clathrate Hydrates. <b>2022</b> , 119553			0
121	Robust, Efficient and Automated Methods for Accurate Prediction of Protein-Ligand Binding Affinities in AMBER Drug Discovery Boost. 161-204			1
120	Simulating the Hydration Structure of Low- and High-Spin [Fe(bpy) <sub>3</sub> ] <sup>2+</sup> : Long-Range Dispersion and Many-Body Effects.			1
119	On the Temporal Selectivity of Desalination for a Porous Composite Graphene-copper Membrane (Gcum): A Molecular Dynamics Study.			
118	The effects of surface hydration on capillary adhesion under nanoscale confinement.			
117	Combined QM/MM, Machine Learning Path Integral Approach to Compute Free Energy Profiles and Kinetic Isotope Effects in RNA Cleavage Reactions.			2
116	Melting points of water models: Current situation. <i>Journal of Chemical Physics</i> , <b>2022</b> , 156, 216101	3.9		1
115	Sodium and Magnesium Ion Location at the Backbone and at the Nucleobase of RNA: Ab Initio Molecular Dynamics in Water Solution.			
114	Irregular Structure of the Hydrated Ag <sup>+</sup> in Aqueous Solution and its Dynamics: an Insight from Perturbation Theory Hybrid Forces Molecular Dynamics Simulation. <b>2022</b> , 119688			
113	Recent Advances in Density Functional Theory and Molecular Dynamics Simulation of Mechanical, Interfacial, and Thermal Properties of Natural Gas Hydrates in Canada.			0
112	The performance of OPC water model in prediction of the phase equilibria of methane hydrate. <i>Journal of Chemical Physics</i> ,	3.9		
111	Studying the Dynamics of a Complex G-Quadruplex System: Insights into the Comparison of MD and NMR Data.			1
110	Rational Design by Structural Biology of Industrializable, Long-Acting Antihyperglycemic GLP-1 Receptor Agonists. <b>2022</b> , 15, 740			
109	On the Performance of Vertically Aligned Graphene Array Membranes for Desalination. <b>2022</b> , 14, 27405-27412			1

- 108 Towards the correct microscopic structure of aqueous CsCl solutions with a comparison of classical interatomic potential models. **2022**, 361, 119660 1
- 107 Molecular insights into methane hydrate growth in the presence of wax molecules. **2022**, 324, 124743 0
- 106 Nucleation of Water Clusters in Gas Phase: A Computational Study Based on Neural Network Potential and Enhanced Sampling?. **2022**, 80, 598
- 105 A Deep Neural Network Potential for Water Confined in Graphene Nanocapillaries. **2022**, 126, 10546-10553 1
- 104 Fate of Water Molecules on (11-20) and (1-102)  $\gamma$ -Alumina Surfaces: 2D Periodic Self-Consistent Charge-Density Functional Tight-Binding/Molecular Mechanics Molecular Dynamics Study. **2022**, 126, 11148-11157
- 103 Phosphomimetic Mutation at Ser165 of  $\beta$ -Tubulin Promotes the Persistence of GTP Caps in Microtubules. **2022**, 61, 1508-1516 0
- 102 SAA fibrils involved in AA amyloidosis are similar in bulk and by single particle reconstitution: A MAS solid-state NMR study. **2022**, 100069
- 101 RNA Electrostatics: How Ribozymes Engineer Active Sites to Enable Catalysis. 1
- 100 Effect of water film on the nano-scratching process of 4H-SiC under the constant load. **2022**, 175, 107802 0
- 99 Comparative analysis of hydration layer reorientation dynamics of antifreeze protein and protein cytochrome P450. **2022**, 35, 509-515
- 98 Anomalous Infrared Absorbance of S<sub>2</sub>O: A Perturbation Study of EC<sub>1</sub>/D. **2022**, 126, 5490-5496 1
- 97 Water Thermodynamic Behavior Under Influence of Electric Field: A Molecular Dynamics Study. **2022**, 126, 5752-5764
- 96 Local RNA Structure, Ion Hydration Shell and the Energy Barrier for Water Exchange from the Ion Hydration Shell Determine the Mechanism of Ion Condensation on Specific RNA Sites.
- 95 Effect of Solvent Quality on Structure and Dynamics of Lignin in Solution. **2022**, 126, 5752-5764 1
- 94 Enhanced Water Evaporation from  $\beta$ -Scale Graphene Nanopores. 0
- 93 Prediction of self-diffusion coefficients of chemically diverse pure liquids by all-atom molecular dynamics simulations. 1
- 92 Controllable and Gradient Wettability of Bilayer Two-Dimensional Materials Regulated by Interlayer Distance.
- 91 Predicting molecular properties of  $\beta$ -synuclein using force fields for intrinsically disordered proteins. 0

90	Detecting the First Hydration Shell Structure around Biomolecules at Interfaces.	2
89	Molecular design of covalent-organic framework membranes for Li <sup>+</sup> /Mg <sup>2+</sup> separation: Significant charge effect. <b>2022</b> , 662, 120976	1
88	A review of geopolymer and its adsorption capacity with molecular insights: A promising adsorbent of heavy metal ions. <b>2022</b> , 322, 116066	0
87	Designing optimal core-shell MOFs for direct air capture.	0
86	How cryoprotectants work: hydrogen-bonding in low-temperature vitrified solutions. <b>2022</b> , 13, 9980-9984	0
85	The role of structural dynamics in the thermal adaptation of hyperthermophilic enzymes. 9,	0
84	Xponge: A Python package to perform pre- and post-processing of molecular simulations. <b>2022</b> , 7, 4467	0
83	Balanced Force Field ff03CMAP Improving the Dynamics Conformation Sampling of Phosphorylation Site. <b>2022</b> , 23, 11285	1
82	Accelerated ensemble generation for cyclic peptides using a Reservoir-REMD implementation in GROMACS.	0
81	Statistical-mechanical liquid theories reproduce anomalous thermodynamic properties of explicit two-dimensional water models. <b>2022</b> , 106,	0
80	Conjugates of Desmycosin with Fragments of Antimicrobial Peptide Oncocin: Synthesis, Antibacterial Activity, Interaction with Ribosome. <b>2022</b> , 87, 871-889	0
79	Antifouling Bilayer Graphene Slit Membrane for Desalination of Nanoplastic-Infested Seawater: A Molecular Dynamics Simulation Study. <b>2022</b> , 14, 43965-43974	0
78	Proposed Mechanism for Emodin as Agent for Methicillin Resistant Staphylococcus Aureus: In Vitro Testing and In Silico Study. <b>2022</b> , 44, 4490-4499	0
77	High-Throughput Nanopore Fabrication and Classification Using Xe-Ion Irradiation and Automated Pore-Edge Analysis.	0
76	Effects of Familial Alzheimer's Disease Mutations on the Folding Free Energy and Dipole-Dipole Interactions of the Amyloid $\beta$ -Peptide. <b>2022</b> , 126, 7552-7566	0
75	Assessing the effect of forcefield parameter sets on the accuracy of relative binding free energy calculations. 9,	0
74	Alkyl chain length-dependent protein nonadsorption and adsorption properties of crystalline alkyl cellulose assemblies. <b>2022</b> , 112898	0
73	Comparison of the United- and All-Atom Representations of (Halo)alkanes Based on Two Condensed-Phase Force Fields Optimized against the Same Experimental Data Set.	2

- 72 Fast Polarizable Water Model for Atomistic Simulations. 1
- 71 Machine learning-generated TIP4P-BGWT model for liquid and supercooled water. **2022**, 367, 120459 0
- 70 Enhancement of DNAzymatic activity using iterative in silico maturation. 0
- 69 Capturing differences in the regulation of LRRK2 dynamics and conformational states by small molecule kinase inhibitors. 0
- 68 An overview of the SAMPL8 host-guest binding challenge. **2022**, 36, 707-734 0
- 67 Mechanistic basis of the increased methylation activity of the SETD2 protein lysine methyltransferase towards a designed super-substrate peptide. **2022**, 5, 0
- 66 Multireference Generalization of the Weighted Thermodynamic Perturbation Method. 0
- 65 Improving Condensed-Phase Water Dynamics with Explicit Nuclear Quantum Effects: The Polarizable Q-AMOEBA Force Field. **2022**, 126, 8813-8826 1
- 64 Effects of carbon nanotube on methane hydrate formation by molecular dynamics simulation. **2022**, 120621 0
- 63 Chemical transformations and transport phenomena at interfaces. 0
- 62 Hydration Structure of Na<sup>+</sup> and K<sup>+</sup> Ions in Solution Predicted by Data-Driven Many-Body Potentials. 0
- 61 On the temporal selectivity of desalination for a porous composite graphene-copper membrane (GCuM): A molecular dynamics study. **2023**, 546, 116182 0
- 60 Molecular dynamics analysis of water flow through a multiply connected carbon nanotube channel. **2023**, 45, 64-71 0
- 59 Molecular Dynamics Methods for Antibody Design. **2023**, 109-124 0
- 58 Formation of the structure-II gas hydrate from low-concentration propane mixed with methane. **2022**, 1
- 57 Binary Salt Structure Classification with Convolutional Neural Networks: Application to Crystal Nucleation and Melting Point Calculations. 0
- 56 Selectivity and ranking of tight-binding JAK-STAT inhibitors using Markovian milestone with Voronoi tessellations. 0
- 55 Comparison of molecular dynamics simulations of water with neutron and X-ray scattering experiments. **2022**, 272, 01015 0



54	Transferable Potential Function for Flexible H <sub>2</sub> O Molecules Based on the Single-Center Multipole Expansion.	2
53	Capturing the Polarization Response of Solvated Proteins Under Constant Electric Fields in Molecular Dynamics Simulations.	0
52	Practical Guidance for Consensus Scoring and Force Field Selection in Protein-Ligand Binding Free Energy Simulations.	0
51	Unusual Temperature Behavior of Stability of Proteinase K Dimer Formed in Crystallization Solution Defined by Molecular Dynamics. <b>2022</b> , 12, 1645	0
50	Performance evaluation of the balanced force field ff03CMAP for intrinsically disordered and ordered proteins. <b>2022</b> , 24, 29870-29881	1
49	Neuroprotective potential of cinnamoyl derivatives against Parkinson's disease indicators in <i>Drosophila melanogaster</i> and in silico models. <b>2023</b> , 94, 147-157	0
48	On the not so anomalous water-induced structural transformations of choline chloride-urea (reline) deep eutectic system. <b>2022</b> , 25, 439-454	0
47	Suspended water nanodroplets evaporation and its deviation from continuum estimations. <b>2023</b> , 370, 121034	0
46	Molecular dynamics-based analysis of the factors influencing the CO <sub>2</sub> replacement of methane hydrate. <b>2023</b> , 119, 108394	1
45	Densities, Viscosities, Thermal Expansivities, and Isothermal Compressibilities of Carbonated Hydroalcoholic Solutions for Applications in Sparkling Beverages. <b>2022</b> , 126, 10194-10205	0
44	A scheme for rapid evaluation of the intermolecular three-body polarization effect in water clusters.	1
43	Ensemble Generation for Linear and Cyclic Peptides Using a Reservoir Replica Exchange Molecular Dynamics Implementation in GROMACS. <b>2022</b> , 126, 10384-10399	0
42	A Comparison of Methods for Computing Relative Anhydrous Hydrate Stability with Molecular Simulation.	0
41	AMBER Drug Discovery Boost Tools: Automated Workflow for Production Free-Energy Simulation Setup and Analysis (ProFESSA). <b>2022</b> , 62, 6069-6083	0
40	Multi-Scale Computer-Aided Design of Covalent Organic Frameworks for CO <sub>2</sub> Capture in Wet Flue Gas. <b>2022</b> , 14, 56353-56362	0
39	Solvation Structure and Ion-Solvent Hydrogen Bonding of Hydrated Fluoride, Chloride and Bromide: A Comparative QM/MM MD Simulation Study. <b>2022</b> , 2, 445-464	0
38	Personal Precise Force Field for Intrinsically Disordered and Ordered Proteins Based on Deep Learning.	0
37	AMBER Free Energy Tools: A New Framework for the Design of Optimized Alchemical Transformation Pathways.	1

- 36 Thermodynamic Response Functions and Stokes-Einstein Breakdown in Superheated Water under Gigapascal Pressure. ○
- 35 Solving an Old Puzzle: Elucidation and Evaluation of the Binding Mode of Salvinorin A at the Kappa Opioid Receptor. **2023**, 28, 718 ○
- 34 Investigating the Solvent Effects on Binding Affinity of PAHs-Box4+ Complexes: An Alchemical Approach. **2023**, 127, 249-260 ○
- 33 ACES: Optimized Alchemically Enhanced Sampling. ○
- 32 State averaged CASSCF in AMOEBA polarizable water model for simulating nonadiabatic molecular dynamics with nonequilibrium solvation effects. **2023**, 158, 014101 ○
- 31 Influence of conversion on dielectric constant of Dicyandiamide cured epoxy resin: a molecular dynamic simulation and experiment study. **2023**, 267, 125645 ○
- 30 Design of Nanostructured Surfaces for Efficient Condensation by Controlling Condensation Modes. **2023**, 14, 50 ○
- 29 Effect of water film on 4H-SiC nano-indentation process. **2022**, ○
- 28 Spacer-engineered Ionic Channels in Covalent Organic Framework Membrane toward Ultrafast Proton Transport. 2211004 ○
- 27 Water model determines thermosensitive and physicochemical properties of poly(N-isopropylacrylamide) in molecular simulations. 10, ○
- 26 Atomistic molecular modeling methods. **2023**, 37-73 ○
- 25 Deconvoluting binding sites in amyloid nanofibrils using time-resolved spectroscopy. **2023**, 14, 1072-1081 ○
- 24 Design of an Electrostatic Frequency Map for the NH Stretch of the Protein Backbone and Application to Chiral Sum Frequency Generation Spectroscopy. **2023**, 127, 2418-2429 ○
- 23 Simulating a flexible water model as rigid: Best practices and lessons learned. **2023**, 158, 134506 ○
- 22 Building a Hofmeister-like series for the maximum in density temperature of aqueous electrolyte solutions. **2023**, 377, 121433 ○
- 21 Effects of  $\text{H}_2\text{S}$ ,  $\text{SO}_2$  and  $\text{N}_2\text{O}$  mole fractions on adsorption behavior and phase equilibrium properties of  $\text{CO}_2$  mixed gas hydrate. **2023**, 380, 121661 ○
- 20 Molecular dynamics study of ion clustering in concentrated electrolyte solutions for the estimation of salt solubilities. **2023**, 571, 113802 ○
- 19 Computational Investigation of Structure-Function Relationship in Fluorine-Functionalized MOFs for PFOA Capture from Water. **2023**, 127, 3204-3216 ○

- 18 Brownian Motion in Optical Tweezers, a Comparison between MD Simulations and Experimental Data in the Ballistic Regime. **2023**, 15, 787
- 17 Scaled charges for ions: An improvement but not the final word for modeling electrolytes in water. **2023**, 158, 054505
- 16 Field-Induced Hydration Shell Reorganization Enables Electro-osmotic Flow in Nanochannels. **2023**, 130,
- 15 What is the Optimal Dipole Moment for Nonpolarizable Models of Liquids?. **2023**, 19, 1790-1804
- 14 Singlet fission as a polarized spin generator for dynamic nuclear polarization. **2023**, 14,
- 13 CBA Test of DNA Force Fields. **2023**, 8, 10253-10265
- 12 Modern semiempirical electronic structure methods and machine learning potentials for drug discovery: Conformers, tautomers, and protonation states. **2023**, 158, 124110
- 11 Fuzzy Drug Targets: Disordered Proteins in the Drug-Discovery Realm. **2023**, 8, 9729-9747
- 10 The T1150A cancer mutant of the protein lysine dimethyltransferase NSD2 can introduce H3K36 trimethylation.
- 9 Computational Prodrug Design Methodology for Liposome Formulability Enhancement of Small-Molecule APIs. **2023**, 20, 2119-2127
- 8 Solvent Model Benchmark for Molecular Dynamics of Glycosaminoglycans. **2023**, 63, 2147-2157
- 7 Identification of the precursor cluster in thermolysin crystallization solution by molecular dynamics methods. **2023**, 33, 225-227
- 6 Selectivity and Ranking of Tight-Binding JAK-STAT Inhibitors Using Markovian Milestoning with Voronoi Tessellations.
- 5 Capturing Differences in the Regulation of LRRK2 Dynamics and Conformational States by Small Molecule Kinase Inhibitors. **2023**, 18, 810-821
- 4 Research and Evaluation of the Allosteric Protein-Specific Force Field Based on a Pre-Training Deep Learning Model.
- 3 Accurate Host-Guest Binding Free Energies Using the AMOEBA Polarizable Force Field.
- 2 Thermodynamic response functions and Stokes-Einstein breakdown in superheated water under gigapascal pressure. **2023**, 142,
- 1 Interlayered Interface of a Thin Film Composite Janus Membrane for Sieving Volatile Substances in Membrane Distillation. **2023**, 57, 7612-7623

